Summer 8-21-2013

Modeling the Production of Microalgal Biodiesel

Mark Henson
Washington University in St. Louis

WASHINGTON UNIVERSITY IN ST. LOUIS

School of Engineering and Applied Science
Department of Energy, Environmental and Chemical Engineering

Dissertation Examination Committee:
Jay R. Turner, Chair
Richard L. Axelbaum
Pratim Biswas
Robert E. Blankenship
David I. Gustafson
Himadri B. Pakrasi

Modeling the Production of Microalgal Biodiesel

by

Mark Henson

A dissertation presented to the
Graduate School of Arts and Sciences
of Washington University in
partial fulfillment of the
requirements for the degree
of Doctor of Philosophy

August 2013

St. Louis, Missouri

TABLE OF CONTENTS

LIST OF FIGURES

LIST OF TABLES

ACKNOWLEDGMENTS

This work was jointly funded by the Archer Daniels Midland Company and the Monsanto Company. Any findings, conclusions, or opinions expressed in this dissertation are solely those of the author, and do not necessarily reflect the views of the Archer Daniels Midland Company or the Monsanto Company. The author gratefully acknowledges the contributions of Professors Jay R. Turner, lead advisor, and Richard L. Axelbaum, co-advisor, for their guidance and support during the performance of the work described in this dissertation.

ABSTRACT OF THE DISSERTATION

Modeling the Production of Microalgal Biodiesel

by

Mark Henson

Doctor of Philosophy in Energy, Environmental and Chemical Engineering

Washington University in St. Louis, 2013

Professor Pratim Biswas, Chair

Biodiesel produced from microalgal lipids is being extensively researched as an alternative to petroleum-derived diesel. Literature reports of prior modeling to estimate the likely energy and carbon footprints and manufacturing cost of microalgal biodiesel are inconclusive, with wide ranges for performance measures such as Net Energy Return and manufacturing cost. The goals of this research are to develop an integrated techno-economic life cycle inventory model of microalgal biodiesel production, create a base case that simulates proven manufacturing processes, identify potential barriers to technical, financial, and/or environmental viability, perform sensitivity analyses that identify the input parameters and modeling assumptions that have significant influence on key biodiesel performance indicators (KPI's), and perform case studies involving alternative microalgal properties, manufacturing processes and operating conditions, modeling time-scales, and geographic locations.

The model created to meet these objectives, called "TELCIM," is the first publicly available, integrated techno-economic life cycle inventory model of microalgal biodiesel manufacture. It consists of a set of interlinked engineering, financial, and life cycle inventory models. It is implemented in Microsoft Excel®, and simulates a five-step manufacturing process consisting of microalgae cultivation, biomass harvesting, lipid extraction, lipid conversion to biodiesel, and anaerobic digestion of residual biomass. Material and energy flows are estimated using mass and energy balances and equipment performance equations. Operating and capital costs are estimated using standard accounting methods, and a "cradle-to-gate" life cycle inventory of energy and resource consumptions and pollutant releases is compiled. Detailed descriptions of TELCIM's component physical models, along with the derivation of their governing equations, are provided.

TELCIM was initially populated with data representing conventional microalgae cultivation and harvesting and vegetable oil extraction and conversion technologies deployed in a southern California location. The Net Energy Return for this case is below 1.0, the minimum threshold for long-term sustainability; the carbon intensity is similar to that of petrodiesel; and the manufacturing cost is uncompetitive with current transportation fuels. Detailed breakdowns show the contributions of each major process step and use category to these performance metrics, allowing identification of the major barriers to viability. Among the biggest obstacles is the large amount of energy used to dry the biomass to the 10% residual moisture content required by the conventional oilseed extraction process.

Two types of single-parameter sensitivity analyses are used to identify input parameters that have significant influence on the KPI's. Tornado plots reveal that biological properties including lipid fraction, intracellular water content, and growth rate are among the most influential with respect to one or more of the KPI's. Trend analyses of several of the anaerobic digester operating parameters show that factors affecting biogas production have much stronger influence on the KPI's than factors relating to nutrient recovery. Several variants to the base case were performed, including cases in which the microalga's growth rate and lipid content conform to R&D targets established by the National Alliance for Advanced Biofuels and Bioproducts; a hypothetical wet extraction process allows the drying step to be bypassed; and there is no anaerobic digestion step. The results from these cases suggest that one or more breakthroughs in cell biology and/or process engineering are necessary to make microalgal biodiesel a sustainable large-scale alternative to petroleum diesel. They also show that including anaerobic digestion in the manufacturing scheme improves the KPI's of greatest interest, and delivers an acceptable financial return on incremental investment.

TELCIM is a steady-state model, and the climatological data used in the base case represents annual average conditions. The effects of monthly variations in sunlight intensity are simulated under several facility design bases and operating strategies; it appears that designing for maximum sunlight intensity is more cost and energy effective, but necessitates underutilization of available carbon dioxide and reduces

the biodiesel production rate. Enhancing the correlation between sunlight intensity and microalgal growth rate to account for the effect of light saturation on photosynthetic efficiency significantly dampens seasonal variations in biomass productivity. Analysis of hourly average versus daily average sunlight intensity indicates that daily average data is sufficiently precise if the long-term average biomass productivity is known; otherwise substantial error can be introduced if biomass productivity is estimated directly from sunlight intensity data, and daily average data is used instead of hourly average data. Five alternative manufacturing locations along the southern rim of the continental United States are simulated using local climatological inputs, including sunlight intensity. The only performance measure that differs significantly among these sites is water intensity, which is predicted to be much lower east of the Rockies due to higher precipitation rates.

Several supporting analyses are also presented in the dissertation, including a comparison of the composition of microalgal and soy lipids, which addresses the assumption that conventional oilseed extraction and conversion technologies will be effective with microalgal biomass as a substrate. The mechanisms of oil extraction, and the effects of residual water on extraction efficiency, are explored in an attempt to optimize evaporation energy load and oil yield. The impact of ambient temperature and relative humidity, dryer operating conditions, and dryer control strategies, on the energy burden imposed by biomass drying, are evaluated. And a multi-parameter sensitivity analysis explores the effect of potential interdependencies among biomass growth rate, intracellular water content, and lipid fraction on the KPI's.

Additional findings from this research include that microalgal properties affect virtually every step of the manufacturing process; TELCIM can be used to identify optimal strain characteristics for a given processing scheme. The bulk of the energy use and carbon dioxide emissions attributable to the cradle-to-gate manufacturing process occur within the biodiesel plant, but offsite emissions resulting from energy and raw material supply and transportation activities are not negligible. The main driver of Net Energy Return, carbon intensity and unit manufacturing cost is electricity usage, primarily for pumping fluids over

long distances. Replacing evaporation losses can impose an enormous water burden, perhaps overwhelming local supplies, especially in the western United States.

TELCIM is a deterministic model; for a given set of input data it returns a set of numerical outputs without any measures of uncertainty or error. Recommendations for future work include an uncertainty analysis involving Monte Carlo simulations. They also include enhancing TELCIM to perform life cycle assessments, by assigning specific fates to byproducts and gauging the environmental impacts of resource usages and pollutant emissions. TELCIM can be modified to simulate alternative manufacturing schemes, such as feeding the biogas produced in the digesters to the central power unit, using the algae ponds for secondary wastewater treatment, and separate growth stages in which biomass production and lipid production are alternately promoted. Finally, the case studies simulating alternative manufacturing sites can be enhanced by using local operating and capital cost structures, especially for those sites in the southeastern United States that appear to have a more acceptable water intensity.

1. INTRODUCTION

1.1. BACKGROUND

1.1.1. Drivers for Renewable Energy Sources

Population growth and improved standard of living are increasing the demand for energy in the United States and around the globe. The U.S. Energy Information Administration predicts that global energy consumption will increase by 49% between 2000 and 2035, from 495 quadrillion BTU to 739 quadrillion BTU per year. In particular, consumption of liquid fuels in the transportation sector, which accounted for 27% of total global energy use in 2007, is expected to rise by 1.3% annually between 2011 and 2035[1]. Most liquid transportation fuels are currently derived from petroleum; in 2009 biodiesel represented less than 1% of the total diesel fuel consumed for transportation, and ethanol represented roughly 8% (by volume) of the gasoline used in vehicles in the United States[2]. The global situation is not much different; the International Energy Administration estimates that biofuels constituted only 2% of the liquid transportation fuel used worldwide in 2009[3].

Many scientists attribute recent global climate variations to an increase in atmospheric carbon dioxide concentration resulting from large-scale combustion of fossil fuels[4]. Despite substantial investment in alternative energy sources, in 2010 fossil fuels still provided 87% of the world's marketed energy[5], as compared to 88% in 2005[6]. For the last quarter century, the ratio of the amount of known oil reserves to annual production (the "R/P Ratio") has hovered between 40 and 50[5]. The combination of increasing world demand and stagnant supply is likely to further drive up the price of liquid petroleum fuels, which has recently undergone dramatic increases - the global spot crude oil price was less than US$24/bbl in August 2001, and more than US$111/bbl in August 2011[7], an almost five-fold increase in one decade. And there is a significant discontinuity between where oil is produced and where it is consumed. For example, for the four weeks ending August 5, 2011, the United States imported 63% of the crude oil it consumed[8]. The dependence of many developed and developing economies on imported oil is expected to grow with time, increasing an already significant risk of geopolitical instability, supply interruptions, and

cost escalation. Conversion from fossil fuels to renewable energy sources will help mitigate these environmental, economic, and political risks.

1.1.2. Biofuels

Prominent among the renewable energy alternatives being developed are biofuels, which are fuels derived directly from biomass[9]. Biofuels are considered to be "carbon-neutral", since the carbon they contain was absorbed from the atmosphere as carbon dioxide during photosynthesis, and their combustion returns that carbon to the atmosphere as carbon dioxide. Among the renewable energy sources, some biofuels are well suited for use in the transportation sector because they are liquid at standard conditions. Biodiesel, which is derived from plant and animal lipids, and bioethanol, which is produced from starch and sugars, are two of the most prominent biofuels suitable for use as transportation fuels, and both are in large-scale commercial production today[10].

In addition to having a more favorable carbon footprint than fossil fuels, bioethanol from sugar and biodiesel from vegetable oil, the so-called "first generation" biofuels, are compatible with existing fuel distribution systems and engine technology[11]. However, first generation biofuels have generated considerable controversy because they compete with food crops for arable land, creating food price and security issues[12]. It is also unclear whether, on a total life-cycle basis, first generation biofuels can be produced sustainably. For example, a recent study indicates that the production and use of nitrogen fertilizers for biofuel crop production may result in N_2O emissions with a global warming potential (GWP) greater than that of the CO_2 emissions from the fossil fuels they displace[13]. To avoid these and other challenges posed by first generation biofuels, researchers are investigating "second generation" biofuels, including bioethanol from lignocellulosics (e.g., agricultural residues, wood processing wastes) and biodiesel derived from microalgae[12], which are expected to be more sustainable than first generation biofuels.

Although chemically distinct, biodiesel closely matches mineral diesel, or "petrodiesel", in performance. Biodiesel has the advantages that it releases less VOC, carbon monoxide, and particulate matter when

burned, does not contain carcinogens, and has a lower sulfur content than petrodiesel. It is also more biodegradable and has higher lubricity[14]. At the same time, biodiesel has lower calorific value, produces more NO_x emissions, and has poorer low temperature flow properties than conventional diesel. In addition, the oxidative stability of biodiesel limits its long-term storage. At present, biodiesel is typically blended with petrodiesel at a 20(biodiesel):80(petrodiesel) ratio and, with further technical development, this ratio is expected to increase[14].

1.1.3. Microalgal Biofuels

Several demonstration plants in which biodiesel is to be produced from microalgal lipids are now under construction or are in operation in the United States. Microalgae comprise a very diverse group of single-celled, photosynthetic, prokaryotic and eukaryotic organisms[15]. They are a primitive form of plant, and are suspected of being one of the oldest forms of life on Earth[12]. They are present in both aquatic and terrestrial ecosystems, and it is estimated that there are more than 50,000 species extant[16]. Some microalgae are capable of growing autotrophically, requiring only CO_2, inorganic salts, and light energy to grow. Others are mixotrophic, meaning they are also capable of heterotrophic growth, in which cells rely upon an external source of organic carbon as an energy source[12]. Microalgae have very fast growth rates, with biomass doubling times typically on the order of 24 hours; during the exponential growth phase, microalgae doubling times as short as 3.5 hours are common[17]. It is estimated that the biomass productivity of microalgae could be 50 times higher than that of switchgrass, which is among the fastest growing terrestrial plants[15]. Microalgae are also capable of accumulating large amounts of lipid; in some cases oil constitutes more than 80% of the dry cell weight, with 20-50% being more typical[17]. In contrast, oil crops such as soybean and palm usually contain less than 5% oil in the total biomass[10]. It is this combination of high growth rate and high lipid content that makes microalgae a promising candidate as a source of biodiesel.

Microalgae have been used as a source of human nutrition for thousands of years, but the intentional cultivation of microalgae has only been practiced since the middle of the twentieth century[18]. Initial development focused on the production of microalgae as a source of protein. Currently, the principal

products obtained from microalgae include ω-polyunsaturated fatty acids and carotenoids such as β-carotene and astaxanthin[18]. The principal markets these products are sold into include human nutrition, animal nutrition, animal feed (single cell protein), and cosmetics. As of 2006, the global market for microalgal biomass was around 5000 tonnes (dry basis) per year, with annual sales on the order of US$1.25 billion. Active microalgae cultures are also used in some municipal wastewater treatment systems as an integral part of the wastewater purification process. However, in almost all such cases, only minimal control over algae productivity and composition is imposed and the algal biomass is not harvested[19]. So although industrial-scale cultivation of microalgae is currently practiced around the world, the size of the industry is very small relative to that required if microalgae is to become a source of meaningful quantities of biofuel.

Microalgal biofuels are reported to have some significant advantages over fuels derived from terrestrial plants. Microalgae can be grown on non-arable land, so there is no direct competition for land upon which to grow food or fodder. Microalgae are capable of year-round growth and harvesting, which leads to substantially higher projected areal biomass productivity compared to oilseed crops[20]. Some investigators estimate that lipid productivity in microalgae will be as much as an order of magnitude higher than in conventional oilseed crops such as rape (canola) or soy[21,22]. Consequently, the amount of land area required to produce a given amount of biodiesel will be far less with microalgae than with a terrestrial oilseed plant. Microalgae cultivation reportedly consumes less water than production of many terrestrial oilseed crops, such as corn or rapeseed, although it exceeds that required by other terrestrial plants such as switchgrass[22]. Many types of microalgae can be cultivated in brackish water, seawater, or other degraded waters, such as municipal, agricultural or industrial wastewater. Microalgae cultivation is therefore expected to consume less fresh water than would be required to irrigate terrestrial oil plants. An additional benefit of using degraded waters is that they often contain essential nutrients, such as nitrogen and phosphorus, which are required by miroalgae and would otherwise have to be supplied as fertilizers[12]. Microalgae cultivation systems can be fed highly concentrated carbon dioxide streams, such as power plant flue gas (150,000 ppm CO_2, or higher), which can sustain very high growth rates. In contrast, terrestrial plants are for all practical purposes limited to extracting carbon dioxide from the

atmosphere (390 ppm CO_2)[15]. The ability to directly use wastewater and concentrated waste gases creates opportunities for coupling microalgal biofuel production with other vital utilities and/or industrial facilities, with potentially significant cost savings and environmental benefits.

A number of processes have been proposed for converting microalgal biomass into energy or energy carriers such as gaseous or liquid fuels; these are similar to processes based upon terrestrial biomass feedstocks. These processes can be generally categorized as thermochemical, biochemical, and direct conversion[12,23], as shown in Table 1.1. Within each category, the conversion process is shown on the left and the resulting energy carrier is shown on the right. For example, it has been proposed to burn microalgal biomass directly in electric power plants, either alone or in combination with other fuels such as coal[24]. It may also be possible to extract a crude bio-oil from microalgae that can be fed into conventional oil refineries to produce renewable diesel. ("Biodiesel" refers specifically to diesel produced by transesterifying animal and/or plant lipids; "renewable diesel" is produced from biomass using other thermal or chemical processes[25].)

Table 1.1: Microalgal Biomass Conversion Technologies	
A. **Thermochemical Processes**	
Gasification	Syngas
Liquefaction	Bio-oil
Pyrolysis	Bio-oil, Syngas, Bio-char
Direct Combustion	Electricity
B. **Biochemical Processes**	
Anaerobic Digestion	Biogas
Fermentation	Ethanol
Photobiological Hydrogen Production	Hydrogen
C. **Direct Conversion Processes**	
Oil Extraction and Transesterification	Biodiesel
Oil Extraction and Hydrogenation	Renewable Diesel

The microalga strain(s) to be grown as a biofuel feedstock and the preferred growth conditions will likely vary based upon the downstream conversion process. For example, a microalga strain and growth conditions that maximize starch production might be chosen if an alcoholic fermentation route will be used, whereas neutral lipid production should be maximized for a biodiesel route. Of the conversion

processes listed in Table 1.1, the microalgal biodiesel route appears to be among the most promising, since biodiesel production from vegetable oil is already an established and growing industry.

1.1.4. Microalgal Biodiesel Production Systems

The U.S. Department of Energy's Aquatic Species Program (ASP) is often cited as the first major effort to develop and evaluate microalgal biodiesel production systems[16,22,26,27,28,29,30]. The ASP was active at the National Renewable Energy Laboratory in Golden, Colorado, from 1978 until 1996. Its research objective was to minimize the cost of producing algal biodiesel by selecting naturally occurring algae strains with the most desirable properties for producing biodiesel, using advanced biotechnological techniques to enhance those properties, and optimizing and demonstrating the industrial processes required to produce mass quantities of algal biodiesel[31]. The program was terminated in 1996 as a result of budget cuts, but the closing report on the program[31] stated "…we fully expect to see renewed interest in algae as a source of fuels and other chemicals…," presumably when conditions become more favorable. The recent spike in petroleum prices to over $100/bbl appears to have created those conditions, and there has been a dramatic increase in research and development on algal biofuels in the last one to two decades, especially microalgal biodiesel. As with the ASP, these efforts are largely focused on two areas: microalgal biology (e.g., strain selection and characterization, metabolic analysis, cultivation conditions) and biofuel production process engineering (e.g., reactor design, process modeling, financial analysis, life-cycle assessment).

Commercial-scale cultivation of microalgae has typically been done in outdoor ponds, but one of the more active areas of research and development in the field of microalgal biofuels is the design of photobioreactors (PBR's) for algae cultivation. PBR's are engineered devices that typically isolate the microalgal cell culture from the environment ("closed system"), allowing greater control over contamination by unwanted organisms, heat and mass transfer, and cultivation conditions, than is achievable in "open" pond systems[15]. Despite these and other advantages over open growth systems, photobioreactors have thus far been shown to have dramatically higher capital costs[32] and consume far more energy than open pond systems producing the same amount of microalgae[33].

A commonly proposed process for producing microalgal biodiesel consists of four major steps: (1) cultivate microalgae under sunlight illumination in open ponds, potentially optimizing the growth conditions to favor lipid production; (2) harvest, dewater, and dry the microalgal biomass; (3) lyse the cells to gain access to the lipids (primarily triacylglycerides, or TAG) and extract them from the cell mass; and (4) chemically convert the acylglycerides to acyl esters and refine them into biodiesel fuel[28]. The first three of these steps (growth, harvesting, and lipid extraction) are currently used for the production of nutritional products from microalgae, albeit at substantially smaller scale than will be necessary to produce relevant quantities of microalgal biodiesel. The fourth step (conversion and refining) is already used commercially to produce biodiesel from oilseed crops, such as canola and soy. Since the composition of the triacylglycerides in microalgal oil is similar to that in vegetable oils such as soybean oil[34,35], it seems reasonable to expect there will be no technological barriers to combining these four process steps into a viable microalgal biodiesel production process. The overall feasibility of such a process will then be determined by such factors as the availability of suitable land and essential inputs, the cost to install and operate it, resource consumption per unit of biodiesel output, and carbon, water and energy footprints.

Despite having some important advantages over terrestrial oilseed crops, microalgae also suffer from some significant handicaps as an oil producer. When grown in open pond systems, the final microalgal cell concentration is typically only on the order of 0.2 - 1.0 grams per liter[11,26,36], so a substantial amount of energy must be expended to concentrate the biomass prior to extracting the lipid fraction. The large illuminated surface area of the ponds relative to the amount of biomass produced can lead to high rates of evaporation, especially in the arid regions that are commonly suggested for algae cultivation (due to their high insolation rates). Open systems are susceptible to contamination by wild-type microalgae, viruses that infect algae, and predators such as protozoa. Microalgal monocultures can be grown by maintaining extreme conditions in the reactor (e.g., high salinity, alkalinity, nutrient concentration, or temperature), such that the desired strain is highly favored over other competing organisms. However, such extremophilic microalgae may not have high growth rate or lipid content, and over long periods,

invading bacteria and other biological contaminants can still take hold[12]. It has been shown that many microalgal strains increase lipid production under conditions such as nitrogen deprivation, but at the expense of a lower growth rate[11], so overall lipid productivity (mass of extractable lipid per unit volume per unit time) remains constrained. In addition to requiring large tracts of flat land, microalgal biodiesel production using the four-step scheme outlined above consumes large amounts of resources, including water, carbon dioxide, fertilizers, and electrical and heat energy. The number of locations in which all of these essential resources are readily accessible is limited. Alternatively, transporting these resources to a production site will involve additional energy consumption, cost, and adverse environmental impacts, offsetting some or potentially all of the benefits garnered by displacing fossil fuel. Finally, microalgal oil production has yet to be demonstrated at a commercial scale, so it is not yet possible to benchmark the technical, financial and environmental performance of large-scale microalgal biodiesel production schemes against other fuel production systems.

1.1.5. Prior Microalgal Biodiesel Production Modeling Efforts

In recent years, many researchers have reported on their efforts to model potential microalgal fuel production systems. All of these analyses include an assumed process model – a set of linked unit operations whose performance can be modeled mathematically. The energy product can vary; in some cases it is microalgal biomass, in others it is a crude oil extract, and in yet other cases it is biogas or a refined diesel fuel. The models typically focus on the cost to produce the microalgal fuel, the energy balance of the production process, or the environmental impacts of the production process and the biofuel in the form of a life-cycle assessment (LCA). None of the studies reviewed for this project address all three critical performance aspects of a potential microalgal biodiesel production scheme: net energy balance, financial performance, and environmental impacts.

Some of the more important original studies of potential microalgal biofuel production systems are listed in Table 1.2.

Table 1.2: Prior Original Publications on Microalgal Biofuel Production Systems			
Author(s)	**Date**	**Analysis Type**	**Fuel Produced**
Oswald and Golueke[37]	1960	Techno-economic	Biogas
Benemann et al.[38]	1982	Techno-economic	Microalgal Oil
Benemann et al.[19]	1996	Techno-economic	Microalgal Oil
Kadam[24]	2001	Life-Cycle Analysis	Microalgal Biomass
Huntley and Redalje[26]	2007	Techno-economic	Microalgal Oil
Alabi et al.[39]	2009	Techno-economic	Microalgal Oil
Lardon et al.[11]	2009	Life-Cycle Analysis	Biodiesel
Batan et al.[40]	2010	Life-Cycle Analysis	Biodiesel
Clarens et al.[41]	2010	Life-Cycle Analysis	Microalgal Biomass
Lundquist et al.[32]	2010	Techno-economic	Microalgal Oil
Pokoo-Aikens et al.[42]	2010	Techno-economic	Biodiesel
Stephenson et al.[33]	2010	Life-Cycle Analysis	Biodiesel
Cooney et al.[43]	2011	Net Energy Balance	Microalgal Oil
Frank et al.[44]	2011	Life-Cycle Assessment	Biodiesel
Murphy and Allen[45]	2011	Net Energy Return	Biodiesel
Razon and Tan[46]	2011	Net Energy Balance	Biogas and Biodiesel

Several of the studies listed in Table 1.2 are particularly noteworthy. The first detailed techno-economic analysis of the potential of producing biofuel from microalgae was published by Oswald and Golueke in 1960[37]. The process proposed by these authors consisted of algae cultivation in open ponds, biomass flocculation and dewatering, anaerobic digestion of whole algal cells to produce biogas, and biogas combustion in an electric power plant. Even in this early study the authors recognized the synergies of using wastewater as a source of nutrients and make-up water, and flue gas from the biogas-fueled power plant as a source of carbon dioxide for the cultivation ponds. The 2010 report by Lundquist et al.[32] is particularly detailed, and was an important source of process and financial data for the modeling efforts described in this dissertation.

In addition to these primary works, there have been a number of recent review articles that survey the field of microalgal biofuels, some of which are listed in Table 1.3. Most of these review articles focus on the current state of microalgal biofuel science and technology, with little information on the relative financial and environmental performance of different microalgal biofuel production schemes. This may be due to the fact that there are no commercial-scale microalgal biofuel production facilities in operation to provide reliable cost and emissions data.

Table 1.3: Prior Review Articles on Microalgal Biofuel Production Systems			
Author(s)	**Date**	**Review Type**	**Microalgal Biofuel(s)**
Spolaore et al.[18]	2006	Technical	Biomass
Dismukes et al.[22]	2008	Technical	Biomass
Li et al.[15]	2008	Technical	Various
Schenck et al.[20]	2008	Technical	Biodiesel
Brennan and Owende[12]	2010	Technical	Various
Harun et al.[47]	2010	Technical	Various
Kumar et al.[48]	2010	Technical and LCA	Biomass
Mata et al.[16]	2010	Technical	Biodiesel
Scott et al.[21]	2010	Technical	Biomass
Singh and Gu[49]	2010	Technical	Biodiesel, Bioethanol and Biogas
Wijffels and Barbosa[50]	2010	Technical	Biomass

A characteristic of prior microalgal biofuel modeling efforts is that they model only one or a very small number of specific scenarios, and provide results based on a narrowly defined set of input parameters. As a result it is usually difficult or even impossible to determine how alternative production processes or different input parameters would impact the results except in the most general terms. And although there have been many such studies, the range of process options, input parameter choices (e.g., microalgae productivity and lipid content, CO_2 concentration in the source gas, nitrogen and phosphorus fertilizers), system boundaries, and fuel type produced is so large that rarely are two studies similar enough to allow detailed comparison. This is especially so for life-cycle assessments, which are usually very site-specific and involve considerable judgment when "assessing" the environmental impacts of a biofuel production scenario. In a 2006 review of published LCA's on liquid transportation biofuels, Eric Larson found wide ranges in the predicted environmental impacts for the same biofuel produced from the same raw material, sometimes reported by the same author[51]. For example, a different basis for allocating greenhouse gas emissions and energy burdens to co-products of biofuel manufacture (such as lipid-extracted algae to be used as animal feed) can make an otherwise unfavorable process look favorable relative to its fossil fuel equivalent, and vice-versa. Decisions about the fate of soil carbon associated with land-use changes can also have a dramatic effect on the apparent performance of a given biofuel and its manufacturing process.

Wide ranges in the critical performance metrics of microalgal oil production schemes, such as manufacturing cost and energy balance, have been reported in the literature. For example, Lardon et al. found that the energy balance of microalgal biodiesel production ranged from 0.74 to 1.95, depending upon whether a wet or dry extraction process was used, and whether the microalgae was grown under high or low nitrogen conditions[11]. (As used here, "energy balance" is the ratio of the energy required to produce a quantity of fuel to the energy content of that fuel. Energy balance is the reciprocal of Net Energy Return (NER). A favorable microalgal biodiesel production scheme is one whose energy balance is less than one, or whose NER is greater than one.)

Table 1.4 lists the Net Energy Return and unit manufacturing cost of microalgal oil predicted by several researchers from their modeling efforts. Differences in input data and system boundaries are among the main reasons for the wide ranges in NER and cost values.

Table 1.4: Reported Values for Net Energy Return and Production Cost of Microalgal Oil

Author(s)	Date	NER	Production Cost ($/gallon)
Lardon et al.[11]	2009	0.51 – 1.35	---
Clarens et al.[41]	2010	1.06 – 13.2	---
Cooney et al.[43]	2011	1.5	---
Murphy and Allen[45]	2011	<0.14*	---
Razon and Tan[46]	2011	0.09 – 0.54	---
Schenck et al.[20]	2008	---	$3.00 - $4.98
Chisti[17]	2007	---	$10.60
Li et al.[15]	2007	---	$9.09
Lundquist et al.[32]	2010	---	$0.67 - $7.91

(: This value is reported on the basis of microalgal biodiesel rather than microalgal oil.)*

It is clear from the number of researchers listed in Tables 1.2 through 1.4 that a considerable amount of work is being done to model the performance of potential microalgal biofuel production schemes. But these studies are yielding widely divergent results, leaving it unclear whether microalgal biofuels are sustainable alternatives to conventional fossil fuels. Some of the large variation in the reported values of key performance metrics, such as unit cost and NER, is due to the differences in assumptions and input parameter selections made by researchers. This state of the science and technology of microalgal

biofuels creates a substantial need for a detailed yet flexible model with which an investigator can systematically vary those assumptions and parameter choices, so that the main drivers of system performance can be identified and the sensitivities of key performance metrics to specific inputs can be determined.

1.2. DESCRIPTION OF THE RESEARCH

1.2.1. Motivation for the Research

There is an urgent and growing need for alternatives to fossil fuels, including alternatives to petroleum-based liquid transportation fuels. The scale of investment required to produce meaningful quantities of alternative fuels is enormous, so it is essential that scarce human and financial resources are focused on alternatives that promise the best performance at the lowest cost and least adverse environmental impact. Even within the scope of a single alternative fuel such as microalgal biodiesel, there is a wide array of possible manufacturing schemes, raw materials, production locations, scale of operations, etc. As yet there is no consensus in the scientific, engineering and financial communities about whether microalgal biodiesel is worthy of large-scale investment.

Modeling is an efficient way to screen proposed microalgal biodiesel production schemes for those that offer the best balance of technical, financial and environmental performance, and to quantify the trade-offs among these performance metrics. For a particular processing scheme, modeling can help identify any significant barriers to technical, financial or environmental viability, so that development efforts can be committed to overcoming them. A reliable model can be used to evaluate claims made for alternative technologies quickly and at minimal cost. And it can help ensure that analyses of different systems are put on common bases, so that their predictions can be fairly compared, and some level of harmonization of the widely divergent results being reported in the literature can be achieved. As yet no such modeling tool is publicly available.

1.2.2. Research Objectives

The goal of this research is to create a techno-economic life-cycle inventory model of microalgal biodiesel production, so that the overall technical, financial and environmental viability of alternative manufacturing schemes can be objectively and accurately assessed. The model is to be sufficiently comprehensive that it includes all of the major processing steps required to produce microalgal biodiesel, rather than an intermediate to that product (such as whole biomass or microalgal oil), or some other energy carrier (such as biogas or electricity). It should account for all of the significant raw material and energy demands of a proposed production process, encompassing activities within the battery limits of the microalgal biodiesel production facility as well as all relevant upstream activities, such as raw material production and transportation. With this level of detail, the model should generate estimates of an intermediate level of accuracy for performance metrics such as: unit manufacturing cost ($/gal), capital cost productivity ($/gal-yr), Net Energy Return (MJ/MJ), volumetric productivity (gal/acre-yr), carbon intensity (gCO2/MJ), and water intensity (gal/gal).

The model should have an open architecture, so that it can be easily adapted to simulate alternative processing schemes, operating conditions, raw materials, microalgae strains, etc. It should be completely transparent, so that all of the embedded assumptions and calculations are visible to the user. It should be readily usable and adaptable by technical professionals who may lack advanced computer programming skills. And it should be constructed on a platform that is widely available and with which most technical professionals are familiar. Once complete, the model should be uploaded to a public space, from which it can be freely downloaded and used.

Once the model is constructed, it should be populated with default values that create a representative scenario for microalgal biodiesel manufacture. The individual contributions to the energy return, cost, and environmental impacts from the various inputs and processing steps should be analyzed, facilitating identification of potential barriers to large scale implementation. Sensitivity analyses should be performed to identify input parameters with the most influence on the key performance indicators. Case studies involving alternative processes, biological properties, and geographic locations should be run to assess

their impact on the viability of microalgal biodiesel production. Finally, the effect of seasonal and diurnal variations on the performance metrics should be investigated by using climate data averaged over different time scales. Inherent in this analysis should be an evaluation of alternative design bases and operating strategies and an assessment of the effect of light saturation on biomass productivity.

1.2.3. The Integrated Techno-Economic Life Cycle Inventory Model (TELCIM)

The microalgal biodiesel manufacturing model created to achieve these research objectives is called "TELCIM", an acronym for "Techno-Economic Life-Cycle Inventory Model". It is implemented in Microsoft Excel®, which is an ideal platform for financial and environmental accounting calculations, and can readily accommodate straightforward engineering calculations. TELCIM is a "Life-Cycle Inventory" (LCI) model rather than a "Life Cycle Assessment" (LCA) tool, because it tabulates resource consumptions and environmental emissions resulting from direct and indirect manufacturing activities without explicitly identifying byproduct fates or assessing the resulting environmental impacts. A schematic of TELCIM's computational structure is shown as Figure 1.1.

At TELCIM's core are its process models, which primarily consist of material and energy balances and equations that predict how individual unit operations perform. Using inputs such as chemical compositions, physical properties, operating conditions, and physical dimensions, the process models predict material and energy flows within the battery limits of the manufacturing plant. TELCIM's economic models estimate the biodiesel's production cost from the consumption rates predicted by the process models and inputs such as raw material and energy prices, and labor and maintenance costs. The economic models also estimate the installed capital cost of the biodiesel manufacturing plant by scaling capital cost structures for basis plants supplied as input. TELCIM's LCI models generate estimates of pollutant emissions and resource consumptions resulting from the production of raw materials and energy, transportation activities, and capital items such as equipment fabrication and construction. The LCI models combine the "indirect" carbon dioxide emissions and energy and water usages with the "direct" emissions and usages predicted by the process models to generate a "cradle-to-gate" inventory

for the microalgal biodiesel manufacturing plant being modeled. More detailed descriptions of TELCIM's component models are provided in Chapter 2.

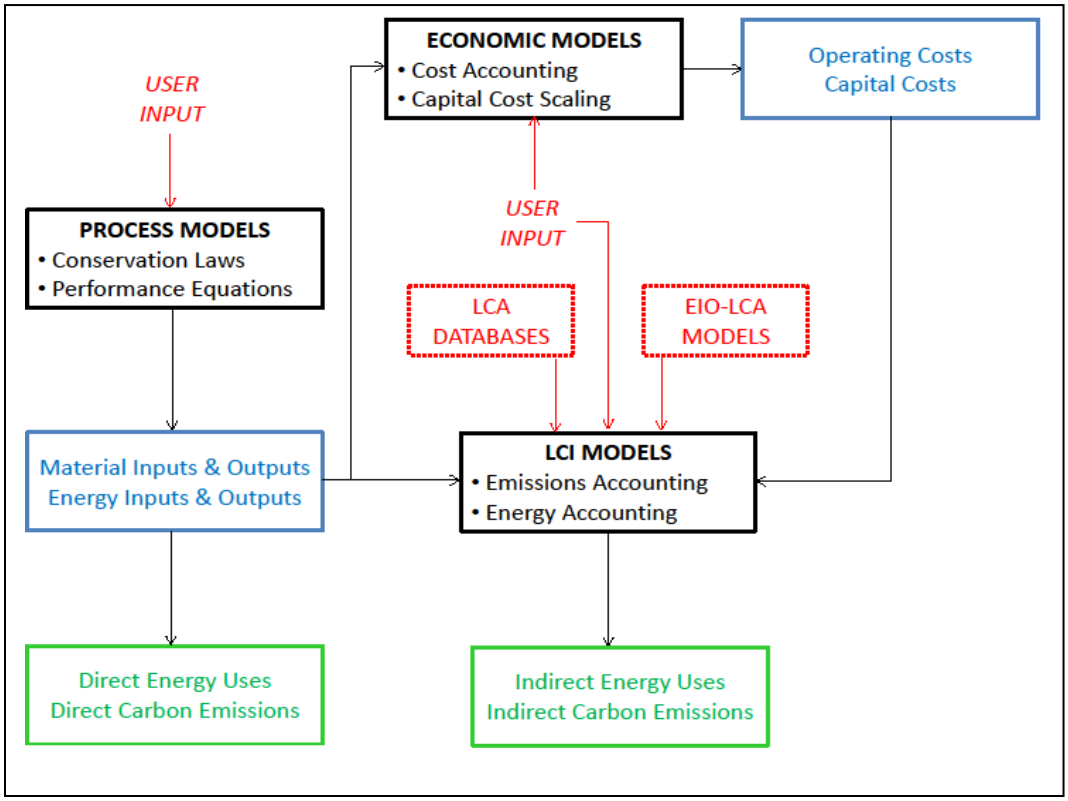

Figure 1.1: Computational Flowchart of TELCIM. The LCA databases and EIO-LCA models shown in dashed boxes are not part of TELCIM; users can access these tools for life cycle inventory data. The sum of the direct and indirect energy uses is used to determine the Net Energy Return of the biodiesel, and the sum of the direct and indirect carbon emissions is used to calculate its carbon intensity.

1.2.4. Methods and Procedures

All of the physical, financial and LCI models comprising TELCIM are contained within a single Excel workbook. The modular structure of Excel is exploited by housing the engineering model for each major process step in a separate spreadsheet within this workbook. There is also one financial model and one LCI model for each major process step, each of which is located in a separate spreadsheet. This arrangement helps compartmentalize the calculations, and limits the number of data exchanges between

models. It also makes it easier to track the flow of information and simplifies making the changes necessary to model different process schemes.

Within each individual spreadsheet, calculations are laid out in a columnar structure, moving from top to bottom. Generally, input data entry cells necessary for a calculation are located immediately above the cells in which those calculations are performed. This layout makes it easier for a user to see exactly what values are being used in each calculation, and to replace or reconfigure particular sub-models.

Excel's open architecture allows a substantial amount of supporting information to be entered directly into the working spreadsheets, but without complicating or cluttering the work space. User notes are embedded directly in the calculation stream and function like comment lines. Literature references are entered in cells alongside input data entry cells, specifying the source of the value used for each parameter. Drop-in comment boxes are used for the same purpose when data is entered into cells located in tables. Original equations are similarly situated alongside cells in which calculations are made; this helps overcome the difficulty in understanding formulas in Excel, which are constructed of cell locations rather than variable names or symbols a user might recognize. For the same reason detailed dimensional analyses are located alongside most of the more complicated calculations. Some of the more complex and lengthy derivations of formulas used in the program's working space are shown in separate spreadsheets. Finally, a User Manual containing detailed instructions on how to use TELCIM in its current configuration and modify it to simulate other process schemes has been written and will be posted on-line alongside the model.

TELCIM's process models are constructed of mathematical expressions, or systems of expressions, that describe the performance of individual unit operations. All of the physical, financial and LCI models have been reduced to sets of expressions that can be solved simultaneously, given all of the required input data. The mass and energy balance equations used in the physical models were derived directly from conservation laws (see the Appendix), while the performance equations for some unit operations were obtained from outside references. In some cases, the physical models used in TELCIM were adopted or

adapted from those used by other biodiesel production modelers. All of the input data are parameters that a user with a reasonable understanding of biology and process engineering should know how to determine or estimate, based on the process scheme and conditions being simulated.

The financial models with which plant operating and capital costs are estimated rely on basic cost accounting principles. They require detailed cost structures as inputs; for the most part TELCIM merely scales capital and operating costs based on biodiesel throughput. Cost structures for the major process steps being simulated were obtained from the open literature; they were not constructed from bottom-up estimates.

The system boundary chosen for TELCIM's LCI models encompasses the biodiesel manufacturing process and all upstream processes that produce and deliver raw materials and energy to the biodiesel plant. This makes TELCIM a "cradle-to-gate" inventory model, however the cradle-to-gate system boundary is violated in one important aspect – the carbon intensity of the biodiesel reported by TELCIM includes the carbon dioxide released when the fuel is combusted, which presumably occurs downstream of the manufacturing process. This is done because TELCIM accounts for the carbon dioxide that is converted into biomass in the ponds as a credit, or negative carbon emission, when calculating the fuel's carbon intensity. (Typically, when computing the carbon intensity of a biofuel, the carbon dioxide from which it is made is ignored, since that carbon is assumed to be released in its entirety as carbon dioxide when the fuel is burned, which is also ignored). TELCIM includes the carbon dioxide taken up during biomass production because it is a more accurate model of the carbon cycles occurring in the manufacturing process, and accounting for the carbon emissions resulting from fuel use puts TELCIM's carbon intensity predictions on the same basis as that used for other fuels, including petrodiesel.

TELCIM generally uses one gallon of biodiesel as the functional unit for the LCI. However, some of TELCIM's outputs such as Net Energy Return and carbon intensity are expressed in terms of the biodiesel product's energy content. These metrics are related to the functional unit by the biodiesel's energy density, which is assumed to be constant and whose numerical value is specified by the user.

The data used to populate the model were all obtained from public sources consisting primarily of articles from the scientific literature, reports published by or on behalf of U.S. government agencies, and U.S. government databases. There was no one source for all of the data needed to populate TELCIM; many independent sources were used. Reasonable care was exercised as input parameter values were chosen to ensure that data was internally consistent, and that in the aggregate, the parameter values used comprise a coherent data set.

1.2.5. Intellectual Merit

TELCIM is the first publicly available, integrated techno-economic life cycle inventory model of microalgal biodiesel manufacture. The integration of process, financial and life cycle models makes it possible for an investigator to rapidly and thoroughly evaluate proposed manufacturing scenarios from a range of perspectives, identify possible barriers to viability, and screen the effectiveness of proposed process improvements. For the first time an investigator can explore potential synergies and trade-offs between important technical, financial and environmental performance characteristics. By implementing it in Excel, providing extensive user instructions and background information, and posting it on a public website as freeware, TELCIM is accessible to a very wide range of technical professionals. It is conceivable that TELCIM may be useful as a template for integrated techno-economic-life-cycle models of other products and processes.

1.3. Structure of Dissertation

Chapter 2 is a detailed description of the component physical, financial and LCI models that make up TELCIM. Examples of the mathematical relationships that comprise the engineering models are included in Chapter 2; the derivation of these and others of the relationships used by the models are included in the Appendix. Much of the text in Chapter 2 is taken from a manuscript that is being prepared for publication.

Chapter 3 describes the data with which TELCIM was originally populated, and the case study this data collectively simulates, which is called the “Test Scenario”. Key outputs from the Test Scenario are presented and discussed, and several sensitivity analyses on these outputs are presented. Some of the text included in Chapter 3 is taken from the same manuscript mentioned in the previous paragraph.

Chapter 4 reviews a number of alternative cases that explore the effect on key biodiesel performance metrics of changes in the biological properties of the microalga, and the processes used to convert it into biodiesel. The effect of seasonal and diurnal variations in sunlight intensity and climate conditions are studied, and the impact of the sunlight saturation effect on biomass productivity is explored. Finally, the effect on the manufacturing process of the climate experienced in different locations in the continental United States is evaluated.

Chapter 5 is a summary of other topics and results generated during the development and deployment of TELCIM.

Conclusions and recommendations arising from this research are presented in Chapter 6.

Detailed derivations of the mathematical relationships underlying the physical models used by TELCIM are presented in the Appendix. Most of the material presented in the Appendix was taken from the Supplemental Information section that accompanies the manuscript from which parts of Chapters 2 and 3 are taken.

Literature references are presented at the end of each individual chapter and the Appendix.

Professors Jay R. Turner and Richard L. Axelbaum are identified as co-authors on the two manuscripts from which sections of this dissertation are taken. Professor Turner served as lead advisor for this research, and Professor Axelbaum served as co-advisor. They contributed to the overall intellectual merit

of the project consistent with their roles as research advisors including editing the manuscripts. They did not perform any programming of the TELCIM.

1.4. References for Chapter 1

[1] Anon., Report # DOE/EIA-0484(2010).

[2] Energy Information Administration 2011: Alternative Transportation Fuels and Alternative Fueled Vehicles, 2009. OMB Control No. 3090-0284. http://www.eia.gove/cneaf/alternate/page/atftables/afv_hist_data.html.

[3] Anon., IEA. World Energy Outlook 2009. Paris, France.

[4] IPCC. Climate Change 2007: Synthesis Report. Contribution of Working Groups I, II and III to the Fourth Assessment Report of the Intergovernmental Panel on Climate Change (Core Writing Team, Pachauri, R. K. and Reisinger, A. (eds.)). IPCC, Geneva, Switzerland.

[5] Anon., BP Statistical Review of World Energy June 2011.

[6] Anon., BP Statistical Review of World Energy June 2007.

[7] Anon., U.S. Energy Information Administration, "Weekly All Countries Spot Price FOB Weighted by Estimated Export Volume", August 10, 2011.

[8] Anon., U.S. Energy Information Administration, "This Week in Petroleum", August 10, 2011.

[9] Anon., REN21. Renewables 2011 Global Status Report, v1.1, July 2011. Paris, France.

[10] Chisti, Y. Biodiesel from microalgae beats bioethanol. Trends Biotech. 26 (2007) 126-131.

[11] Lardon, L., Helias, A., Sialve, B., Steyer, J.P, and Bernard, O. Life-Cycle Assessment of Biodiesel Production from Microalgae. Env. Sci. Tech. 43 (2009) 6475-6481.

[12] Brennan, L. and Owende, P. Biofuels from microalgae – A review of technologies for production, processing, and extractions of biofuels and co-products. Renewable and Sustainable Energy Reviews 14 (2010) 557-577.

[13] Crutzen, P.J., Mosier, A. R., Smith, K.A., and Winiwarter, W. N_2O release from agro-biofuel production negates global warming reduction by replacing fossil fuels. Atmos. Chem. Phys. 8 (2008) 389-395.

[14] Sharma, Y.C. and Singh, B. Development of biodiesel: Current scenario. Renewable and Sustainable Energy Reviews 13 (2009) 1646-1651.

[15] Li, Y., Horsman, M., Wu, N., Lan, C., and Dubois-Calero, N. Biofuels from Microalgae. Biotechnol. Prog. 24 (2008) 815-820.

[16] Mata, T.M., Martins, A.A., and Caetano, N.S. Microalgae for biodiesel production and other applications: a review. Renewable and Sustainable Energy Reviews 14 (2010) 217-232.

[17] Chisti, Y. Biodiesel from Microalgae. Biotech. Adv 25 (2007) 294-306.

[18] Spolaore, P., Joannis-Cassan, C., Duran, E., and Isambert, A. Commercial Applications of Microalgae. J. Biosci. Bioeng. 101 (2006) 87-96.

[19] Benemann, J.R., and Oswald, W.J. Systems and Economic Analysis of Microalgae Ponds for Conversion of CO_2 to Biomass – Final Report. Department of Energy, Pittsburgh, PA, 1996, 201 pp.

[20] Schenck, P., Thomas-Hall, S., Stephens, E., Marx, U.C., Mussgnug, J.H., Posten, C., Kruse, O., and Hankamer, B. Second Generation Biofuels: High-Efficiency Microalgae for Biodiesel Production. Bioenerg. Res. 1 (2008) 20-43.

[21] Scott, S.A., Davey, M.P., Dennis, J.S., Horst, I., Howe, C.J., Lea-Smith, D.J. and Smith, A.G. Biodiesel from algae: challenges and prospects. Current Opinion in Biotechnology 21 (2010) 277-286.

[22] Dismukes, G.C., Carrieri, D., Bennette, N., Ananyev, G.M., Posewitz, M.C. Aquatic autotrophs: efficient alternatives to land-based crops for biofuels. Current opinion in Biotechnology 19 (2008) 235-240.

[23] U.S. DOE 2010. National Algal Biofuels Technology Roadmap. U.S. Department of Energy, Office of Energy Efficiency and Renewable Energy, Biomass Program.
[24] Kadam, K.L. Microalgae Production from Power Plant Flue Gas: Environmental Implications on a Life Cycle Basis. NREL/TP-510-29417, June 2001.
[25] Oregon Department of Environmental Quality (2011), Oregon Low Carbon Fuel Standards – Final Report, Appendix K: Review of Biodiesel and Renewable Diesel Use Considerations. Recovered from http://www.deq.state.or.us/aq/committees/docs/lcfs/appendixK.pdf
[26] Huntley, M.E. and Redalje, D.G. CO_2 mitigation and renewable oil from photosynthetic microbes: a new appraisal. Mitigation and Adaptation Strategies for Global Change 12 (2007) 573-608.
[27] Weyer, K.M., Bush, D.R., Darzins, A., and Wilson, B. D. Theoretical Maximum Algal Oil Production. Bioenerg. Res. 3 (2010) 204-213.
[28] Robertson, D.E., Jacobson, S.A., Morgan, F., Berry, D., Church, G.M., and Afeyan, N.B. A new dawn for industrial photosynthesis. Photosynth. Res. 107 (2011) 269-277.
[29] Wijffels, R.H. and Barbosa, M.J. An Outlook on Microalgal Biofuels. Science (2010) 329:796-799.
[30] Pfromm, P.H., Amanar-Boadu, V. and Nelson, R. Sustainability of algae derived biodiesel: A mass balance approach. Bioresource Technology 102 (2011) 1185-1193.
[31] Sheehan, J., Dunahay, T., Benemann, J., and Roessler, P. A look back at the U.S. Department of Energy's aquatic species program: biodiesel from algae. NREL/TP-580-24190. National Renewable Energy Laboratory. 1998. USA.
[32] Lundquist, T.J., Woertz, I.C., Quinn, N.W.T., and Benemann, J.R. A Realistic Technology and Engineering Assessment of Algae Biofuel Production. Energy Biosciences Institute, University of California. October 2010. Berkeley, California.
[33] Stephenson, A.L., Kazamia, E., Dennis, J.S, Howe, C.J., Scott, S.A., and Smith, A.J. Life-Cycle Assessment of Potential Algal Biodiesel Production in the United Kingdom: A Comparison of Raceways and Air-Lift Tubular Bioreactors. Energy Fuels 24 (2010) 4062-4077.
[34] Kubatova, A., Luo, Y., Stavova, J., Sadramele, S.M., Aulich, T., Kozliak, E., and Seames, W. New path in the thermal cracking of triacylglycerols (canola and soybean oil). Fuel 90 (2011) 2598-2608.
[35] Dunstan, G.A., Volkman, J.K., Jeffrey, S.W., and Barrett, S.M. Biochemical composition of microalgae from the green algal classes Chlorophyceae and Prasinophyceae. 2. Lipid classes and fatty acids. J. Exp. Mar. Biol. Ecol. 161 (1992) 115-134.
[36] Uduman, N., Qi, Y., Danquah, M.K., Forde, G.M., and Hoadley, A. Dewatering of microalgal cultures: A major bottleneck to algae-based fuels. J. Renewable Sustainable Energy 2 (2010) 012701.
[37] Oswald, W.J. and Golueke, C.G., Biological Transformation of Solar Energy. Advances in Applied Microbiology 2 (1960) 223-262.
[38] Benemann, J.R., Goebel, R.P., Weissman, J.C., and Augenstein, D.C. Microalgae as a Source of Liquid Fuels. Final Technical Report. 1982. DOE/ER/30014—T1.
[39] Alabi, A.O., Tampier, M. and Bibeau, E. Microalgae Technologies & Processes for Biofuels/Bioenergy Production in British Columbia: Current Technology, Suitability & Barriers to Implementation. Final report submitted to the British Columbia Innovation Council, January 14, 2009.
[40] Batan, L., Quinn, J., Wilson, B. and Bradley, T. Net Energy and Greenhouse Gas Emission Evaluation of Biodiesel Derived from Microalgae. Environ. Sci Technol. 44 (2010) 7975-7980.
[41] Clarens, A.F., Resurreccion, E.P., White, M.A., and Colosi, L.M. Environmental Life Cycle Comparison of Algae to Other Bioenergy Feedstocks. Environ. Sci. Tech 44 (2010) 1813-1819. (From Supporting Information, available at http://pubs.acs.org.)
[42] Pokoo-Aikins, G., Nadim, A., El-Halwagi, M. and Mahalec, V. Design and analysis of biodiesel production from algae grown through carbon sequestration. Clean Techn. Environ. Policy 12 (2010) 239-254.
[43] Cooney, M.J., Young, G., and Pate, R. Bio-oil from photosynthetic microalgae: Case study. Bioresource Technology 102 (2011) 166-177.

[44] Frank, E.D., J. Han, I. Palou-Rivera, A. Elgowainy and M.Q. Wang. Life Cycle Analysis of Algal Lipid Fuels with the GREET Model. Argonne National Laboratory, Energy Systems Division, ANL/ESD/11-5, August 2011.
[45] Murphy, C.F. and D.T. Allen. Energy-water nexus for mass cultivation of algae. Environ. Sci. Technol. 45 (2011) 5861-5868.
[46] Razon, L.F. and Tan, R.R. Net energy analysis of the production of biodiesel and biogas from the microalgae: *Haematococcu pluvialis* and *Nannochloropsis*. Applied Energy 88 (2011) 3507-3514.
[47] Harun, R., Singh, M., Forde, G.M., and Danquah, M.K. Bioprocess engineering of microalgae to produce a variety of consumer products. Renewable and Sustainable Energy Reviews 14 (2010) 1037-1047.
[48] Kumar, A., Ergas, S., Yuan, X., Sahu, A., Zhang, Q., Dewulf, J., Malcata, F.X., and van Langenhove, H. Enhanced CO_2 fixation and biofuel production via microalgae: recent developments and future directions. Trends in Biotechnology 28 (2010) 371-380.
[49] Singh, J. and Gu, S. Commercialization potential of microalgae for biofuels production. Renewable and Sustainable Energy Reviews 14 (2010) 2596-2610.
[50] Wijffels, R.H. and Barbosa, M.J. An Outlook on Microalgal Biofuels. Science 329 (2010) 796-799.
[51] Larson, E.D. A review of life-cycle analysis on liquid biofuel systems for the transport sector. Energy for Sustainable Development. X 2 (2006) 109-126.

2. TELCIM*

2.1 Introduction

TELCIM consists of a set of interlinked engineering, financial, and life cycle inventory models, as illustrated in Figure 1.1. The purpose of this chapter is to explain how these models function, and to describe the types of outputs TELCIM is capable of generating.

2.2. The Process Models

A commonly proposed microalgal biodiesel production scheme consists of four major process steps: microalgae cultivation, biomass harvesting, lipid extraction, and lipid conversion to fatty acid esters[1,2,3,4]. TELCIM simulates this scheme and adds a fifth major step - anaerobic digestion of the residual (non-lipid) biomass for the purpose of energy and nutrient recovery[5,6]. A simplified flowsheet of the manufacturing process modeled by TELCIM is shown as Figure 2.1. For clarity, the only energy stream shown in this flowsheet is that which is recovered from the biogas produced in the anaerobic digestion step, but it should be noted that energy is consumed in every major process step.

Within the context of this five-step manufacturing process, TELCIM retains modeling flexibility by treating some unit operations as generic processes. For example, the harvesting step includes "dewatering" operations that can represent sedimentation, filtration, centrifugation, etc. In other cases TELCIM models more than one type of unit operation for a given processing step, and the user selects which alternative's output is to be used in subsequent calculations. For example, the harvesting step simulates contact and non-contact biomass drying, as well as no drying. For some processing steps, due to factors such as process complexity (e.g., transesterification) or a lack of sufficient engineering design and cost data for novel alternatives (e.g., wet extraction), TELCIM models only one specific type of unit operation. A prime example is the type of reactor in which microalgae are grown; only cultivation in raceway ponds is simulated. A user wishing to evaluate an alternative to raceway ponds, such as photobioreactors, can

* *Some of the text and figures included in this chapter were taken from a manuscript that is being prepared for publication.*

replace the raceway pond models with suitable alternatives. Or the alternative models can be installed alongside the default models, allowing direct comparison of their respective impacts on the key performance indicators (KPI's) of interest. In any event, TELCIM's modular structure facilitates modifying, replacing, or deleting operations, or rearranging the entire process scheme.

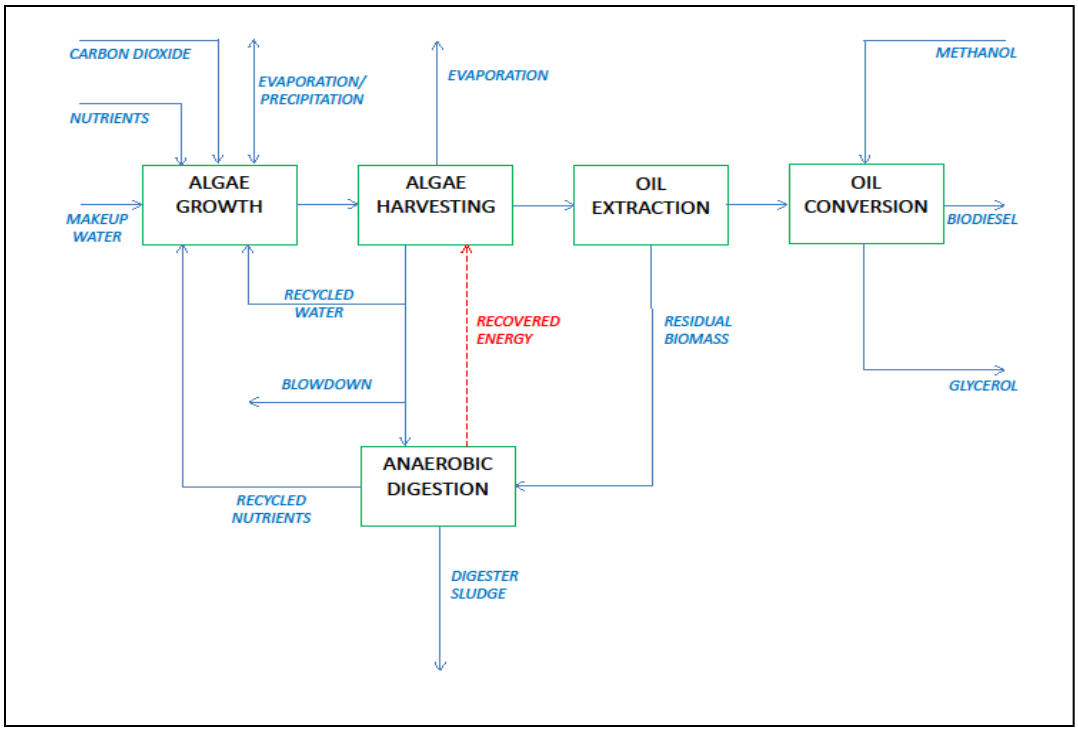

Figure 2.1: Simplified Flowchart of the Microalgal Biodiesel Manufacturing Process modeled by TELCIM. The energy recovered from the digester biogas is shown feeding the algae harvesting step, but it can be used elsewhere within the plant or exported.

TELCIM is intended to simulate biodiesel plants with production capacities on the order of hundreds of thousands of gallons per day. At that scale, the physical layout of the facility is critical, since large amounts of energy are consumed moving materials within the plant. Several assumptions about the facility layout are built into TELCIM. To minimize gas-pumping distances, the source of carbon dioxide is situated at the center of the plant (Figure 2.2). Ponds, harvesting equipment and digesters are clustered together in biomass production "modules", minimizing water-pumping distances. Dewatered biomass is transported by truck from the production modules to a centralized lipid extraction plant. The residual biomass is backhauled to the modules, where it is slurried in water and fed to anaerobic digesters. The

extracted lipid is transformed into biodiesel in a centralized conversion plant located alongside the extraction plant.

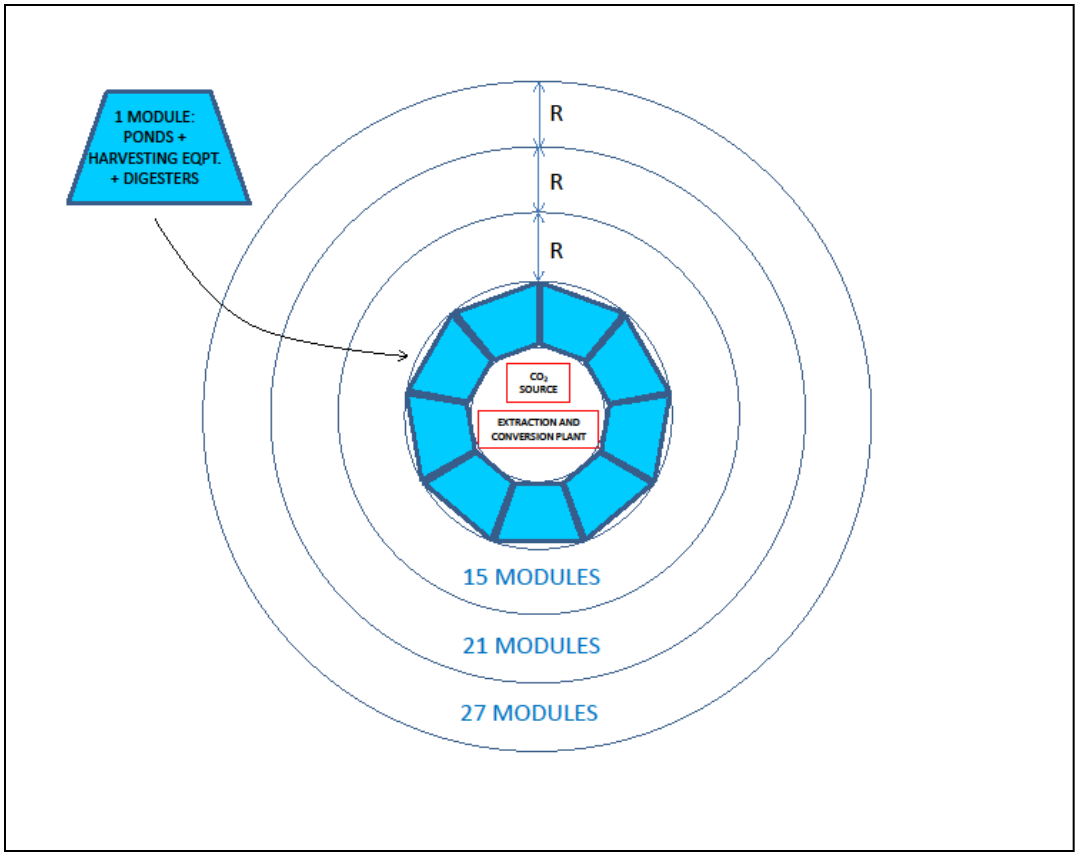

Figure 2.2: Pumping Distance Model. The conceptual layout of the biodiesel manufacturing facility and how TELCIM estimates the distances that CO_2-containing gas must be pumped. The inset shows one "biomass production module," consisting of ponds, harvesting equipment and digesters. TELCIM calculates the number of modules needed, and assigns them to annular rings from the innermost ring outward until all modules are assigned. The pumping distance to a particular module is taken as the outer radius of the ring in which it is located. The first annular ring holds nine biomass production modules, the second 15, and so on.

2.2.1. The Growth Step Process Model

The main function of the Growth Step Process Model is to predict the quantities of chemical fertilizers and water that must be supplied, the illuminated surface area required, and the electricity used, when a given quantity of carbon dioxide is converted into microalgal biomass. Critical inputs include:

- The chemical compositions of the microalga, the additives that supply nitrogen, phosphorus and sulfur, and the gas that contains carbon dioxide;
- The physical dimensions of a cultivation pond; and
- The areal productivity of the microalga, in units of mass per illuminated surface area per time (g/m^2-day).

The carbon dioxide feed rate is either entered directly or is calculated from a power plant capacity rating and a CO_2 emission factor. This feed rate is corrected to a carbon uptake rate by a CO_2 conversion efficiency, which accounts for losses from the ponds due to offgassing. In the event that the microalga's areal productivity is unknown, TELCIM includes two subroutines with which it can be estimated. The first is a photosynthetic efficiency model that estimates biomass yield based on the intensity of incident sunlight[7,8]. The second is a chemical reactor model in which the microalga's doubling time is used to calculate a pseudo-first order rate constant, and the ponds are assumed to be perfectly mixed flow-through reactors at steady state. (The derivation of the governing equations used in these two subroutines is shown in the Appendix.) Because TELCIM is a time-averaged, steady-state model, a correction factor may have to be applied to the areal productivity to ensure it is valid for the time-scale being modeled. For example, if a single TELCIM run is intended to predict annual plant performance metrics, the value used for the areal productivity should account for losses arising from maintenance and sanitation downtime, effects of temperature on growth rate, variation in the number of daylight hours, etc.

Once the amount of biomass to be grown has been determined, TELCIM employs a "Stoichiometry Model" to close mass balances around the growth step. Inputs to this model include chemical composition data and information about the recycle water and nutrient streams generated by the harvesting step and digestion step process models (Fig. 2.1). The Stoichiometry Model allows that treated sewage water containing usable nitrogen and phosphorus may be used as an input to the growth step, reducing the demand for chemical fertilizers. It accounts for any carbon present in the nitrogen source (e.g., urea), and recognizes that fertilizers may contain combinations of macronutrient elements (e.g., ammonium phosphate). The Stoichiometry Model computes the minimum quantities of the specified chemical fertilizers that must be added to satisfy the mass and composition of the microalga to

be grown. It also predicts the mass of water consumed and oxygen produced in photosynthesis reactions. The mass balance equations for carbon, nitrogen, phosphorus and sulfur, the microalga's primary nutrients, are shown here. The derivation of these and the other equations used by the Stoichiometry Model is given in the Appendix.

$$C_{TOT} = \begin{cases} \dfrac{(C_{CO_2} - k_{CN} n_{SEW} Q_{SEW})}{[1 - k_{CN} k_{NA}(1 - f_N)]}, & if\ n_{SEW} Q_{SEW} < k_{NA}(1 - f_N) C_{CO_2} \\ C_{CO_2}, & if\ n_{SEW} Q_{SEW} \geq k_{NA}(1 - f_N) C_{CO_2} \end{cases} \quad (2.1)$$

$$N_N = \begin{cases} k_{NA}(1 - f_N) C_{TOT} - n_{SEW} Q_{SEW}, & if\ n_{SEW} Q_{SEW} < k_{NA}(1 - f_N) C_{TOT} \\ 0, & if\ n_{SEW} Q_{SEW} \geq k_{NA}(1 - f_N) C_{CO_2} \end{cases} \quad (2.2)$$

$$P_P = \begin{cases} k_{PA}(1 - f_P) C_{TOT} - p_{SEW} Q_{SEW} - k_{PN} N_N, & if\ (p_{SEW} Q_{SEW} + k_{PN} N_N) < k_{PA}(1 - f_P) C_{TOT} \\ 0, & if\ k_{PA}(1 - f_P) C_{TOT} \geq (p_{SEW} Q_{SEW} + k_{PN} N_N) \end{cases} \quad (2.3)$$

$$S_S = \begin{cases} k_{SA}(1 - f_S) C_{TOT} - s_{SEW} Q_{SEW} - k_{SN} N_N, & if\ (s_{SEW} Q_{SEW} + k_{SN} N_N) < k_{SA}(1 - f_S) C_{TOT} \\ 0, & if\ k_{SA}(1 - f_S) C_{TOT} \geq (s_{SEW} Q_{SEW} + k_{SN} N_N) \end{cases} \quad (2.4)$$

where:

C_{TOT} = the total amount of carbon to be converted to microalgae [kg-mol/day];

C_{CO_2} = amount of carbon in carbon dioxide to be converted to microalgae [kg-mol/day];

k_{CN} = molar ratio of carbon to nitrogen in the nitrogen source (k_{PN}, k_{SN} by analogy);

k_{NA} = molar ratio of nitrogen to carbon in the microalgae (k_{PA}, k_{SA} by analogy);

n_{SEW} = concentration of usable nitrogen in the sewage wastewater [kg-mol/m^3] (p_{SEW}, s_{SEW} by analogy);

Q_{SEW} = volumetric flowrate of sewage wastewater [m^3/day];

f_N = fraction of usable nitrogen in the microalgae exiting the ponds that is recycled to the growth step (f_P, f_S by analogy);

N_N = amount of nitrogen in the nitrogen source added to the growth step [kg-mol/day];

P_P = amount of phosphorus in the phosphorus source added to the growth step [kg-mol/day]; and

S_S = amount of sulfur in the sulfur source added to the growth step [kg-mol/day].

The water of reaction computed by the Stoichiometry Model is an input to the "Water Balance Model," which is the TELCIM subroutine that determines how much make-up water must be added to the raceway

ponds to replace losses. To reduce the demand for make-up water, it is assumed that as much supernatant (filtrate) as possible is recycled from the dewatering operations; Figure 2.3 illustrates the microalgae cultivation water balance. Three linearly independent water balance equations, a mass balance on a dissolved constituent (e.g., Total Dissolved Solids), and limits representing physical constraints, are used to solve for the amount of water that must be added (q_{fresh}) to maintain the system water balance and control salt accumulation. (The derivations of the water flowrate and dissolved constituent mass balance equations, along with TELCIM's solution strategy for the Water Balance Model, can be found in the Appendix.)

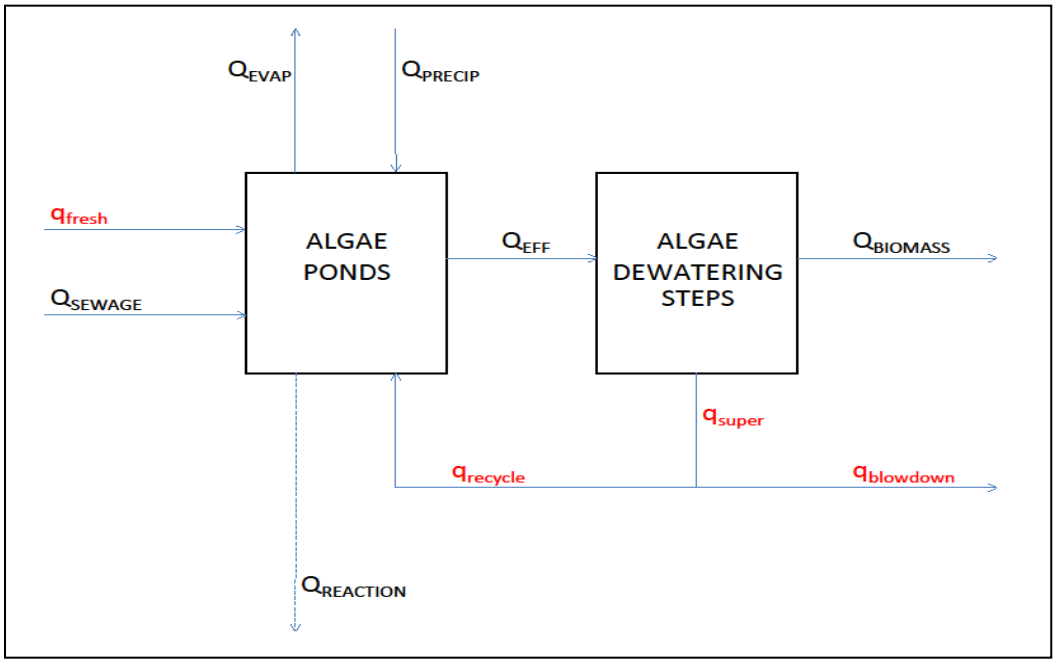

Figure 2.3: The Water Balance around the Ponds and Dewatering Operations. Q_i or q_i is the volumetric flowrate of stream 'i'. Streams with uppercase tags are specified by user input or the Stoichiometry Model; those with lowercase tags are calculated by the Water Balance Model. $Q_{REACTION}$ is shown as a dotted line because it is a virtual rather than an actual process stream.

TELCIM uses the mass of carbon to be converted to biomass, and the carbon content and areal productivity of the microalga, to calculate the required pond surface area. This fixes the number of ponds in the facility, which are all assumed to be identical. The model uses the following equation to compute the power required to provide vigorous mixing in the ponds:

$$P = k \frac{Q\rho(\Delta D + h_L)}{e} \quad (2.5)$$

where:

P = electrical power usage [kW];

k = conversion factor = 0.0098066 kW-sec/kg-m;

Q = volumetric flowrate [m^3/sec];

ρ = fluid density [kg/m^3];

e = motor efficiency [none];

ΔD = hydraulic gradient required to induce the desired mean channel velocity [m]; and

h_L = head loss due to changes in flow direction [m].

The hydraulic gradient (ΔD) is calculated using the Manning Equation for open channel flow[9]. Both head loss terms (ΔD and h_L) are proportional to the square of the velocity in the ponds; separate velocities can be entered for daytime and nighttime operations under the presumption that less vigorous mixing is required at night. (The derivation of the equations with which the pond mixing energy demand is calculated can be found in the Appendix.)

Although identical for the purpose of computing mixing energy, the ponds are not equivalent with respect to the power required to distribute to them the CO_2-containing gas (hereafter assumed to be a flue gas from an industrial plant), since they are located at different distances from the central CO_2 source. TELCIM uses a simple geometric model (the "Pumping Distance Model") to estimate these distances, as shown in Figure 2.2. Each biomass production module contains a specified number of ponds and associated harvesting and digestion equipment. Once the number of ponds needed to provide the required illuminated surface area is determined, the number of biomass production modules becomes fixed. The surface area of one module is estimated by applying to its pond surface area an escalation factor that accounts for the footprint of the harvesting equipment, digesters, and infrastructure items (roads, pipe bridges, buildings, etc.). The overall facility is visualized as a set of concentric rings whose radii are integer multiples of the radius of the innermost circle ('R'). That radius is scaled so that the first annular ring has an area equal to that of exactly nine biomass production modules. This results in a

number series in which each successive ring holds six more modules than its next inner neighbor. Rings are filled from the innermost ring outward, until the required number of modules has been assigned.

Estimating the power required to pump flue gas to the ponds in a given module involves two calculations. The first estimates the pressure drop in the gas main, using the following form of the Bernoulli Equation[10]:

$$\dot{m} = \left(\frac{\pi}{8}\right)\sqrt{\frac{(P_1^2 - P_2^2)g_c D^5 M}{fLRT}} \tag{2.6}$$

where:

$\dot{m}$ = gas mass flowrate [lb_m/sec];

P_1 = header inlet pressure [lb_f/ft^2];

P_2 = header outlet pressure [lb_f/ft^2];

g_c = gravitational constant = 32.174 lb_m-ft/lb_f-sec^2;

D = pipe inside diameter [ft];

M = gas molecular weight [lb_m/lb-mole];

f = Fanning friction factor [none];

L = pipe length [ft];

R = Universal Gas Law constant =1546 ft-lb_f/lb-mole-^oR; and

T = absolute temperature [^oR].

The header outlet pressure (P_2) is supplied as input (it can be estimated from the pressure drop in the local pipes and fittings and across the gas sparger, and the liquid head in the ponds above the sparger), and TELCIM calculates the gas mass flow rate ($\dot{m}$) in each gas header from the carbon dioxide loading and gas properties. The model then uses Equation 2.6 to find the header inlet pressure (P_1) necessary to overcome the pressure drop due to friction. Since the pressure drop for a given flowrate varies with the length of the pipe, different compressor outlet pressures are calculated for the modules in different rings. Once each header's inlet pressure is determined, the following equation for adiabatic compression is used to calculate the head required to compress the gas to that pressure[10]:

$$H_{ad} = \left(\frac{k}{k-1}\right) RT \left[\left(\frac{P_{out}}{P_{in}}\right)^{(k-1)/k} - 1\right] \quad (2.7)$$

where:

H_{ad} = adiabatic head [kJ/kg-mole];

k = ratio of heat capacities = C_P/C_V [none];

P_{out} = compressor outlet pressure [atm]; and

P_{in} = compressor inlet pressure [atm].

The adiabatic head is converted to a power load, and TELCIM compiles the electrical power used to feed gas to each module.

The remaining calculations in the Growth Step Process Model estimate the power load for water pumping. Three streams are addressed: the make-up water (q_{fresh} in Fig. 2.3), any sewage water used as make-up (Q_{SEWAGE}), and the effluent from the ponds (Q_{EFF}), which is pumped to the first dewatering operation. The head loss due to friction is calculated using the following form of the Darcy Equation[11]:

$$h_L = \frac{2fLv^2}{Dg} \quad (2.8)$$

where:

h_L = head loss [m];

f = Fanning friction factor [none];

L = pipe length [m];

v = gas velocity [m/sec];

D = pipe diameter [m]; and

g = acceleration due to gravity = 9.81 m/sec^2.

The frictional head loss is summed with any change in elevation, and the total is converted to a power load. The electrical power loads for water pumping are combined with the pond mixing and flue gas compressor loads, as well as any other specified auxiliary power uses, to estimate the total electricity usage in the growth step.

2.2.2. The Harvesting Step Process Model

The purpose of the harvesting step is to dewater the biomass to the extent required by the lipid extraction step. The Harvesting Step Process Model allows for as many as five sequential mechanical dewatering steps to remove extracellular water, followed by as many as five sequential drying steps to remove intracellular water. Specifying the biomass recovery efficiency and solids concentration in the concentrate from each harvesting step allows the model to predict the composition and flowrate of each concentrate and supernatant (filtrate) stream. The supernatant flowrates from all of the dewatering steps (q_{super} in Fig. 2.3) are combined and provided as an input to the Water Balance Model.

TELCIM computes the drying energy loads using two separate drying models. The first assumes the dewatered biomass is contacted with heated surfaces, such as in a plate or drum dryer. The theoretical evaporative heat loads are scaled using specified thermal efficiency factors for each dryer, and then summed to estimate the total drying heat load. The second drying model assumes the biomass is contacted with hot air, such as in a fluidized bed or moving belt dryer. The thermodynamic model for air drying involves two changes of state, as illustrated in Figure 2.4. Simultaneous mass and enthalpy balances are used to estimate the theoretical drying heat load (Q), based on specified dryer outlet conditions. (These conservation equations are derived in the Appendix.) TELCIM also accounts for the additional thermal efficiency losses that occur assuming steam is used to heat the dryers in the first model, and to preheat the air in the second model. Based on these heat loads and transfer efficiencies, the model calculates the amount of natural gas that must be burned to supply the required thermal energy for biomass drying.

The Harvesting Step Process Model calculates the electrical power load for pumping the concentrate from each dewatering operation to the next process step, the recycled filtrate back to the ponds, and the blowdown to an outfall. These calculations are performed in the same manner as those described above for water pumping in the growth step. The power load for compressing the air used in the dryers is estimated using the same approach as that used for flue gas compression in the growth step, except that the pressure drops in the air piping, heat exchangers, and dryers can be specified separately. Finally, the

power loads for any other electricity consumers in the harvesting step are entered (e.g., clarifier rakes, evaporator rotors), and TELCIM computes the total electrical power load for the harvesting step.

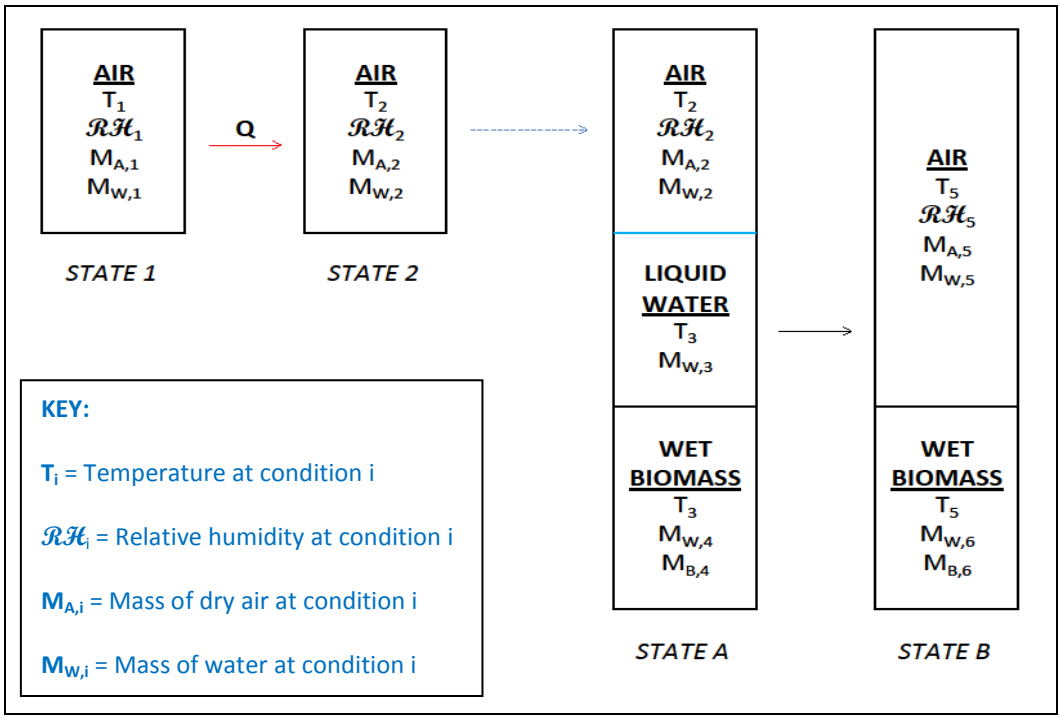

Figure 2.4: Thermodynamic Model of Air Drying. In the first change of state, heat (Q) is added to a mass of ambient air ($M_{A,1}$), raising its temperature and reducing its relative humidity. In the second change of state, sensible heat is converted to latent heat, and the relative humidity of the air is increased. The model solves for Q and $M_{A,1}$ based on the composition and temperature of the incoming wet biomass and user-specified dryer outlet conditions.

2.2.3. The Extraction Step Process Model

The purpose of the lipid extraction step is to separate nonpolar lipids (assumed to be entirely composed of triacylglycerides, or TAG) from the remainder of the microalgal biomass. It is assumed that the same lipid extraction process commonly used for soybean oil extraction will be used to recover TAG from the biomass[1,2,3,6]. TELCIM uses as its "basis" extraction plant the lipid extraction facility modeled by Lundquist et al. in their study of algal oil production[6], which includes the following operations:

- Forming the microalgal biomass into cassettes in an extruder/expander;
- Leaching neutral lipids from the cassettes with hexane in a moving belt extractor;

- Stripping solvent from the residual biomass using hot air;
- Separating the extraction solvent from the solvent-oil mixture (miscella) in a series of evaporators and strippers;
- Condensing the solvent vapors and passing the condensate through an oil-water separator; and
- Recycling the recovered solvent and discarding the separated water.

Because the lipid extraction step involves several complex mass transfer operations, it is treated as a single "black box" in which the consumptions of solvent, electricity, and process heat, and the generation of wastewater, are assumed to scale linearly with oil production. The scaling factors are calculated from the mass and energy flowrates for the basis plant, which are provided as TELCIM inputs. Additional inputs to the extraction process model include the lipid fraction in the harvested microalgal biomass, and the overall lipid recovery efficiency of the extraction process. TELCIM scales these consumption/generation rates based on the ratio of oil production in the microalgal biodiesel plant being modeled to that in the basis plant.

2.2.4. The Conversion Step Process Model

The role of the conversion step is to convert TAG into biodiesel and glycerol by reacting it with a short chain monoalcohol. The U.S. Department of Agriculture recently developed a techno-economic model of an industrial-scale plant for producing biodiesel from soybean oil[12]. TELCIM's lipid conversion process model is based on the USDA's proposed process, which uses sodium methoxide as a homogeneous catalyst and methanol as the esterifying alcohol, and includes the following operations:

- Two continuous transesterification reactors in series;
- Centrifugal separation of the crude ester phase from the aqueous glycerol phase;
- Acid washing of the crude ester to neutralize catalyst and convert soaps to free fatty acids, and centrifugal separation followed by vacuum drying to produce refined biodiesel;

- Acid washing and caustic neutralization of the glycerol phase, followed by distillation to recover and recycle unreacted methanol;
- Further distillation of the crude glycerol/water mixture to produce a semi-refined glycerol co-product (80% aq.), and water suitable for recycle to the wash step; and
- Steam generation in a natural-gas fired boiler (steam is used to heat the reactors and distillation tower reboilers).

Selection of this lipid conversion process model extends the earlier assumption that microalgal oil can be converted to biodiesel using the same process technology currently used to convert soybean oil to biodiesel. This assumption appears to be reasonable because the compositions of microalgal TAG[13] and soybean oil TAG[14] are similar, and transesterification processes are used to produce biodiesel from a wide variety of animal and vegetable oils with very different fatty acid profiles[15].

As with the extraction step, the conversion step process model is treated as a unitary "black-box". Consumption rates for alcohol, catalyst, acid, caustic, water, electricity and natural gas are entered for a basis conversion plant at a specified oil feed rate, and the model calculates normalized consumption rates. Except for the esterifying alcohol, these consumption rates are scaled based on the mass flowrate of oil recovered in the extraction step. Methanol consumption is instead calculated based on the molar flowrate of TAG in the incoming oil; this accounts for potential differences in fatty acid profiles between the algal lipids and the soybean oil assumed by the USDA model. TELCIM predicts biodiesel, glycerol, wastewater, and free fatty acid production rates based on molar and mass balances around the transesterification process. It also estimates carbon dioxide production from the natural gas burned in the steam generator using an appropriate emission factor[16]. Finally, several vital statistics about the biodiesel product are displayed, including the area normalized production rate (gal/acre-year), fuel energy productivity (MJ/day), and the mass ratio of biodiesel to microalgal biomass.

2.2.5. The Anaerobic Digestion Step Process Model

Anaerobic digestion is commonly used to break down biomaterials, such as wastewater treatment sludges, while generating methane as a valuable byproduct. Several prior studies have proposed

anaerobic digestion of the microalgal biomass that remains after lipid extraction as a means of reducing the demands for purchased nitrogen and phosphorus fertilizers, electricity and natural gas[3,6,17,18].

The TAG fraction of the biomass is characterized by its average carbon chain length and number of double bonds, which fixes its chemical composition. Because the chemical composition of the microalgal biomass is known, the elemental composition of the residual biomass (also referred to as "lipid-extracted algae," or LEA) is calculated by difference. Because TAG is pure hydrocarbon, all of the nitrogen and phosphorus contained in the microalgal biomass is assumed to partition to the LEA during extraction. As digestion of this material proceeds, a fraction of these elements is liberated as water-soluble species. TELCIM calculates the amounts of nitrogen and phosphorus that are recycled to the growth step by applying recovery efficiency factors to the amounts present in the residual biomass.

Biogas yield from biological wastes is typically predicted on the basis of the chemical oxygen demand (COD) of those materials[19,20]. The COD of the residual biomass is calculated by TELCIM based on its chemical composition and standard oxidation chemistries (typical oxidation reactions are shown in the Appendix), but this can be overwritten with a measured COD value. Other essential inputs include the COD removal efficiency in the digesters, the estimated biogas yield per kilogram of COD removed, and the estimated methane content of the biogas. After the methane production rate and the biogas's energy content are calculated, the carbon dioxide production rate in the digester is estimated using a carbon balance. The model also calculates the rate of CO_2 production from biogas combustion. Finally, the production of digester sludge (anaerobic bacteria plus unreacted LEA) is estimated based on a specified carbon fraction and the assumption that it contains all of the carbon not present in the biogas.

TELCIM models the conversion of biogas to electricity in microturbine generators located alongside the anaerobic digesters. This choice of distributed power generation is made to avoid the large capital and operating costs of compressing and conveying biogas to a centralized power unit. The amount of electrical power produced from the biogas is predicted using a conversion efficiency factor. The residual thermal energy of the exhausted biogas is estimated by subtracting the electrical energy produced from

the heat of combustion of the biogas. This thermal energy is assumed to be exported to the harvesting step, where it displaces an equivalent amount of thermal energy from natural gas.

2.3. The Financial Models

The purpose of TELCIM's financial models is to estimate the capital cost of a microalgal biodiesel manufacturing plant of the size specified by the process models, and the unit production cost of the biodiesel produced in that plant. The capital cost of each major process step is estimated by scaling the capital costs of a basis plant to match the production capacity of the biodiesel plant being modeled. Most variable operating costs are calculated by multiplying a material or energy usage rate by a unit price. Some fixed operating costs are estimated as percentages of certain capital or variable costs, while others are entered directly.

There is one financial model for each of the five major process steps. Each of these models assembles operating and capital cost structures for its process step. These five models are sufficient if detailed cost data is available for all of the major process steps, but TELCIM includes a sixth, auxiliary financial model (the "Summary Cost Model") which is used when only aggregated cost structures are available as input. The Summary Cost Model is used to allocate aggregated costs among the applicable major process steps. (If this allocation is not performed, the model is unable to isolate the contributions of each of the individual steps to the overall cost structures.) The Summary Cost Model also organizes capital cost data in a way that allows Economic Input - Output LCA models to be interrogated, which is how the contributions of capital spending categories to the LCI of the biodiesel plant are estimated.

Because the growth, harvesting, and digestion steps are of modular design, their financial models are configured slightly differently than those for the extraction and conversion steps. The subsequent description of the growth step financial model applies as well to the harvesting and digestion step financial models, while that for the extraction step also applies to the conversion step.

The capital cost structure for a basis plant is entered into each process step's financial model. Because capital costs for the growth step are scaled on the basis of the number of modules in the overall biodiesel plant, its basis plant is defined as the equipment and facilities comprising the growth step in one biomass production module. This selection ensures continuity between the growth step's process and financial models. The total capital cost structure for the growth step is obtained by multiplying the cost structure for one module by the number of production modules in the overall facility. In contrast, the capital cost structure of the basis plant for the extraction step is adjusted using a power law method for scaling the capital costs of chemical plants of different sizes[11]. The capital cost structures for the basis plants can be entered directly into each step's financial model or imported from the Summary Cost Model if the allocation method was used.

The operating cost structure for each basis plant is entered into the corresponding financial model. Since some operating costs are calculated from capital costs (e.g., maintenance and depreciation), the operating cost structure should match the basis plant selected for the capital cost estimate. These operating cost structures can also be entered directly into each step's financial model or imported from the Summary Cost Model, depending on the specificity of the available input data.

TELCIM adjusts for cost/price inflation that occurred between the time the cost estimate for a basis plant was generated and the time period being modeled. Applicable construction, commodity, and labor cost indices for the appropriate dates are entered into each financial model. The Growth Step Financial Model displays the inflation-adjusted capital cost structure for the growth step in one production module, and for the growth step in the entire facility. The Extraction Step Financial Model adjusts for inflation and scales the capital cost structure (based on production capacity) in a single calculation. Each process step's operating cost structure is similarly displayed in its financial model. For the growth step, the inflation-adjusted operating cost structure for a single production module is presented, along with the operating cost structure for that step across the entire facility. For the extraction step, the inflation-adjusted, capacity-scaled operating cost structure is displayed in its model. Grand totals are displayed in each model, and are exported to several tabular and graphical output summaries.

2.4. The Life Cycle Inventory Models

The purpose of TELCIM's LCI models is to estimate the energy and water usage and air pollutant emissions resulting from indirect activities attributable to the manufacture of microalgal biodiesel, including:

- Raw material manufacture and transportation;
- Electricity production;
- Natural gas production, distribution, and use;
- On-site transportation (i.e., biomass hauling);
- Capital equipment manufacture; and
- Construction activities.

In general, these indirect environmental impacts are estimated by multiplying a consumption rate predicted by the TELCIM's process models by an appropriate energy use, water use, or air pollutant emission factor. These factors must be supplied as inputs, and can be obtained from process knowledge or external LCA databases (as illustrated in Figure 1.1), such as Argonne National Lab's GREET model[21], or Carnegie Mellon University's EIO-LCA Model[22]. There is one LCI model for each major process step, helping to isolate the indirect environmental impacts attributable to each step, and making it easier to model alternative process schemes.

For raw material manufacture, each ingredient's identity and usage rate are imported from the corresponding process model. These usage rates are multiplied by factors corresponding to various air pollutants (including greenhouse gases), energy use categories, and water use, yielding the total emissions and resource usages attributable to each raw material. Resource usages and pollutant emissions arising from the delivery of these raw materials to the biodiesel plant are also estimated. Additional inputs required for these calculations include the transportation mode, fuel type and energy density, distance traveled, and load factors. TELCIM calculates the rate of fuel consumption for delivering each raw material, and estimates the air emissions and resource usages resulting from fuel

production and combustion. A similar set of calculations is performed in the extraction and digestion step LCI models for the transportation of biomass within the facility. For these internal shipments, TELCIM uses the average distance between the production modules and the center of the facility, as calculated by the growth step's Pumping Distance Model (Fig 2.2).

An LCI is assembled for the electricity that is imported into the facility from off-site. The energy use and emissions factors for imported electricity should reflect the appropriate fuel mix (i.e., specific percentages of coal, gas, nuclear, wind, biomass, etc.). When determining the biodiesel's NER, TELCIM accounts for the energy content of the fuels used to generate electricity, reflecting the efficiency of fuel-fired electric power generation. This avoids distortions that might arise if all forms of energy, including electricity, are considered equivalent in the NER calculation.

A similar LCI is constructed for thermal energy on the basis that imported natural gas is the sole source of process heat, except for that obtained from the combusted biogas. Any thermal efficiency losses that occur in the use of natural gas and biogas are reflected in the process models, whereas inefficiencies associated with natural gas production and distribution are accounted for by the energy use factors entered into the LCI models.

The LCI models account for the resource usages and air pollutant emissions resulting from the manufacture of capital items and the performance of construction activities. The same list of capital expense categories that appears in each process step's financial model is entered into the corresponding LCI model, and TELCIM imports the total capital spending, by category. This list forms one axis of a matrix; the other axis consists of spending categories for which an EIO-LCA model can be probed (e.g., machinery, instrumentation, construction, concrete, steel pipe, tanks/vessels, and plastics). The percentage of each capital cost that is attributable to each spending category is entered into the corresponding matrix cell; these percentages can be determined from detailed capital cost estimates, project experience, or engineering judgment. The total spending in each of these expense categories is

multiplied by factors obtained from an EIO-LCA model to estimate the indirect energy and water usages and air emissions attributable to capital items.

TELCIM includes the indirect energy uses tabulated by the LCI models when computing the NER of the biodiesel manufacturing process. It similarly includes the indirect carbon dioxide emissions reported by the LCI models when computing the biodiesel's carbon intensity. However it does not include the CO_2-equivalence of other greenhouse gases when calculating the carbon intensity of the biodiesel. The other information compiled by the LCI models, such as indirect emissions of air pollutants like VOC and NO_x, can be used to inform site-specific studies, such as a Life Cycle Assessment.

2.5. TELCIM Outputs

TELCIM extracts important outputs from the process, financial and LCI models and presents them in summary tables and graphics. Outputs reported in the "Summary Results" section include:

- The energy content of the produced biodiesel (MJ/gal);
- The Net Energy Return of the biodiesel manufacturing process (MJ/MJ);
- The direct and indirect energy use by major process step, and by category (e.g., direct electricity use, direct natural gas use, and embedded energy in capital items);
- Net carbon dioxide emissions, by major process step, and by category of CO_2 flux (e.g., pond uptake, electricity production, natural gas combustion, and transportation activities);
- A system carbon balance showing the amount of CO_2 taken up in the ponds, and the carbon content of the biodiesel product and other byproduct and waste streams;
- The contribution of each major process step to the carbon intensity of the produced biodiesel, the net CI of the production process, and the CI of biodiesel combustion;
- The annual operating and capital cost contributions from each of the major steps and grand totals;
- The biodiesel's unit production cost ($/gal);

- The capital productivity of the manufacturing plant, defined as the total capital investment divided by the annual biodiesel production capacity ($/gallon/year); and
- The water intensity of direct biodiesel manufacturing activities, defined as the volume of water used per volume of fuel produced [gal/gal].

Note that the reported water intensity does not include indirect water usages, due to a paucity of water use data in the LCI databases that were accessed when TELCIM was being developed.

2.6. Conclusion

TELCIM is an integrated techno-economic LCI model with which an analyst can generate estimates of numerous financial, technical and environmental performance metrics for a proposed microalgal biodiesel manufacturing scheme. Implementation in Excel makes it accessible to a broad audience, including those with limited computer programming skills. Its modular structure limits the number of connections between individual models, making it easily adapted to simulate alternative raw material and energy inputs, microalgal species, and/or production processes. Excel's open architecture allows background information to be loaded directly into the model, facilitating information organization, sharing and recordkeeping. The layout and approach used in TELCIM might serve well as a template for combined techno-economic life cycle inventory models of other products and processes.

2.7. References for Chapter 2

[1] Lardon, L., A. Helias, B. Sialve, J.P. Steyer, and O. Bernard. Life-cycle assessment of biodiesel production from microalgae. Env. Sci. Tech. 43 (2009) 6475-6481.

[2] Batan, L., J. Quinn, B. Wilson, and T. Bradley. Net Energy and Greenhouse Gas Emission Evaluation of Biodiesel Derived from Microalgae. Environ. Sci. Technol. 44 (2010) 7975-7980.

[3] Razon, L.F. and R.R. Tan. Net energy analysis of the production of biodiesel and biogas from the microalgae : *Haematococcus pluvialis* and *Nannochloropsis*. Applied Energy 88 (2011) 3507-3514.

[4] Robertson, D.E., S.A. Jacobson, F. Morgan, D. Berry, G.M. Church, and N.B. Afeyan. A new dawn for industrial photosynthesis. Photosynth. Res. 107(3) (2011) 269-277.

[5] Benemann, J.R., and W. J. Oswald. Systems and Economic Analysis of Microalgae Ponds for Conversion of CO_2 to Biomass – Final Report. 1996. Department of Energy, Pittsburgh, PA, 201 pp.

[6] Lundquist, T.J, I.C. Woertz, N.W.T. Quinn, and J.R. Benemann. A Realistic technology and engineering assessment of algae biofuel production. 2010. Energy Biosciences Institute, University of California, Berkeley, California, USA.

[7] Weyer, K.M., D.R. Bush, A. Darzins, and B.D. Wilson. Theoretical maximum algal oil production. Bioenerg. Res. 3 (2010) 204-213.
[8] Wigmosta, M.S., A.M. Coleman, R.J. Skaggs, M.H. Huesemann, and L.J. Lane. National microalgae biofuel production potential and resources demand. Water Resources Research 47 (2011) W00H04 doi:10.1029/2010WR009966.
[9] Oswald, W.J., and C.G. Golueke. Biological transformation of solar energy. Advances in Applied Microbiology 2 (1960) 223-262.
[10] Perry, R.H. and C.H. Chilton. Chemical Engineers' Handbook, 5th ed. 1973. McGraw-Hill Inc. USA.
[11] Welty, J.R., C.E. Wicks, R.E. Wilson, and G. Rorrer. Fundamentals of Momentum, Heat and Mass Transfer (4th ed.). 2001. John Wiley & Sons, Inc. Hoboken, NJ, USA.
[12] Haas, M.J., A.J. McAloon, W.C. Yee, and T.A. Foglia. A process model to estrimate biodiesel production costs. Bioresource Technology 97 (2006) 671-678.
[13] Dunstan, G.A., J.K. Volkman, S.W. Jeffrey, and S.M. Barrett. Biochemical composition of microalgae from the green algal classes Chlorophyceae and Prasinophyceae. 2. Lipid classes and fatty acids. J. Exp. Biol. Ecol. 161 (1992) 115-134.
[14] Kubatova, A., Y. Luo, J. Stavova, S.M. Sadrameli, T. Aulich, E. Koziak, and W. Seames. New path in the thermal cracking of triacylglycerols canola and soybean oil). Fuel 90 (2011) 2598-2608.
[15] Demirbas, A.H.. Inexpensive oil and fats feedstocks for production of biodiesel. Energy Education Science and Technology Part A: Energy Science and Research 23(1) (2009) 1-13.
[16] U.S. Environmental Protection Agency. AP 42, Fifth Edition, Volume I, Chapter 1: External Combustion Sources, Section 1.4: Natural Gas Combustion. 1998. Accessed at: http://www.epa.gov/ttn/chief/ap42/ch01/final/c01s04.pdf.
[17] Benemann, J.R., R.P.Goebel, J. C. Weissman, and D. C. Augenstein. Microalgae as a Source of Liquid Fuels. Final Technical Report DOE/ER/30014—T1. 1982.
[18] Chisti, Y. Biodiesel from microalgae beats bioethanol. Trends in Biotechnology 26(3) (2007), 126-131.
[19] Tchobanoglous, G. and F. L. Burton. Wastewater Engineering; Treatment, Disposal, Reuse. 3rd ed. Section 8-9: Anaerobic suspended-growth treatment systems. 1991. McGraw-Hill, Inc., USA.
[20] Grady, C.P.L., G.T. Daigger and H.C. Lim. Biological Waste Treatment. 2nd ed. Chap. 13: Anaerobic processes. 1999. Marcel Dekker, New York, USA.
[21] Wang, M. The Greenhouse Gases, Regulated Emissions, and Energy Use in Transportation Model (GREET), v.1.8d.1, Copyright 1999, University of Chicago Argonne LLC. Accessible at http://www.greet.es.anl.gov.
[22] Carnegie Mellon University Green Design Institute. Economic Input-Output Life Cycle Assessment (EIO-LCA). 2008. Accessible at http://www.eiolca.net.

3. THE TEST SCENARIO*

3.1 Introduction

Since production of microalgal biodiesel is a complex process that has yet to be demonstrated at large scale, a single reference for all of the data required to populate TELCIM is not yet available. To test the model, input parameter values were obtained from several scientific journals, government reports and other reliable open source materials. The values selected were all deemed to be individually reasonable, and in combination create a coherent input data set. The case which these input data case simulate is called the "Test Scenario". The primary purpose of the Test Scenario is to demonstrate TELCIM's integrity and functionality. A secondary purpose is to generate output values that broadly characterize the expected technical, economic, and environmental performance of a microalgal biodiesel production scheme that simulates commercially demonstrated process technologies.

A particularly important source of the capital cost data used in the Test Scenario is the techno-economic analysis of microalgal oil production performed by Lundquist et al[1]. To ensure consistency between that economic data and the physical facility it describes, the Test Scenario also uses the pond dimensions, site location, and extraction process assumed in Lundquist's analysis. For the same reason, the operating cost structures and climate conditions chosen for the Test Scenario are consistent with the Salton Sea, California, location modeled by Lundquist.

There are two significant differences between the processing scheme modeled by Lundquist and that simulated by the Test Scenario. Lundquist's harvesting step involves solids sedimentation, gravity thickening, open bed solar drying (from 3% to 80% solids, by weight), and natural gas fired flash drying to the target dryness of 90-95%[1]. The harvesting step simulated in the Test Scenario simulates three dewatering steps (sedimentation, gravity thickening, and vacuum filtration), and two steps of forced air drying. (This harvesting scheme is adapted from that commonly used in industry to produce dry baker's

* *Some of the text, tables and figures included in this chapter were taken from a manuscript that is being prepared for publication.*

yeast.) The capital cost structure assembled by Lundquist for the harvesting step was left unchanged – it was assumed that the capital cost of the filters and first-stage dryers envisioned by TELCIM will be similar to that of the large, low-rate solar drying beds and spreading and collection equipment. The other major difference is that Lundquist's techno-economic model stopped at the oil extraction step; it does not include a transesterification plant. The Test Scenario uses the capital cost structure developed by the USDA for a techno-economic model of a soy oil tranesterification plant as the basis for the Test Scenario's lipid conversion plant[2].

3.2 Inputs to the Test Scenario

The Test Scenario simulates a microalgal biodiesel plant processing the flue gas from a 1000 MW_e coal-fired electric power plant. Table 3 lists some of TELCIM's most significant input parameters, and the values assigned to those parameters in the Test Scenario.

Table 3.1: Examples of Test Scenario Inputs

Parameter	Input to the Test Scenario
Flue Gas Composition	15.5% CO_2, 3.8% O_2, 80.7% N_2 (by volume)
Carbon Dioxide Feed Rate	11,400 tonnes/day
Microalga Composition	*Chlorella vulgaris* ($C_{106.6}H_{174.1}O_{25.9}N_{10.3}PS_{0.22}$)
Carbon Dioxide Conversion Efficiency	75%
Microalga Productivity	24.75 g/m^2/day
Sewage Water Availability	10^8gallons per day (100 MGD)
Surface Area per Pond	4.06 hectares (40,600 m^2)
Nutrients	Urea, Superphosphate, Sodium Sulfate
Net Evaporation Rate	79 inches/yr (Salton Sea, Calif.)
Electricity Price	$0.10/kWh
Natural Gas Price	$8.28/GJ
Interest on Debt	5% p.a.
Oil Content	25% (wt./wt.)
Final Pond Cell Density	0.34 g/L (ash-free, dry weight basis)
Final Dewatering Moisture Content	73.5%
Final Drying Moisture Content	10%
COD Removal Rate	65%
Methane Yield	0.3 m^3/kg COD rem.
Nitrogen Recovery Efficiency	75%
Phosphorus Recovery Efficiency	50%

3.3 Outputs from the Test Scenario

Table 3.2 lists some of the significant outputs from the Test Scenario.

Table 3.2: Examples of Test Scenario Output Values	
Parameter	**Output From the Test Scenario**
Total Pond Surface Area	15,300 hectares
Total Facility Footprint	193 square kilometers
Number of Ponds	3758
Microalga Production	3780 tonnes/day
Biodiesel Production	850 tonnes/day (255,000 gal/day)
Biodiesel Productivity	1950 gal/acre/yr
Make-up Water Requirement	334,000,000 gal/day
Urea Consumption	121 tonnes/day
Superphosphate Consumption	59 tonnes/day
Facility Capital Cost	$4,253,000,000
Annual Operating Cost	$889,000,000
Biodiesel Production Cost	$9.56 per gallon
Net Energy Return	0.40 joules out per joule in
Biodiesel Carbon Intensity	76.7 gCO_2/MJ
Biodiesel Water Intensity	1300 gallons water/gallon biodiesel

The surface area of the facility required to process the flue gas from a 1000 MWe coal-fired power plant is on the order of 80 square miles. A plant of this size produces roughly one-quarter million gallons of biodiesel per day. As a point of reference, domestic consumption of diesel fuel for transportation in 2010 was around 114 million gallons per day[3], so close to 450 microalgal biodiesel plants of the size envisioned by the Test Scenario would be needed to meet that demand. The combined footprint of these facilities encompasses an area roughly equivalent to the size of the State of South Carolina.

The amount of make-up water required by this facility is roughly one-third of a billion gallons per day (including the 100 million gallons per day of treated sewage wastewater assumed to be available). Roughly 1300 gallons of water is used for each gallon of biodiesel produced. This enormous water burden is driven by the high evaporation and negligible precipitation rates experienced in the Salton Sea area of southern California. Water availability is likely to represent a substantial barrier to facility siting in the western United States, even if degraded water can be used.

Like water intensity, other key performance metrics for the biodiesel are problematic. The Net Energy Return of the biodiesel is much less than the minimum threshold for long-term sustainability of 1.0. While this may be acceptable for a niche fuel, such as for military use, it would be unsustainable as a general transportation fuel – based on the current fuel mix used in the United States, producing biodiesel this way will cause an increase in fossil fuel consumption. The unit cost of manufacturing is considerably higher than the selling price of conventional diesel fuel derived from petroleum, meaning there is a large financial disincentive to producing biodiesel in this way. That will make it impossible to find private funding for the large capital costs to build production plants. And the carbon intensity of this biodiesel is only slightly better than that of conventional diesel (84.3 gCO_2/MJ)[4], so using it instead of petrodiesel will not contribute significantly to a reduction in carbon dioxide emissions.

In addition to the summary results presented in Table 3.2, TELCIM provides a substantial amount of detail on the technical, financial and environmental performance of the biodiesel plant. For example, a breakdown of the energy used in the plant is shown in Figure 3.1.

TELCIM computes energy and raw material consumptions (and costs) for the growth, harvesting, extraction and conversion steps on the basis that there are no anaerobic digesters. This allows the effects of the digesters to be displayed as credits which offset some of those consumptions (and costs). For example, the anaerobic digestion step reduces the overall power consumption by roughly 45% (52% for indirect energy and 45% for direct energy usage).

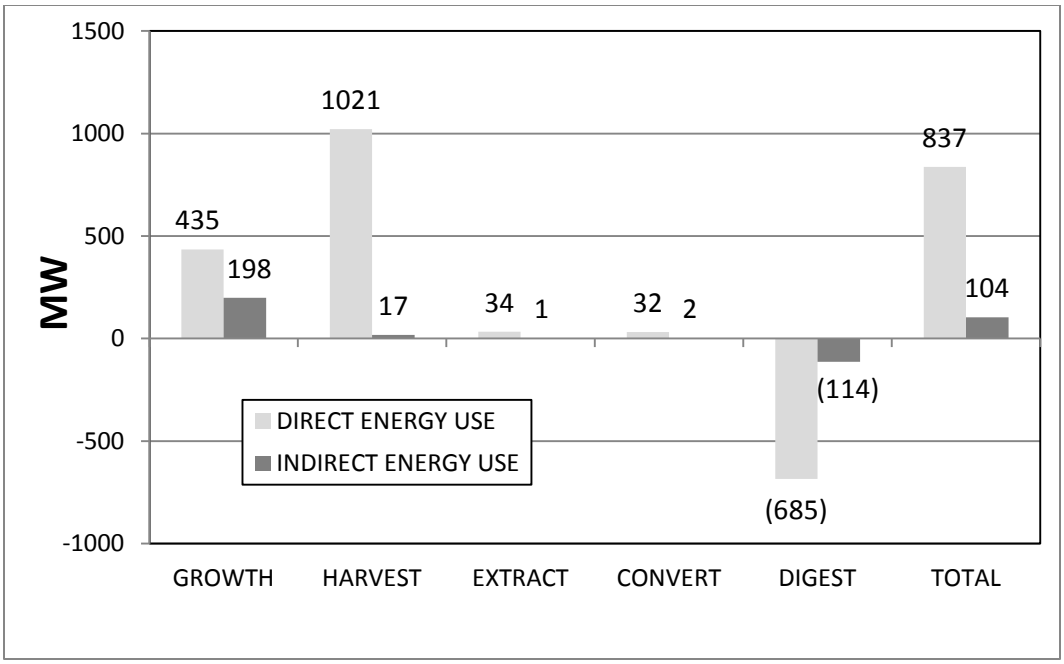

Figure 3.1. Net Energy Use by Major Process Step, and overall. Direct energy use reflects energy used within the battery limits of the biodiesel plant. Indirect energy use measures energy used to conduct indirect activities necessary for biodiesel manufacture, including raw material production, transportation activities, and capital equipment fabrication. (Energy use is reported in units of megawatts, or energy per time.)

Energy use in the harvesting step, and particularly in the drying operations, dominates the energy footprint of the biodiesel plant. This creates a large incentive to improve the water tolerance of the lipid extraction process; this topic will be discussed in more detail in Section 5.2. Indirect energy usage represents 11% of the total consumption; while small, this is not negligible. This outcome confirms the importance of the indirect energy accounting performed by TELCIM's LCI models. The extraction and conversion steps each contribute only between 3 and 4% of the total energy demand of the biodiesel manufacturing process.

Figure 3.2 displays energy use by usage category. In TELCIM, electricity is converted to chemical energy on the basis of the fuel(s) used to produce it. In the Test Scenario, fuel energy usage factors corresponding to the U.S. national electricity fuel mix were used[4]. With this conversion, electricity accounts for around 59% of the total fuel energy used to manufacture microalgal biodiesel (including

indirect uses). Transportation activities, both on-site and off-site, account for around 0.1% of total energy use.

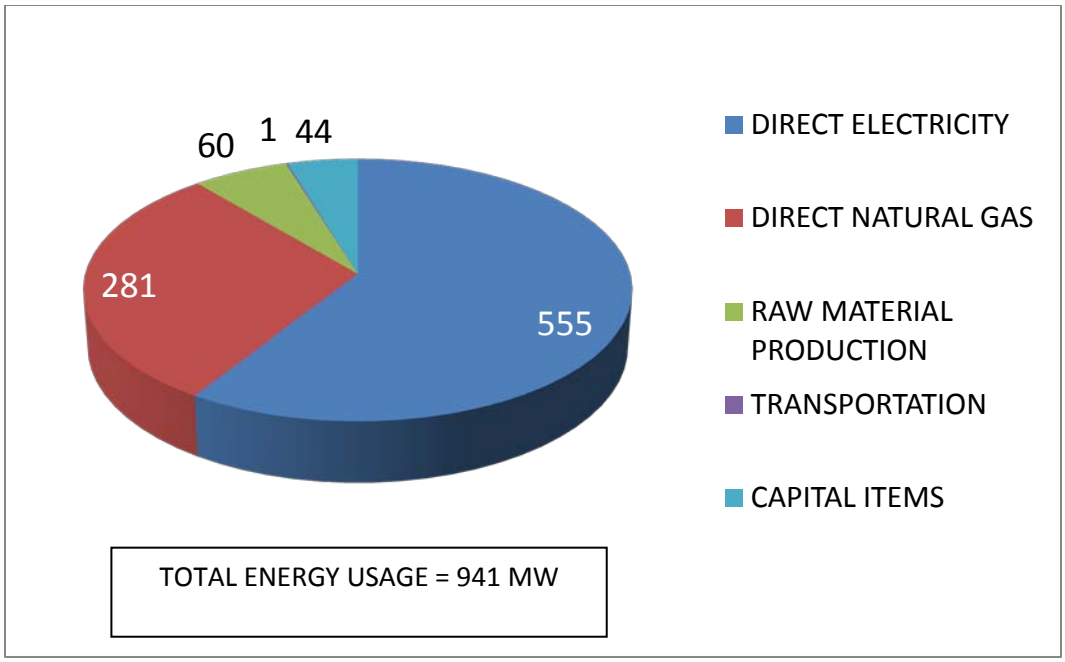

Figure 3.2 Net Energy Use by Category. Breakdown of total energy use in the Test Scenario. The electricity and natural gas use are only for purchased energy - the figures shown are net of offsets resulting from on-site biogas combustion. (Energy use is reported with units of megawatts, or energy per time.)

Figure 3.3 provides an inventory of the actual carbon dioxide inflows (negative) and emissions (positive) from the major steps comprising the manufacturing process. In this accounting, indirect carbon dioxide emissions are attributed to the process step that caused them (e.g., the CO_2 emitted when fertilizers are produced is attributed to the growth step). The large negative value reported for the growth step includes the carbon dioxide taken up by the biomass in the ponds, partially offset by the CO_2 emitted when the electricity and raw materials used in the growth step are produced. As with energy use, the CO_2 fluxes reported for the harvesting and other steps ignores the effects of the anaerobic digesters. It is noteworthy that the net carbon dioxide emissions from the digesters is negative; this suggests that generating electricity on-site in microturbines results in lower carbon dioxide emissions than would have occurred if the equivalent amount of electricity was obtained from the U.S. grid. Based on the total carbon dioxide

emissions, the biodiesel manufacturing process involves the release of slightly more carbon dioxide than is taken up in the ponds. Since this accounting does not address the CO_2 created when the biodiesel is burned, it appears that using biodiesel produced this way instead of petrodiesel will not result in a significant reduction in net carbon dioxide emissions.

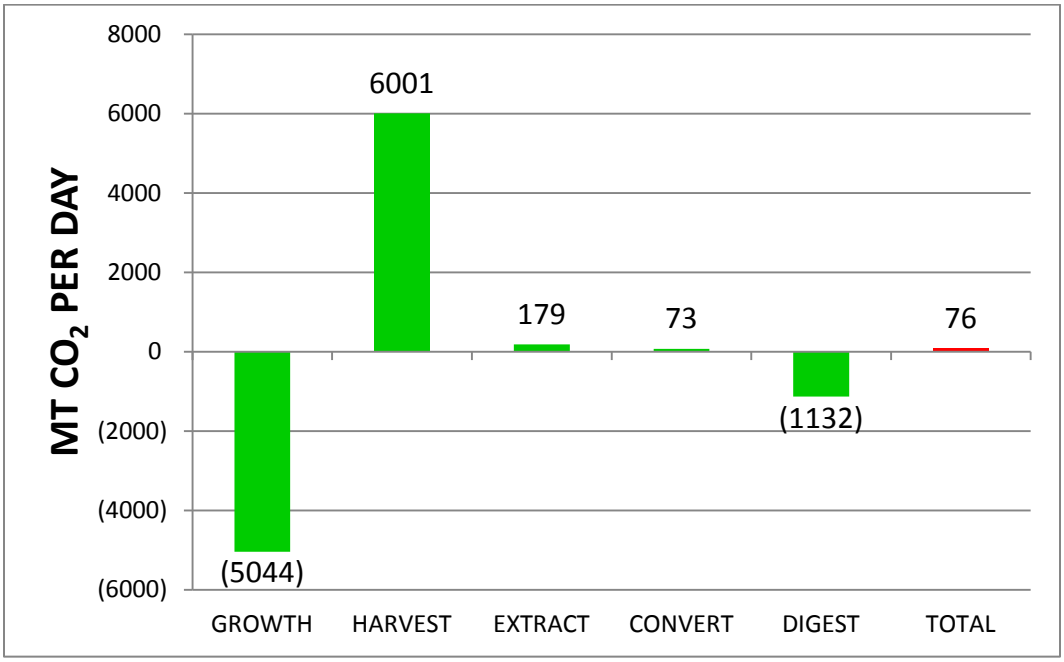

Figure 3.3. Carbon Dioxide Emissions by Major Process Step, and overall. The negative value for the growth step indicates net carbon dioxide uptake. The negative value for the anaerobic digestion step indicates avoided carbon dioxide emissions, offsetting a portion of the CO_2 emissions that are included in the growth step for raw material production, and in the harvesting step for electricity and natural gas use. (Carbon dioxide emissions are reported in units of metric tonnes of CO_2 per day.)

TELCIM tracks all of the carbon that enters and leaves the manufacturing process. Figure 3.4 displays a system carbon balance, expressed in terms of carbon dioxide equivalents - this is done to make it easier to compare the results shown in Figures 3.3 and 3.4. For example, from Figure 3.4 we see that 8553 metric tonnes per day of CO_2, and another 45 MT per day of carbon (as CO_2 equivalents) in the form of urea, is converted to biomass in the ponds. When this sum is compared to the net CO_2 flux for the growth step shown in Figure 3.3, it becomes clear that the difference, or 3554 MT per day of CO_2, is emitted when the energy and raw materials used in that step are produced and delivered to the biodiesel plant.

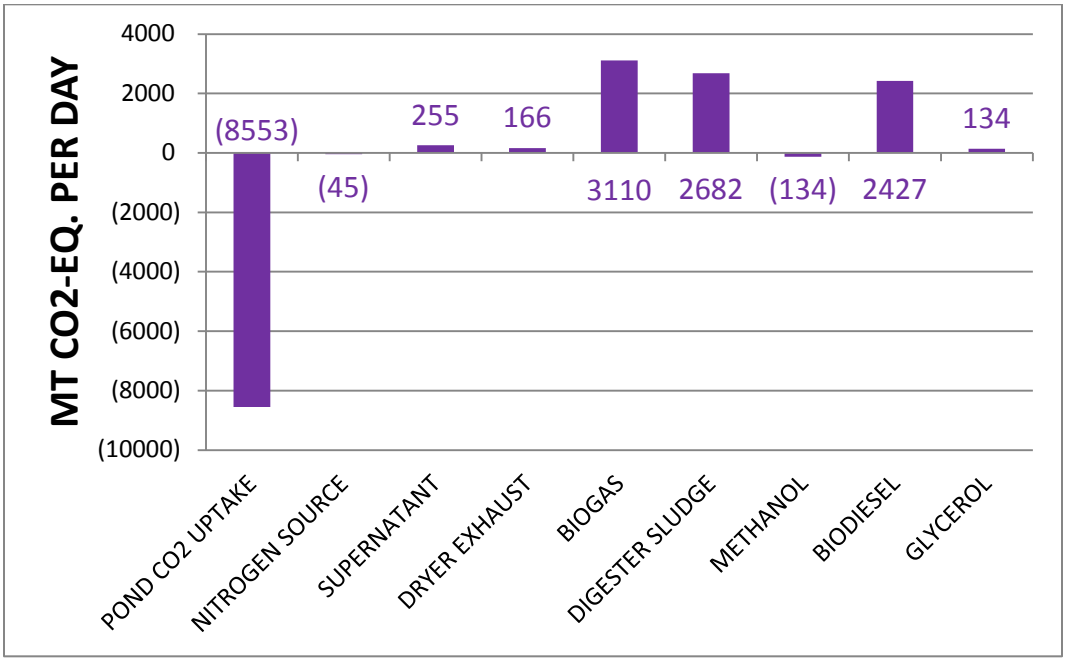

Figure 3.4. System Carbon Balance. Carbon mass fluxes expressed as carbon dioxide equivalents. Negative values indicate carbon inputs to the system; positive values indicate carbon discharges from the system. (Carbon fluxes are reported in units of metric tonnes of equivalent carbon dioxide per day.)

Note that roughly 31% of the carbon taken up in the ponds exits the system in the form of digester sludge, which is a mixture of anaerobic bacteria and undegraded LEA. The fate of this material is important in determining the ultimate carbon footprint of the biodiesel. It is also reassuring to find that the carbon entering the system as methanol exactly offsets the carbon exiting as glycerol. This matches the transesterification reaction stoichiometry, in which three moles of a single-carbon compound displace one mole of a three-carbon molecule.

Estimates of the annual plant operating costs are shown in Figure 3.5. These costs are based on southern California cost structures, including energy prices. The digestion step creates a net annual operating credit of $175MM. Without that credit, the unit manufacturing cost of the fuel would increase by roughly $1.75 per gallon. The impact of anaerobic digestion on the manufacturing process is explored more fully in Section 4.2.

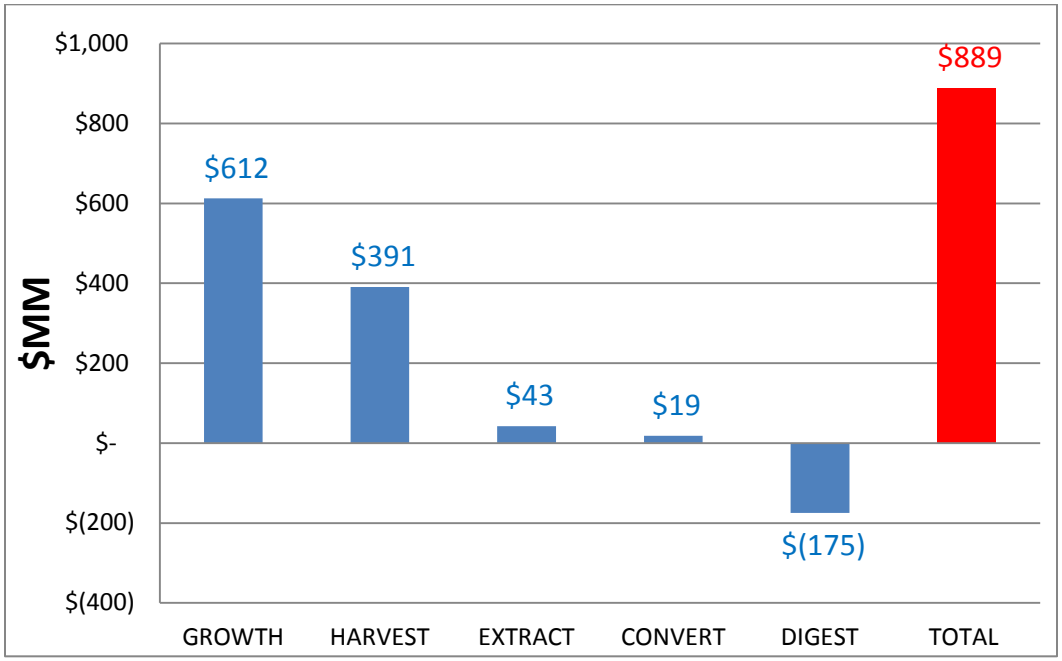

Figure 3.5. Annual Manufacturing Costs by Major Process Step, and overall. The costs for each major process step are determined without consideration of the nutrient recovery and energy recovery accomplished by the anaerobic digesters. The net cost of the digestion step represents the value of those recovered inputs, less the operating and maintenance costs of the digesters. (Annual costs are reported in units of millions of dollars.)

Although the cost of the harvesting step is high due to the high energy demand of the drying operations, the growth step has the largest contribution to total manufacturing cost. The full cost of nitrogen and phosphorus is roughly $250MM per year (this assumes no nutrient recycle from the digesters). The extraction and conversion steps each contribute less than 5% of the net cost of production.

A breakdown of the capital cost for the facility by major process step is shown in Figure 3.6. The cost of the lipid extraction and conversion plants is minor at the scale of this facility. Because of the different scaling rules used for estimating the capital cost of these two steps versus the other three (growth, harvesting and digestion), these percentages will be higher at smaller plant sizes.

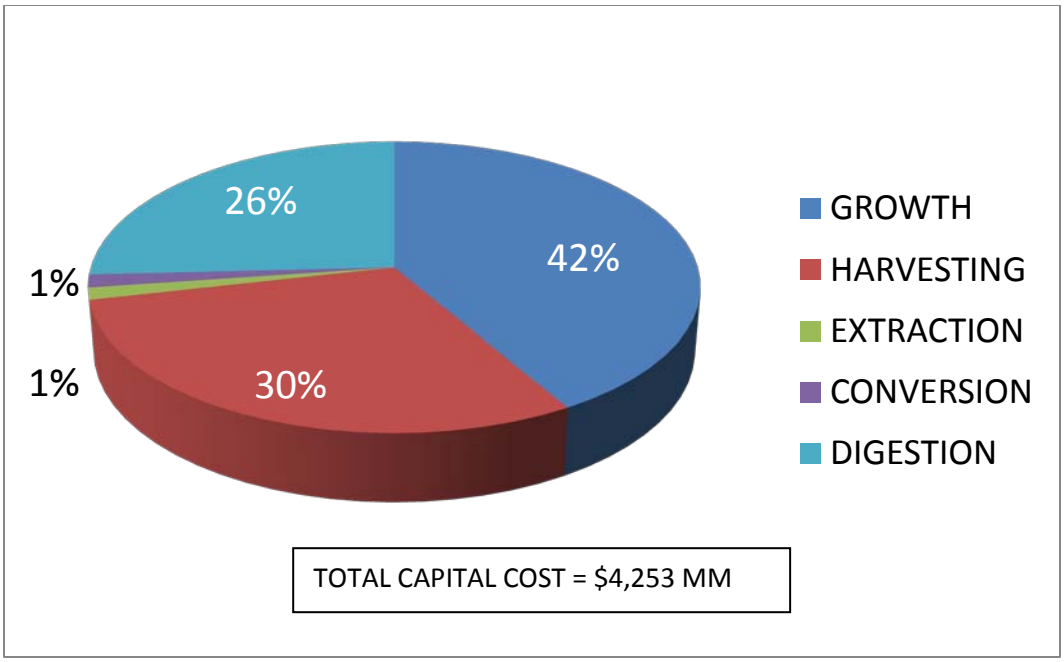

Figure 3.6. Facility Capital Cost, by Major Process Step. The extraction and conversion steps each contribute less than 1% to the total capital cost of the plant.

3.2 Sensitivity Analyses

TELCIM has a large scope; it models the technical, financial and environmental performance of a complex, multi-step, biochemical manufacturing process. Hundreds of input parameter values are required to run the model, and it is useful to know which parameters have strong influence on the performance characteristics of greatest importance (such as NER, CI, and unit manufacturing cost), and which inputs have little or no influence. One way to identify influential input parameters is to run multiple simulations in which only one input is varied, and the effect of that variation on key performance measures is evaluated. Finding the influential variables has several important implications. The modeler should be most concerned about ensuring the accuracy of highly influential inputs, since errors in those variables propagate most strongly. And more strategically, it is the influential parameters that should be the targets of research and development, since improvements in those aspects of the process will deliver the greatest benefits.

Two types of single-parameter sensitivity analyses are described in this section: tornado plots and trend plots. In these analyses, input parameters are treated as independent variables, which may not be the case in an actual production system.

3.2.1. Tornado Plots

The tornado plots in Figures 3.7, 3.8 and 3.9 illustrate the sensitivity of NER, CI, and manufacturing cost (respectively) to six input parameters that were individually varied by ±20%. "Oil Content" is the weight percent concentration of recoverable lipid in the microalgal cell mass, on an ash-free dry weight basis. "Dewatered Algae Conc." is the weight percent concentration of ash-free dry cell mass in water after dewatering and before drying. "Microalgae Productivity" is the average microalgal growth rate. "COD Removal Efficiency" is the percentage of chemical oxygen demand removed in the anaerobic digesters. "CO_2 Concentration" is the volume percent concentration of carbon dioxide in the flue gas feeding the ponds. "Power Plant Size" is a surrogate for the carbon dioxide feed rate.

Figure 3.7 indicates that among the variables selected, two biological properties – intracellular water content and oil content - have the greatest influence on the NER of the biodiesel. The areal productivity of the microalgae has little impact on NER; the energy footprint of the biodiesel is dominated by the energy and material inputs that vary with biomass production, and not productivity. The NER is completely insensitive to the size of the facility, for the same reason.

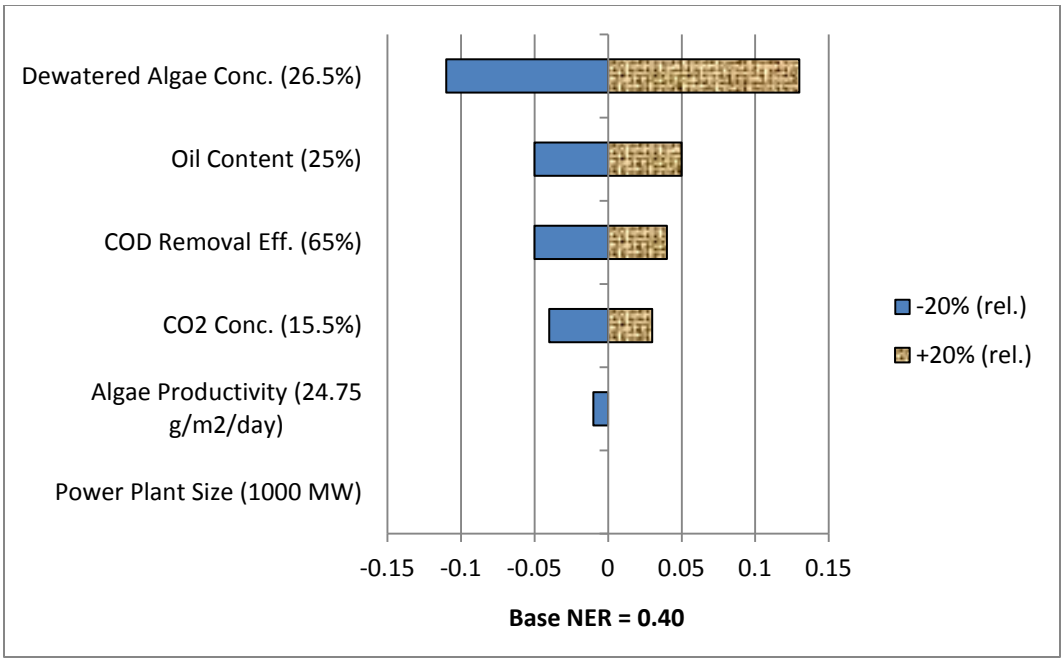

Figure 3.7. Tornado Plot Indicating the Sensitivity of Net Energy Return (NER) to several input parameters. Shown in parentheses after the name of each input variable is the value used in the Test Scenario. The solid bars indicate the change in NER from its base value of 0.40 when the input parameter value is decreased by 20% (relative), and the hatched bars indicate the results when the parameter value is increased by 20%. For example, when the oil content of the microalgae is assumed to be 20%, the NER is reduced to 0.35. The horizontal axis values indicate the deviation from the base value.

Of the six input parameters evaluated in Figure 3.8, the dry solids concentration exiting the dewatering operations is the most influential. This relates to the energy load imposed by drying the biomass to the Test Scenario target of 90% dry solids. As the residual water content of the cells increases, the drying load increases, and the amount of natural gas used for thermal energy goes up accordingly. The top solid (blue) bar shows that if the dry solids concentration of the biomass exiting the dewatering operations falls to 21.2%, the carbon intensity of the fuel almost doubles, to 137 gCO_2/MJ. The second most influential input parameter with respect to carbon intensity is the carbon dioxide concentration in the flue gas feeding the ponds. If the gas is more concentrated in CO_2, the volume of flue gas that must be pumped is lower, reducing electricity consumption.

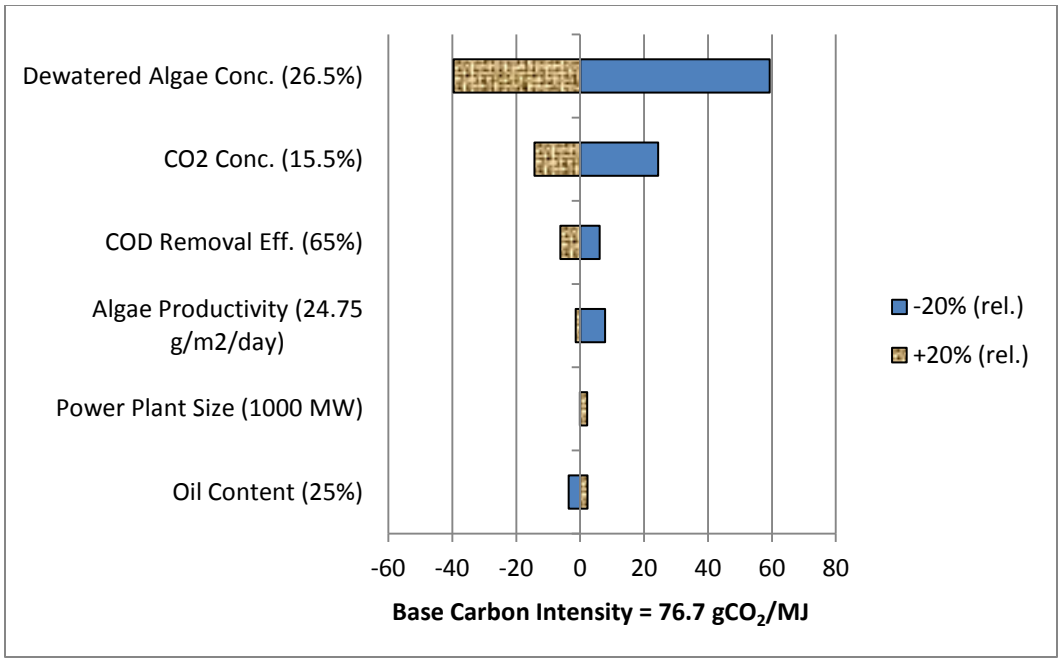

Figure 3.8. Tornado plot indicating sensitivity of biodiesel Carbon Intensity (CI) to several input parameters.

It might seem surprising that the carbon intensity is insensitive to oil content, since the biodiesel production rate is directly proportional to the oil content of the microalgae, and fuel energy content is in the denominator of the CI calculation. When there is less oil, there is more LEA going to the digestion step, which increases the amount of biogas produced. And because biogas has a lower carbon footprint than the purchased energy it displaces, these two effects tend to cancel one another, and the CI remains nearly constant.

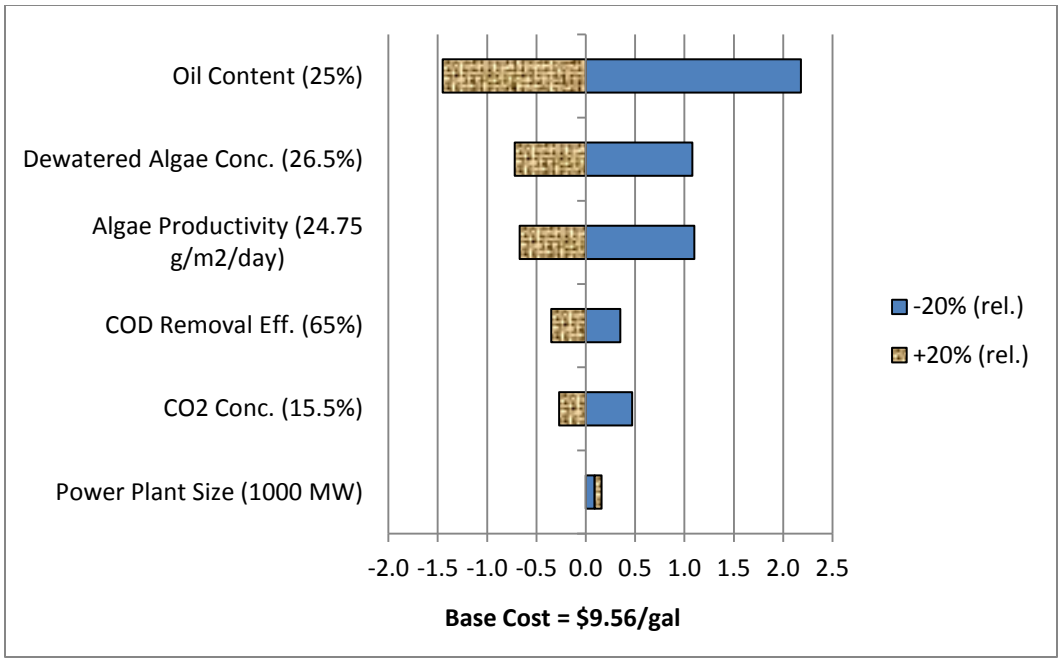

Figure 3.9. Tornado Plot Indicating the Sensitivity of Unit Biodiesel Manufacturing Cost to several input parameters.

Although carbon intensity is insensitive to the microalga's oil content, Figure 3.9 shows that the unit biodiesel manufacturing cost is highly sensitive to oil content. This reflects the direct dependence of biodiesel production rate on oil content. Considering that the cost of producing a unit of biomass is almost independent of its composition, increasing the oil content spreads those costs over a larger amount of fuel, lowering its unit cost. The dewatered algae concentration is also influential, due to the cost of purchased energy for the drying operations. Finally, algae productivity also strongly influences unit cost. This is because productivity affects facility size, and hence capital costs. And many of the operating costs, such as maintenance and interest on debt, are related to the capital cost of the facility.

3.2.2. Trend Analysis

Another type of single-parameter sensitivity analysis that can be used to identify input parameters with significant influence on critical system performance metrics is trend analysis. A base case simulation is created in which the most probable values of all input parameters are entered. Additional simulations are performed in which an individual input parameter is systematically varied over its expected range, and the

predicted values of important output parameters are plotted against the input parameter. The shape of the resulting curve indicates the nature of the relationship between the input and output parameters (e.g., linear, non-linear). The direction of a curve's slope indicates whether the variables are directly or inversely correlated, and the magnitude of the slope indicates the sensitivity of the output parameter to the input that was varied. No consideration is given for the probability distribution of the input parameters; the purpose of the trend analysis is to assess the response of important output parameters to changes in particular input variables.

Once influential variables are identified, the modeler can focus on improving their accuracy. These parameters should also be the preferred targets for research and development efforts, since they offer the greatest potential impacts on the performance characteristics of interest. Input parameters identified by trend analysis as being influential (i.e., those to which KPI's are most sensitive) are the ones that should be studied in an uncertainty analysis. Trends will also indicate whether a change in an input will cause all or some of the KPI's of interest to vary in the same or opposite direction (favorable or unfavorable). Otherwise, trade-offs will arise between improvements in some categories and deterioration in others.

To illustrate how one might use this technique with TELCIM, an analysis was made of the impact on the biodiesel Net Energy Return, carbon intensity, and unit manufacturing cost, of the following inputs to the anaerobic digestion process model:

- Nitrogen recovery efficiency factor (no units; base case value = 0.75)
- Phosphorus recovery efficiency factor (no units; base case value = 0.50)
- COD removal efficiency (no units; base case value = 0.65)
- Methane yield (cubic meters per kg of COD removed; base case value = 0.35)

Upper and lower bounds for these four variables were selected arbitrarily, but are intended to represent realistic limits for the corresponding parameters. Cases were run at the limits for each of the four parameters, and at increments of 0.05 in between. The biodiesel's NER, CI and unit manufacturing cost for each simulation were recorded, and are plotted below.

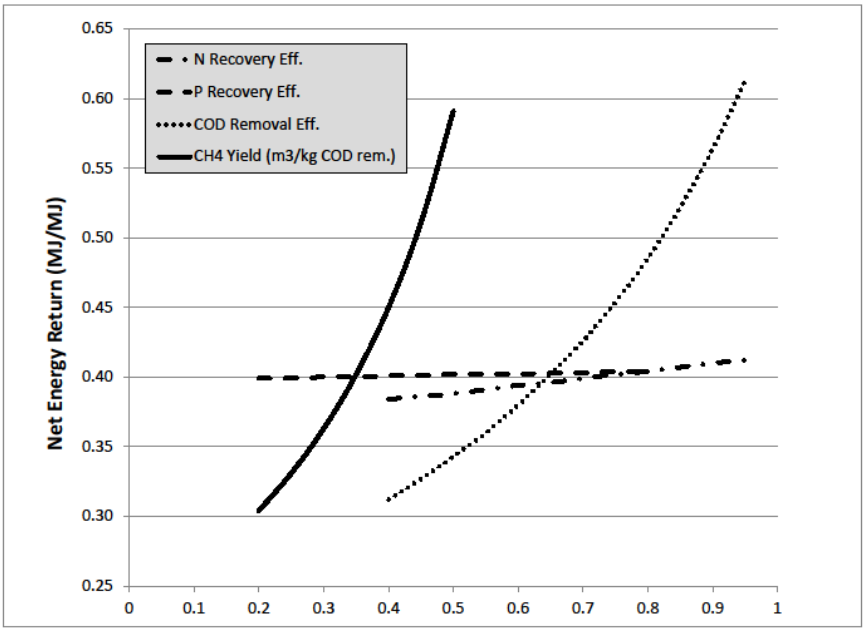

Figure 3.10. Trend Analysis of Anaerobic Digestion – Net Energy Return. Values for the four input parameters are shown on the horizontal axis

A plot of Net Energy Return as a function of several anaerobic digestion input variables is shown as Figure 3.10. It is apparent that the NER is relatively insensitive to the nitrogen and phosphorus recovery efficiency factors. This indicates that the energy consumed to produce and transport the nitrogen and phosphorus fertilizers used in the growth step contributes little to the overall energy footprint of the biodiesel. As expected, both curves have a positive slope, indicating that recycling nitrogen and phosphorus reduces overall energy use. The slope of the curve for the nitrogen recovery efficiency factor is larger than that for the phosphorus recovery efficiency factor, indicating that there is more embedded energy in the nitrogen source being added to the system than in the phosphorus source.

The NER is moderately sensitive to the COD removal efficiency factor, and is quite sensitive to methane yield. Both variables are positively correlated with NER. These conditions reflect the large impact that energy recovery in the digestion step has on the biodiesel's overall energy footprint. An increase in COD removal efficiency means more biogas is generated, reducing the demand for externally sourced energy.

(Since the biogas is part of an internal carbon loop, its energy content is not included in the calculation of the NER.) An increase in methane yield means the biogas has a higher energy content, also reducing the amount of energy that must be purchased from off-site.

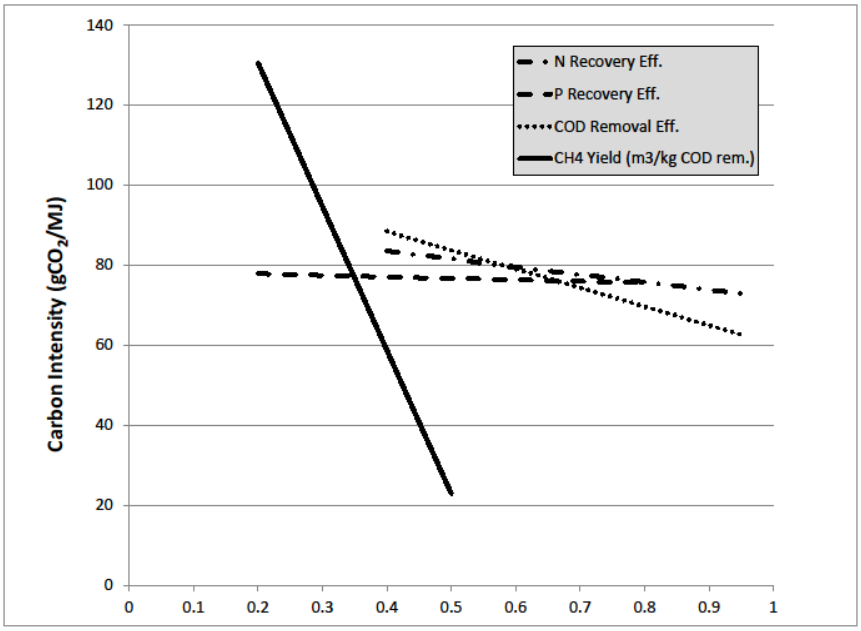

Figure 3.11. Trend Analysis of Anaerobic Digestion – Carbon Intensity.

The sensitivity of the biodiesel's carbon intensity to the input parameters of interest is shown in Figure 3.11. Varying the nitrogen and phosphorus recovery efficiencies has little impact on the carbon intensity of the biodiesel. As with energy, the manufacture and delivery of the nitrogen and phosphorus fertilizers does not contribute significantly to the overall carbon intensity of the biodiesel manufacturing process. The negative slope of each of these curves indicates that recycling nitrogen and phosphorus entails lower carbon dioxide emissions than manufacturing and delivering them to the biodiesel plant.

The biodiesel's carbon intensity is also relatively insensitive to the COD removal efficiency. If less COD is removed, more carbon remains fixed in the un-degraded material, and less is converted back to CO_2 in the combusted biogas. But the energy that would have been extracted from the biogas has to be supplied from external sources, so the carbon emissions are similar; they simply occur elsewhere. The

negative slope indicates that using biogas has a lower carbon intensity than relying on purchased energy streams. In contrast, the CI is very sensitive to the methane yield. When the carbon in the residual biomass is broken down in the digesters, it is mostly converted either to methane or carbon dioxide (the ratio of these two products is a function of the oxidation state of the biomass being degraded). So as the methane yield goes down, there is a corresponding increase in the amount of carbon dioxide generated. This is in addition to the carbon dioxide generated off-site, to supply the site's energy demand.

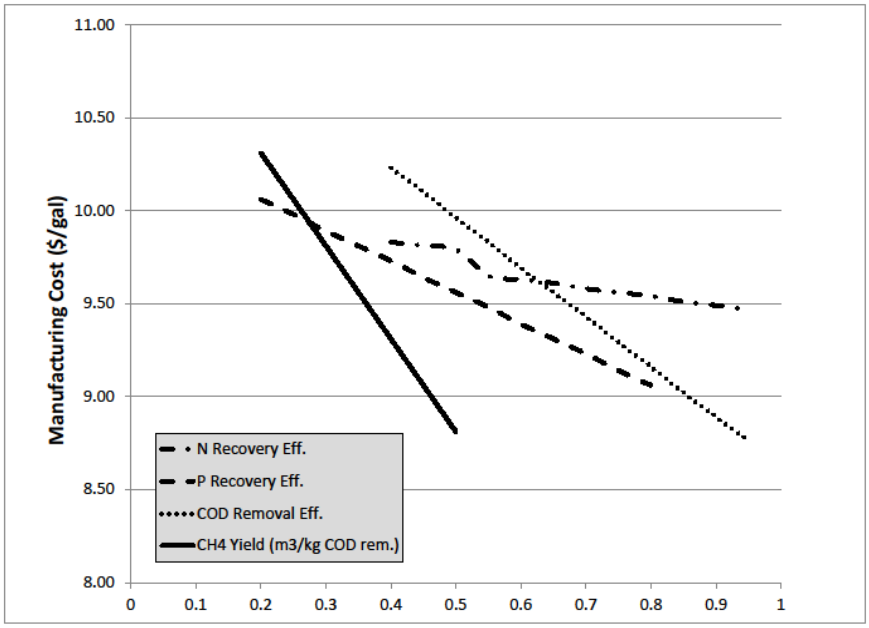

Figure 3.12. Trend Analysis of Anaerobic Digestion – Manufacturing Cost.

Of the four variables shown in Figure 3.12, unit biodiesel manufacturing cost appears to be least sensitive to the nitrogen recovery efficiency. The curve for this parameter has a negative slope, and contains an inflection point. As the nitrogen recovery efficiency in the digesters declines, the amount of nitrogen fertilizer being added must increase commensurately. But the nitrogen source used in the Test Scenario, urea, contains carbon, and the model adds this carbon to the carbon dioxide which is converted into biomass. At a fixed biomass productivity, a larger carbon load requires more illuminated surface area, and the model computes the number of additional ponds needed. But because TELCIM aggregates

ponds into modules, and the number of modules is a discrete quantity, and at some point TELCIM determines that an additional module is required. An additional module brings with it many fixed costs, such as operating labor, maintenance, and other overheads, causing an apparent step change in biodiesel cost. The “knuckle” in the nitrogen curve occurs at the total carbon loading at which TELCIM models that another biomass production module is required.

Surprisingly, the slope of the phosphorus recovery factor curve is greater than that for the nitrogen recovery factor curve. Because the mole ratio of nitrogen to phosphorus in the microalga is more than ten to one, the same relative increase in these two recovery factors means that more than ten times as many moles of nitrogen are being recovered than are moles of phosphorus. But the cost of the phosphorus fertilizer (superphosphate), on a molar basis, is so much higher than that of urea that it more than offsets this 10:1 ratio. And because superphosphate contains no carbon, there are no inflections points in that curve.

Manufacturing cost is moderately sensitive to the COD removal efficiency; if the LEA is more degradable than is modeled by the Test Scenario, the biodiesel cost could be reduced by as much as $0.50-$1.00 per gallon. Unit cost is slightly more sensitive to methane yield, and COD removal efficiency and methane yield are both negatively correlated with manufacturing cost.

3.3. Conclusions

The microalgal biodiesel production cost and NER predicted by the Test Scenario fall well within the ranges predicted by other modeling efforts reported in the literature, helping to validate TELCIM’s integrity and functionality.

TELCIM is designed to isolate the impacts of the anaerobic digestion step on biodiesel cost and energy, carbon and water footprints. In the Test Scenario, anaerobic digestion reduces net manufacturing cost and improves sustainability by lowering the demand for purchased nutrients and energy. It predicts that the equivalent monetary value of the residual biomass is on the order of $175 per tonne, and roughly 30%

of the carbon dioxide converted to biomass in the cultivation step is tied up in the biomass exiting the digesters. The ultimate fate of this byproduct is critical in assessing the overall carbon footprint of the modeled microalgal biodiesel manufacturing process, and highlights an important difference between a cradle-to-gate LCI and a cradle-to-grave LCI. If the digester sludge is managed in a way that its constituent carbon is ultimately released as CO_2, then the Test Scenario predicts that the overall carbon intensity of the biodiesel will be substantially higher than that of petrodiesel.

It is apparent from the tornado plots that the modeled biodiesel production scheme has almost no economies of scale; changing plant size has little impact on the KPI's. Capital costs are largely driven by illuminated surface area, which scales linearly with biomass production. Similarly, operating cost, NER and CI are dominated by variable inputs such as ingredients and energy. While this suggests that the penalties for distributed manufacturing will be small, the number of viable manufacturing sites will be limited by the availability of large tracts of flat land near sources of carbon dioxide and make-up water. In particular, water requirements in dry climates may represent a barrier to facility siting. The tornado plots also show that the KPI's respond quite differently to different input parameters, demonstrating that there can be trade-offs among the KPI's, and system optimization will depend on the relative weights placed upon them.

From the Trend Analysis, it appears that the COD removal efficiency and methane yield are influential variables – one or more of the NER, CI, and manufacturing cost are sensitive to those inputs. In comparison, the nitrogen and phosphorus recovery efficiencies are less influential. As a result, the digestion step should be optimized for biogas production, and not for nutrient recovery. And because they are influential, COD removal efficiency and methane yield might be included among those variables that would be studied in an uncertainty analysis. This topic will be covered in more detail in Chapter 6. All four of the input variables evaluated in the Trend Analysis have a positive slope with respect to NER and a negative slope with respect to CI and cost across their entire range. This means that increases in nutrient recovery, COD removal, and methane yield improve all three of the KPI's; in no case did a

change in an input variable improve one KPI and degrade another. And in none of the simulations run for these sensitivity analyses did the NER exceed 1.0.

These preliminary results from the Test Scenario underscore the need for continued research on microalgal biology and biodiesel manufacturing process technologies. There is also a need for large-scale demonstration plants, to provide coherent data sets for further modeling and reduce uncertainty in the model's predictions.

3.4. References for Chapter 3

[1] Lundquist, T.J, I.C. Woertz, N.W.T. Quinn, and J.R. Benemann (2010). A Realistic technology and engineering assessment of algae biofuel production. Energy Biosciences Institute, University of California, Berkeley, California, USA.

[2] Haas, M.J., A.J. McAloon, W.C. Yee, and T.A. Foglia (2006). A process model to estrimate biodiesel production costs. Bioresource Technology 97, 671-678.

[3] U.S. Energy Information Agency (2011). Annual Energy Review 2010. Table 5.13c. Washington D.C., USA.

[4] Wang, M. (1999). The Greenhouse Gases, Regulated Emissions, and Energy Use in Transportation Model (GREET), v.1.8d.1, Copyright 1999, University of Chicago Argonne LLC. Accessible at http://www.greet.es.anl.gov.

4. CASE STUDIES*

4.1. Introduction

Washington University in St. Louis recently released, as freeware, a techno-economic life-cycle inventory model ("TELCIM") of microalgal biodiesel manufacture. Implemented in Microsoft Excel®, the model is accessible at www.openscholarship.wustl.edu. It simulates a biodiesel manufacturing process consisting of five major steps. Microalgal biomass is cultivated continuously in raceway ponds fed an industrial gas containing carbon dioxide. The biomass is then concentrated by consecutive sedimentation, thickening, filtration, and forced air drying operations. Neutral lipids are extracted from the dry biomass using hexane leaching, and are then converted to methyl esters in an aqueous alkali-catalyzed transesterification process. Finally, the residual biomass (lipid-extracted algae, or LEA) is anaerobically digested to recover nutrients for recycle to the growth step, and to produce biogas, which is burned to produce electricity and process heat.

A review of prior microalgal biodiesel modeling efforts showed that there is considerable uncertainty in the financial viability and environmental sustainability of this alternative fuel[1]. These models also generally focused on either the economics or environmental footprint of the biodiesel manufacturing process, which motivates the development of an integrated techno-economic-environmental model of biodiesel production. That manuscript also provided detailed descriptions of TELCIM's component physical, financial and life cycle inventory (LCI) models, listed many of the input parameter values used to populate a base case (the "Test Scenario") and key results from that case, and showed examples of sensitivity analyses used to identify influential input parameters. The purpose of this article is to report on several variants to the Test Scenario in which the impacts of alternative production processes, manufacturing site locations, and modeling time-scales, were investigated.

---

* *This chapter in its entirety is taken from a manuscript that is being prepared for publication; only the Abstract and Acknowledgments section of that manuscript are not reproduced here. Some of the formatting of the original document has been altered to conform to the format of the remainder of the dissertation.*

The Test Scenario models commercially demonstrated process technologies deployed near the Salton Sea in the southern California desert. This hypothetical biodiesel plant uses flue gas from a 1000MW_e coal-fired electric power plant as its carbon dioxide source, and 100 million gallons per day of municipal secondary effluent as a supplemental source of nutrients and make-up water. Urea and superphosphate are used as nitrogen and phosphorus sources, respectively, and all of the microalga's other nutritional requirements are assumed to be supplied directly from the environment or are inconsequential to the analysis.

4.2. Variants of the Test Scenario

Several variants of the Test Scenario were generated to predict the likely effects on key biodiesel performance indicators (KPI's) of potential improvements in process technology and microalga properties. Table 4.1 identifies these variant cases, the major input parameters that were varied, and TELCIM's predictions for three benchmark KPI's: biodiesel manufacturing cost ($/gal), Net Energy Return (defined as the ratio of biodiesel fuel energy to the total life cycle fuel energy consumed in its manufacture, with units of MJ/MJ), and carbon intensity (defined as the ratio of total life cycle carbon dioxide mass emissions to fuel energy content, with units of gCO_2/MJ). Also shown for comparison are estimates of the Net Energy Return (NER) and carbon intensity (CI) for diesel fuel produced from petroleum[2,3]. (Note that the carbon intensity for biodiesel reported here includes CO_2 emissions resulting from biodiesel production and use; an exception to the "cradle-to-gate" basis for TELCIM. This puts the carbon intensity estimates generated by TELCIM on the same basis as those typically reported for other fuels.)

Table 4.1: Variants to the Test Scenario						
	INPUTS			OUTPUTS		
	Algae Productivity (g/m^2-day)	Lipid Content (%,afdw)	Water Content at Extraction (%, wt.)	Production Cost ($/gal)	Net Energy Return (MJ/MJ)	Carbon Intensity (gCO_2/MJ)
Petro-Diesel	N/A	N/A	N/A	(?)	4.35	84.3
Test Scenario	24.75	25	10	9.56	0.40	76.6
NAABB R&D Targets	20	50	10	5.72	0.56	87.3
No Drying	24.75	25	73.5	6.28	1.34	(40.4)
NAABB Targets and No Drying	20	50	73.5	4.08	1.43	16.7
No Anaerobic Digestion	24.75	25	10	11.32	0.22	117.1

The National Alliance for Advanced Biofuels and Bioproducts (NAABB) is a government-industry consortium that funds research in the area of algal biofuels. NAABB has promulgated several R&D targets for microalgal biofuel processes, including an areal productivity of 20 g/m^2-day and a recoverable lipid content of 50% (dry weight basis)[4]. The "NAABB R&D Targets" variant is identical to the Test Scenario except for these two microalgal properties. As shown in Table 4.1, the improved lipid yield envisioned by the NAABB case dramatically reduces unit biodiesel manufacturing cost versus the Test Scenario, since a much higher percentage of the carbon dioxide taken up in the ponds is ultimately converted to biodiesel rather than a byproduct. For the same reason the NER increases, but not enough to achieve a positive energy balance (i.e., NER > 1.0). And although the NER improves, the CI does not. Because a higher percentage of the carbon taken up in the ponds is converted to fuel, more of it is ultimately returned to the atmosphere as CO_2, and less of it is sequestered in the form of byproducts (e.g., glycerol, anaerobic digester sludge).

Drying the microalgal biomass to the residual moisture content required by conventional oilseed extraction technology consumes a large amount of energy, with corresponding environmental impacts. A

water-tolerant, or “wet” extraction process has the potential to improve the energy, environmental, and economic performance of microalgal biodiesel. Without knowing any of the details of such an alternative process, it is possible to estimate its impact on the KPI’s by increasing the moisture content entering the extraction step to 73.5%, a value based on the intracellular water content of a typical microalga[5], and which should be achievable by mechanical dewatering alone. Since the capital and operating cost structures of such a hypothetical process are unknown, the “No Drying” variant retains the capital and non-energy operating cost structures for the drying and extraction steps used in the Test Scenario. The reduction in energy usage in the “No Drying” case leads to a significant cost reduction and large improvements in NER and CI. Although the NER indicates a positive energy balance, it is still well below the target of 3.0 for algal biofuels acknowledged by the National Research Council of the National Academies[6]. The negative CI value indicates net carbon sequestration, even when accounting for the carbon released upon biodiesel combustion. (Because TELCIM is a “cradle-to-gate” LCI model, it is assumed that the carbon present in the byproducts of biodiesel manufacture remains fixed).

The variant labeled “NAABB Targets and No Drying” combines the microalgal productivity targets of the NAABB case and the revised process conditions of the No Drying case. It is intended to simulate the effects of improvements in both microalgal biology and process technology. Combining the NAABB productivity targets with wet extraction gives the lowest cost and highest NER of the variants considered. Even so, at an NER of 1.43, if the biofuel produced was used to supply the energy required by the biodiesel manufacturing process (including upstream life cycle usages), roughly 70% of the fuel would be consumed and only 30% would be available as product. The CI for this variant is considerably lower than that of petroleum diesel.

Anaerobic digestion is not integral to the manufacture of microalgal biodiesel, but it has often been incorporated into proposed biodiesel manufacturing schemes because it is expected to reduce operating cost and external energy use[7,8,9,10]. These assumptions were tested by simulating a facility without anaerobic digestion. The “No Anaerobic Digestion” variant is the same as the Test Scenario, except that all of the cost and process impacts of the digesters are nullified. (This was achieved by adjusting several

input parameters, including setting to zero all of the capital and operating costs assigned or allocated to the digestion step, the digester nutrient recovery efficiency factors, and the biogas generation rate). The inclusion of anaerobic digestion in the overall process scheme appears justified, since it reduces unit manufacturing cost, improves NER, and reduces carbon intensity. Because TELCIM is a "cradle-to-gate" life cycle inventory model, these results do not account for the ultimate fate of the waste biomass from the digesters, which in the Test Scenario accounts for roughly 30% of the carbon taken up in the ponds. The unfavorable manufacturing cost variance for the No Digestion case can be eliminated or even reversed if the LEA is sold at a high enough price. (For the conditions modeled in the Test Scenario, TELCIM predicts the break-even price of the LEA is around $175 per tonne.) The NER and CI of the biodiesel could also be improved or worsened, depending on the fate of the LEA, and in particular, what other products it might displace (e.g., animal feed), and the environmental burdens resulting from the production and use of those displaced products. The wide variety of options for the fate of the byproducts from the microalgal biodiesel manufacturing process is one of the reasons TELCIM is limited to a "cradle-to-gate" LCI model.

Additional outputs from the Test Scenario and the "No Anaerobic Digestion" variant are shown in Table 4.2 ("With Anaerobic Digestion" and "Without Anaerobic Digestion", respectively). This table illustrates how TELCIM reports cost structures, energy profiles, and carbon balances. For example, TELCIM computes energy and resource burdens in the other major process steps assuming that no nutrients or energy are recovered in the anaerobic digestion step. The energy and nutrients recovered in the digesters are treated as credits, which offset equivalent amounts of purchased raw materials and energy. (The small differences in values for the growth, harvesting, extraction and conversion steps between the Test Scenario and the "No Anaerobic Digestion" case arise because urea was used as the nitrogen source in the growth step. Since urea contains carbon, and more urea is used in the "No Anaerobic Digestion" case, slightly more biomass is produced in that case, leading to small differences in the cost, energy and carbon profiles.)

Table 4.2: Impact of Anerobic Digestion								
	OPERATING COST ($MM/yr)		**CAPITAL COST ($MM)**		**NET ENERGY USAGE (MW)**		**CARBON INTENSITY (gCO2/MJ)**	
	With Anaerobic Digestion	Without Anaerobic Digestion	With Anaerobic Digestion	Without Anaerobic Digestion	With Anaerobic Digestion	Without Anaerobic Digestion	With Anaerobic Digestion	Without Anaerobic Digestion
Growth Step	612	623	1769	1857	633	634	(154.5)	(148.7)
Harvesting Step	391	407	1270	1337	1038	1078	183.8	183.8
Extraction Step	43	44	56	57	35	36	5.5	5.5
Conversion Step	19	19	61	63	34	35	2.2	2.2
Digestion Step	(175)	0	1096	0	(799)	0	(34.7)	0
Production Total	889	1093	4253	3314	941	1783	2.3	42.8
	UNIT MANUFACTURING COST ($/gal)		CAPITAL COST PRODUCTIVITY ($/gal/yr)		NET ENERGY RETURN (MJ/MJ)		CARBON INTENSITY INCLUDING FUEL COMBUSTION (gCO_2/MJ)	
Overall	9.56	11.32	45.71	34.32	0.40	0.22	76.6	117.1

The capital cost for the facility with anaerobic digestion is roughly 33% higher than for the facility without it, but its operating costs are lower due to reduced raw material and energy purchases. The net cost savings (after accounting for the operating and maintenance costs of the digestion step) generate an IRR of 17% on the incremental capital investment. The effect of anaerobic digestion on the energy footprint of the biodiesel is very large; burning biogas on-site reduces energy purchases by almost half. Anaerobic digestion also has a large impact on the carbon footprint of the biodiesel; with anaerobic digestion the overall biodiesel manufacturing process is almost carbon neutral (assuming the carbon in the byproducts remains fixed).

4.3. Seasonality Analysis

TELCIM models continuous, steady-state operation of the biodiesel manufacturing plant. The assumption of steady state operation may be suitable for a well-controlled industrial process, but microalgae cultivation in ponds will be subject to variable ambient conditions. In the Test Scenario, annual average values were used for input parameters such as climatological conditions and the microalga's areal productivity. However, it is clear that in the continental United States these parameters will be inconstant over the span of an entire year. The areal productivity, for instance, will be affected by seasonal and diurnal variations in solar irradiance. The following analysis is intended to determine to what extent seasonal variations in sunlight intensity might affect the KPI's for the biodiesel manufacturing process.

TELCIM includes a photosynthetic efficiency model with which the microalga's areal productivity can be estimated from sunlight intensity[12,13]:

$$P_{mass} = E_s \left[\frac{C_{PAR} \tau_p \varepsilon_f \varepsilon_s \varepsilon_a M_A}{Q_r C_c \hat{E}_p} \right] \tag{4.1}$$

where P_{mass} is algal productivity (kg/m^2-day), E_s is sunlight intensity (kJ/m^2-day), C_{PAR} is the fraction of sunlight that is photosynthetically active, τ and ε represent efficiency factors for transmission, fluorescence, light saturation and biomass conversion, C_c/M_A is the mole concentration of carbon in the

microalga (kg-mol/kg), Q_r is the quantum yield, and $\hat{E}_p$ is the average energy content of photosynthetically active radiation (kJ/kg-mol). Most of the parameters in the brackets in Equation 4.1 are constant or near-constant for a given organism and reactor design. As a first approximation, a linear relationship between productivity and incident sunlight intensity can be assumed:

$$P_{mass} = kE_s \tag{4.2}$$

where k is a proportionality constant (kg/kJ). Once this constant is known, changes in areal productivity can be estimated from the seasonal variations in sunlight intensity. Equation 4.2 represents an idealized model in which every incremental photon of photosynthetically active sunlight is converted to biochemical energy with equal efficiency. The proportionality constant for the "NAABB R&D Targets" case was calculated by substituting into Equation 4.2 the annual average daily sunlight intensity in the Salton Sea area of southern California (5.67 kWh/m^2-day) and the NAABB areal productivity target (20 g/m^2-day). The Western Regional Climate Center, an arm of the National Oceanic and Atmospheric Administration (NOAA), was the source of daily sunlight intensity data for the Salton Sea site[14]. The average daily sunlight intensity for each month of the year for the period 1994-2010 was computed from the WRCC data, and are plotted in Figure 1. Equation 4.2 was then used to calculate the areal productivity for each month of the year from the average daily sunlight intensity during that month. The WRCC database also reports the monthly average temperature, relative humidity, and precipitation for each year in this time range; long-term averages for these TELCIM input parameters for the 1994-2010 time period were also computed. The monthly average pan evaporation rate (the only other climatological input required by TELCIM) was obtained from the California Climate Data Archive for the Indio, California, reporting station, for the period 1927-2002[15]. (The time span over which pan evaporation data was averaged differed from that used for the other climatological inputs because the CCDA database only reports the monthly pan evaporation rate averaged over this entire time span; it does not report separate monthly figures for each year within that range. In addition, CCDA's database does not include a Salton Sea monitoring station; the Indio and WRCC's Salton Sea monitoring stations are approximately 30 miles apart.)

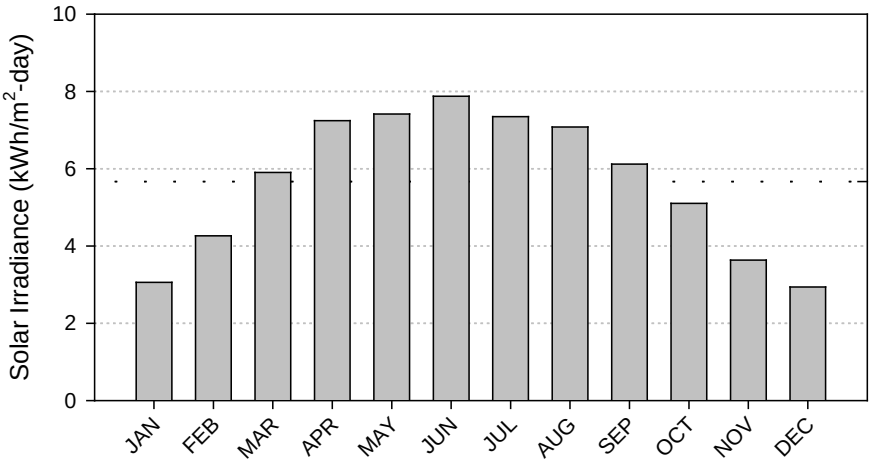

Figure 4.1: Average Sunlight Intensity for Salton Sea, California. Data from the California Climate Data Archive for the time period 1994 through 2010. The dashed line indicates the annual average (5.67 kWh/m^2-day) over this time span.

TELCIM uses the microalga's areal productivity to predict the illuminated surface area required to convert a specified amount of CO_2 to biomass. However, for this analysis it was necessary to determine how much biomass will be produced in a facility of fixed size under different productivity conditions. To specify the size of the facility, it was necessary to define a design basis for the facility. There are two cases which represent the bounds of realistic design bases: the facility either maximizes sunlight utilization or carbon dioxide uptake. These alternatives nicely conform to two simple design bases. In the first, sunlight utilization is maximized by sizing the facility based on the highest monthly productivity (June in the Salton Sea area; Fig. 4.1). As productivity falls off in other months, the ponds convert less carbon dioxide to biomass, and the excess carbon dioxide is vented. In the other design basis, carbon utilization is maximized by sizing the facility based on the lowest productivity month. This ensures that all of the carbon dioxide that is available for conversion to biomass is converted every month. In months with higher sunlight intensity, less illuminated surface area is required to achieve the same biomass production rate. So, as sunlight intensity and hence biomass productivity increases, some ponds are taken out of service, avoiding some operating costs.

Variant cases representing these two alternative design bases were modeled, each as a set of 12 monthly TELCIM simulations. The "base case" for this analysis was the "NAABB R&D Targets" case described earlier (Table 4.1), in which the annual average areal productivity of 20 g/m^2-day, and annual average climate data were used. The proportionality constant in Equation 4.2 was determined using this base case (k = 3.529 g/kWh), and for the monthly simulations, the areal productivity was calculated using the monthly average sunlight intensity in Equation 4.2. To isolate the impacts on the KPI's of using monthly productivity values instead of the assumed annual average of 20 g/m^2-day, annual average climate data were used in these simulations rather than monthly average data. The simulation outputs were then annualized, using volume-averaging when appropriate (e.g., unit production cost). The results, which are shown in Table 4.3, clearly indicate that the maximum productivity design basis has a much better cost structure – in the minimum productivity case too much capital equipment is idle too much of the time. The maximum productivity case also has a smaller environmental footprint, as indicated by the values returned for NER, CI and water intensity.

Table 4.3: Seasonality Analysis for Salton Sea Location

	Biodiesel Production Volume (Mgal/yr)	Biodiesel Production Cost ($/gal)	Areal Productivity (gal/acre-yr)	Capital Productivity ($/gal)	Net Energy Return (MJ/MJ)	Carbon Intensity (gCO_2/MJ)	Water Intensity (gal/gal)
Petro-Diesel	N/A	N/A	N/A	(?)	4.35	84.3	(?)
NAABB R&D Targets	187	5.72	3171	25.14	0.56	87.3	781
Max. Productivity & Annual Average Weather Data	134	5.74	3165	26.95	0.56	86.9	825
Min. Productivity & Annual Average Weather Data	187	8.00	1643	44.18	0.53	96.4	865
Max. Productivity & Monthly Avg. Weather Data	134	5.74	3166	26.95	0.57	87.0	827

The first of the 12 simulations run for the maximum productivity case was for the month of June, which had the highest sunlight intensity and hence the highest predicted biomass productivity (Fig. 4.1). This fixed the size of the facility at 3347 4-hectare ponds, as compared to 4650 ponds in the base case. For

each of the other months, the carbon dioxide feed rate was iterated until the model predicted that 3347 ponds were required (Excel's "Goal Seek" function was used to perform these iterations). As a consequence of the assumption of proportionality between sunlight intensity and productivity, the production cost, NER and carbon intensity in the maximum productivity case are virtually unchanged from the base case. On the other hand, the annual biodiesel production volume is substantially lower, consistent with the smaller illuminated surface area. Another important difference between the maximum productivity case and the annual base case is with regard to water intensity. Because less biomass is produced in all but the peak sunlight month, but the rate of evaporation is held constant at the annual average, the water intensity is higher for the month-by-month simulation. The capital productivity in this case is also slightly poorer than in the annualized base case, as would be expected of a facility with a large turndown ratio over a full annual cycle.

In contrast, the initial simulation for the minimum productivity case modeled December, which had the lowest predicted monthly productivity (Fig. 4.1). This fixed the facility size at 8972 ponds, almost double the illuminated surface area of the base case. In the remaining monthly simulations TELCIM predicted the minimum number of ponds necessary to process the desired amount of carbon dioxide, based on the higher biomass productivity. This led to some electricity savings, but operating labor and maintenance costs were held constant - it was assumed that the labor force could not be upsized and downsized throughout the year as the number of ponds in operation changed. As expected, the annual biodiesel production volume for this case is the same as in the base case, but the capital cost productivity is much worse ($44.18 vs. $25.14 per gallon/year of installed capacity), and the unit manufacturing cost is much higher. Both the NER and CI are less favorable for this case compared to the maximum productivity design basis, so all four of these performance metrics appear to favor the facility designed to maximize sunlight utilization.

Another goal of the seasonality analysis was to determine whether there is any significant difference in the KPI's using climate data averaged over shorter timescales. Another set of 12 simulations was run, using the maximum productivity design basis, and month-by-month climate data. Key outputs from this

set of simulations, which are reported on the bottom line of Table 4.3, suggest that using annual average data instead of monthly climate data does not change the model's predictions for the Salton Sea location.

4.4. The Light Saturation Effect

Since it appears that seasonality effects can be significant, it is appropriate to reconsider how areal productivity is expected to vary with season. A linear relationship between sunlight intensity and biomass productivity assumes that the light energy of every photon is converted to biochemical energy with the same efficiency. But it is known that photosynthetic systems, including those present in microalgae, saturate at relatively low light intensity[16,17], so this assumption may be too optimistic. By including a correction for the light saturation effect (LSE) when calculating biomass productivity, it is possible to determine to what extent light saturation affects the KPI's.

The light saturation efficiency factor that appears in Equation 1 can be estimated using the Bush Equation[18]:

$$\varepsilon_s = \begin{cases} \frac{E_0}{E_s}\ln\left(\frac{E_s}{E_0}+1\right), if\ E_s > E_0 \\ 1 \qquad\qquad\qquad\quad , if\ \ E_s \le E_0 \end{cases} \tag{4.3}$$

where E_0 is a species-specific light saturation constant. A plot of the Bush Equation is shown as Figure 4.2, with E_0 taken as 150 μmol/m^2-sec, a value used previously to characterize microalgae[13].

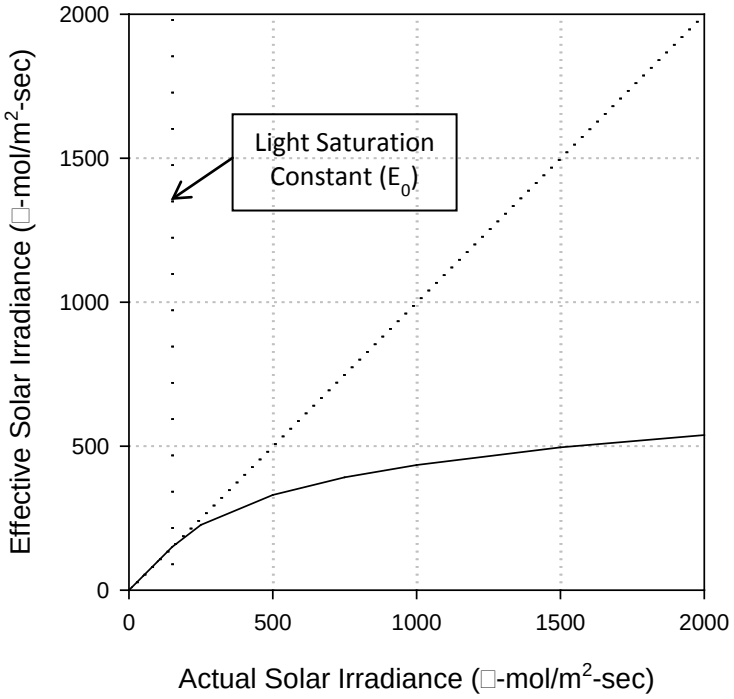

Figure 4.2: Plot of the Bush Equation. Effective solar irradiance as a function of total solar irradiance (E_s), with the light saturation constant (E_0) equal to 150 μmol/m^2-sec. The diagonal dotted line represents no light saturation effect (i.e., $\varepsilon_s = 1$ for all values of E_s).

Assuming the other factors in Equation 4.1 remain constant, Equation 4.2 can be rewritten as:

$$P_{mass} = k' \varepsilon_s E_s \tag{4.4}$$

where k' is a new proportionality constant. The predicted monthly average areal productivities using Equations 4.2 and 4.4 were calculated based on sunlight intensity and weather data obtained for Memphis, Tennessee. The annual average direct plus diffuse sunlight intensity at a Memphis monitoring station for the period 1991-2005 was obtained from NREL's National Solar Radiation Database[19]. That value is 5.68 kWh/m^2, almost exactly the same intensity reported for the Salton Sea site in the California Climate Data Archive. The NSRDB lists the average daily sunlight intensity for each month of the year for the span 1991-2005, as well as for each individual year in that span. First, the normalization constant assuming a linear relationship between light intensity and biomass productivity (k in Equation 4.2) was calculated for the Memphis site assuming the NAABB areal productivity target of 20 g/m^2-day. The

productivity for each month was then calculated by scaling the sunlight intensity to that annual average, using Equation 4.2. The resulting monthly average areal biomass productivities are shown in Figure 4.3a ("Memphis without LSE"). The annual average solar intensity at Memphis was then used in Equation 4.3 to calculate ε_s. This value (0.441) was used in Equation 4.4, along with the NAABB productivity target of 20 g/m^2-day, to calculate a new scaling constant (k' = 8.383 g/kWh), and then Equation 4.4 was used to estimate month-by-month values of the areal biomass productivity. These productivities, which are corrected for light saturation ("Memphis with LSE"), are plotted alongside the "uncorrected" values in Figure 4.3a. Also shown are the standard deviation and range for each data set; applying the correction for light saturation greatly reduces the variation in monthly biomass productivity values.

To determine whether similar results obtain for another geographic location, the same analysis was performed for Bakersfield, California, using monthly average sunlight intensity data for that site obtained from the NSRDB for the period 1991-2005. To retain the effect on biomass productivity of any difference in overall sunlight intensity at the two sites, the correlation factors derived for the Memphis cases (k and k') were also used in the Bakersfield simulations. The results are shown in Figure 4.3b.

At both sites, applying the light saturation effect significantly reduces the month-to-month variation in effective sunlight intensity. The expected advantage in biomass productivity of the site with higher average sunlight intensity is retained - compare Bakersfield without LSE to Memphis without LSE, or Bakersfield with LSE to Memphis with LSE - but that advantage is significantly diminished when the light saturation effect is accounted for.

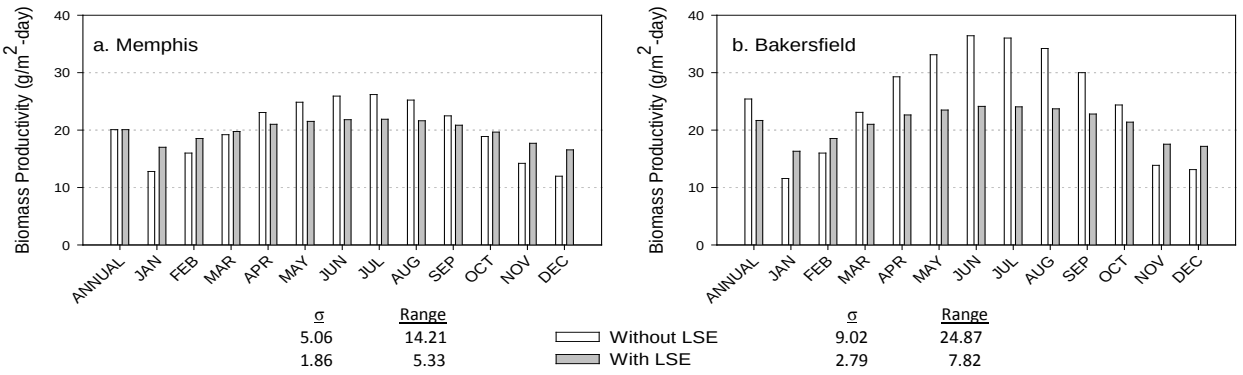

Figure 4.3: Impact of Light Saturation Effect (LSE) on Microalgal Productivity at Memphis, TN, and Bakersfield, CA. Data from the National Solar Radiation Database for 1991-2005. Shown beneath each graph are the standard deviation and range of the data sets with and without the correction for light saturation. The annual average sunlight intensity in Memphis was normalized to a biomass productivity (P_{mass}) of 20 g/m^2-day for the simulations both with and without the LSE. The higher sunlight intensity in Bakersfield translates into higher annual average biomass productivity values than for Memphis, but it is also apparent that the light saturation effect diminishes that difference.

While this analysis suggests that applying the light saturation effect is important, it involved applying a correction to daily average sunlight intensity values. While this may account for seasonal variations in sunlight intensity, it does not address diurnal variations. Since the Bush Equation is highly non-linear, one might expect that applying it to a daily average sunlight intensity value (kWh/m^2-day) can introduce significant distortion. In addition to monthly average daily sunlight intensity values, the NSRDB also includes hourly average sunlight intensity statistics, by month[20]. For the Bakersfield site, plots of the hourly average sunlight intensity for the months of January (which had the lowest average daily sunlight intensity) and July (highest average intensity), 1991, are shown in Figure 4.4. Also shown in Figure 4.4 are the plots of the January and July, 1991, hourly sunlight intensity data after correcting them for the light saturation effect using the Bush Equation, on an hour-by-hour basis. It is obvious from Fig. 4.4 that a substantial amount of attenuation occurs in both curves. It is also interesting to note that both curves corrected for light saturation peak at about the same effective light intensity. Thus any additional biomass productivity in July compared to January is due primarily to the longer day length, and not to the higher sunlight intensity.

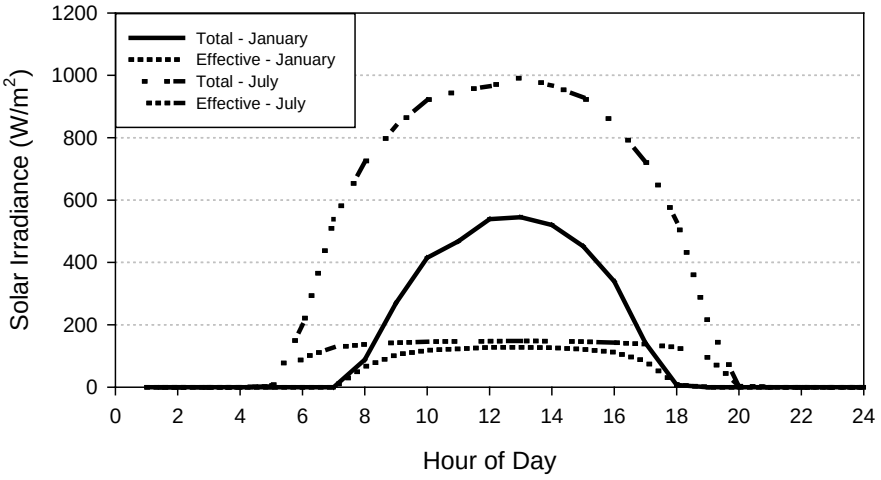

Figure 4.4: Average Hourly Sunlight Intensity in Bakersfield, CA for January and July. Data from the National Solar Radiation Database for 1991. After correcting for light saturation, the increase in effective sunlight intensity in July compared to January is almost entirely due to the longer day.

Hourly sunlight intensity data for 1991 for the Memphis and Bakersfield sites were obtained from the NSRDB and corrected using the Bush Equation to obtain effective sunlight intensity, on an hour-by-hour basis, for each month in that year. Hourly effective sunlight intensity values were then summed to obtain the average effective daily sunlight intensity for each month. The correlation factor k' was calculated from Equation 4.4 using the annual average daily sunlight intensity in Memphis and the NAABB biomass productivity target of 20 g/m^2-day, and a light saturation efficiency factor calculated from Equation 4.3. (The daily average sunlight intensity of 5.278 kWh/m^2-day for 1991 was attenuated to 1.380 kWh/m^2-day, yielding a value for k' of 14.50 g/kWh.) This conversion factor was then used to recalculate the average daily biomass productivity (kg/m^2-day) for each month, using the attenuated sunlight intensity calculated on an hour-by-hour basis. Again, to retain the relative differences between the Memphis and Bakersfield sites, the effective sunlight intensity data for Bakersfield was converted to biomass productivity values using the same conversion factor calculated by normalizing the Memphis data to 20 g/m^2-day.

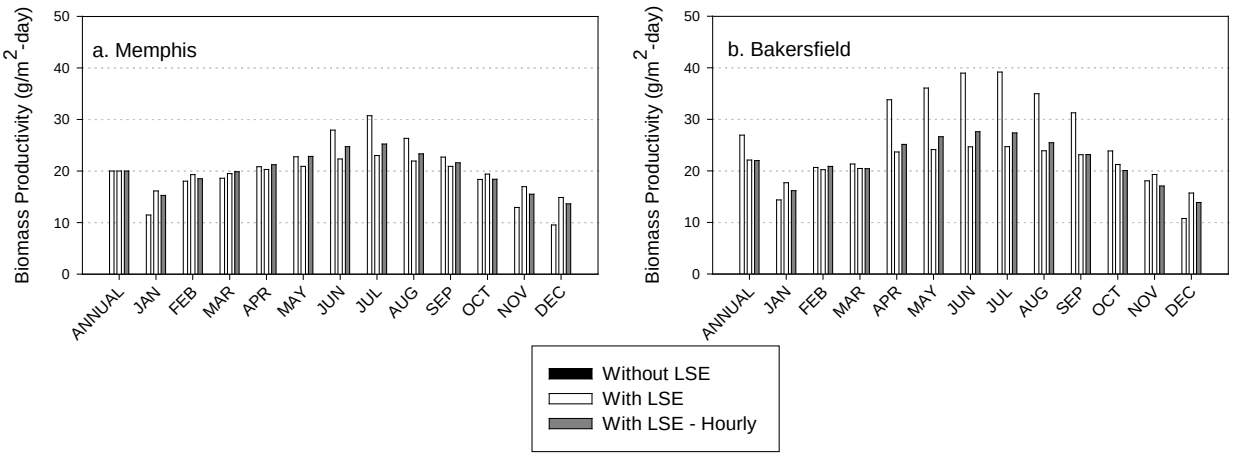

Figure 4.5: Biomass Productivities Based on Sunlight Intensity Data Averaged over Different Time Scales. These graphs show predicted biomass productivities for Memphis, TN, and Bakersfield, CA, calculated from daily average sunlight data from the National Solar Radiation Database for 1991, without correcting for light saturation ("Without LSE"), from daily average sunlight data after correcting for light saturation ("With LSE"), and from hourly average sunlight data after correcting for light saturation ("With LSE – Hourly"). The annual average sunlight intensity in Memphis was normalized to a biomass productivity (P_{mass}) of 20 g/m^2-day for all three cases.

Figure 4.5 presents the monthly average productivities for Memphis (on the left) and Bakersfield (on the right) based on hourly sunlight intensity data, alongside the productivity values based on daily average sunlight intensity with and without the correction for light saturation. It is clear from the graphs for both sites that the productivity predicted using hourly data much more closely resembles the results generated from the daily average data with the correction for light saturation, and in almost all cases the productivity predicted using hourly sunlight intensity data lies between the productivity predicted using daily average sunlight data with the light saturation effect, and that predicted using daily average sunlight intensity without correcting for light saturation.

The "flattening" effect of the LSE is readily apparent when the annual average productivities at Memphis and Bakersfield are compared. With the linear assumption, the annual average productivity at Bakersfield is 26.9 g/m^2-day (with Memphis normalized to 20 g/m^2-day). With the LSE correction, it is 22.1 g/m^2-day using daily average sunlight intensity, and 22.0 g/m^2-day using hourly average sunlight intensity (again, with Memphis normalized to 20 g/m^2-day in each case). The light saturation effect tends to reduce the

benefit in microalgal productivity that one might expect from higher sunlight intensity (35% higher annual average sunlight intensity yields only a 10% increase in biomass productivity).

The very small difference between the productivity values calculated for Bakersfield using hourly average and daily average sunlight intensities (22.1 vs. 22.0 g/m^2-day) suggests that using daily average data is sufficient, and the 24-fold increase in computations necessary to calculate hourly average productivities is probably unnecessary. But it is important to recognize that in each case the Bakersfield productivity data was compared to data from Memphis that was separately normalized to 20 g/m^2-day.

Figure 4.6 illustrates the impact of applying the Bush Equation correction to the daily average sunlight intensity versus applying it to the hourly data and then summing that data to arrive at the effective daily average sunlight intensity. Because of the asymptotic behavior of the Bush Equation at high sunlight intensities, there is a marked difference in the net daily effective sunlight intensity, with the average computed from hourly data being on the order of half of that derived from the daily average data. This has a profound implication if an investigator is attempting to predict biomass productivity directly from sunlight intensity data, without "pegging" a gross overall average to some arbitrary value, such as using 20 g/m^2-day in Memphis as a basis. In other words, if an investigator is attempting to predict a biomass productivity from sunlight intensity data, it is essential to use sunlight intensity at the smallest time-scale available, and to apply the Bush Equation to that data rather than applying it to data representing time scales of days or longer.

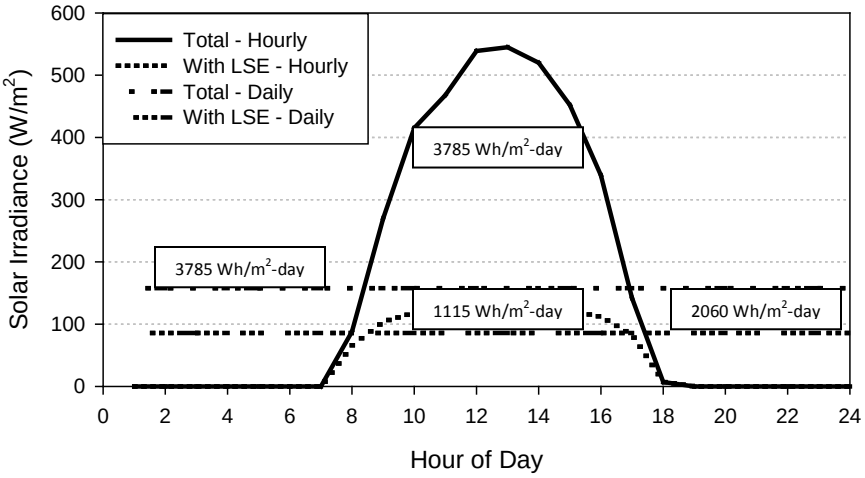

Figure 4.6: Impact of Applying Light Saturation Effect to Hourly versus Daily Average Sunlight Intensity. Data from the NSRDB for Bakersfield, CA, for January, 1991. The text boxes indicate the area under each curve. Due to the non-linearity of the Bush Equation, applying it to the daily average sunlight intensity instead of the hour-by-hour intensity almost doubles the effective daily sunlight intensity, and thus the estimated daily biomass production rate.

4.5. Alternative Site Analysis

Prior modeling at the Pacific Northwest National Laboratory predicted that the Gulf Coast and lower Atlantic seaboard regions might have the most suitable combination of resource availability and site conditions for mass algae cultivation[13]. To evaluate the impact of differences in climatic conditions at locations along the southern rim of the continental United States, a set of TELCIM simulations was performed for potential biodiesel manufacturing sites in each of: Bakersfield, California; Tucson, Arizona; Memphis, Tennessee; Baton Rouge, Louisiana; and Jacksonville, Florida. This includes sites in the desert southwest, Gulf Coast, lower Atlantic seaboard, and lower Mississippi River Valley. Monthly average sunlight intensity, temperature, and relative humidity data were obtained for these locations from the National Solar Radiation Database for the span 1991-2005[19]; the sum of direct and diffuse sunlight was used throughout. Monthly average precipitation and pan evaporation data for these locations (except Bakersfield) were obtained from the National Climatic Data Center[21] for the same time period. (There were no monitoring stations near the Salton Sea area in the NSRDB and NCDC data sets used for this geographic analysis, so to ensure that all of the sunlight intensity data was obtained from a single source,

the Bakersfield site was selected as an alternative southern California location.) Unfortunately, very few monitoring locations are common to both the NSRDB and NCDC databases, so several compromises had to be made when compiling input climate data for these simulations:

- The pan evaporation and precipitation data for the Tucson site covers only the 1991-1999 period (pan evaporation data collection was discontinued at Tucson after 1999).
- The pan evaporation and precipitation data for the Jacksonville simulations was that reported for Lake City, Florida, some sixty miles distant.
- Pan evaporation and precipitation data for the Bakersfield locations were obtained from the California Climate Data Archive[15]. The precipitation data was averaged over the period 1981-2010, and the pan evaporation rates were reported to have been estimated using a form of the Penman Equation for an unspecified time period.
- Pan evaporation data for Memphis for the 1991-2005 time period was reported only for the months of April through October, the normal growing season. An older NOAA data set, for the period 1956-1970, included pan evaporation rates at Memphis for all twelve months of each year[22]. A linear regression analysis between these two data sets (r^2 = 0.970) was used to estimate the pan evaporation rates for the missing months in the 1991-2005 NCDC data sets.

The TELCIM simulations performed in this study of alternative production locations were all based on the Test Scenario with the NAABB productivity targets (20 g/m^2-day at 50% lipid content). The southern California cost structures used in the Test Scenario were retained for all sites, ensuring that any changes in the KPI's are solely attributable to the differences in sunlight intensity and other climatic conditions. For each site, twelve simulations were performed, one for each month of the year, using the average sunlight intensity and climate data for that month. The maximum productivity design basis was used in these simulations, with the result that the size (i.e., illuminated surface area) of the facility varied from one site to another, based on each location's peak sunlight month. Memphis was again used as the "base" site – the annual average biomass productivity (P_{mass}) there was assumed to be 20 g/m^2-day. The annual average sunlight intensity in Memphis of 5.68 kWh/m^2-day and a light saturation constant (E_0) of 150 µmol/m^2-sec (equivalent to 0.811 kWh/m^2-day at an average photon energy content of 225.3 kJ/g-mol)

were used in Equation 4.3 to calculate a base light saturation efficiency factor (ε_s) of 0.421. When substituted into Equation 4.4, this resulted in a value for k' of 8.389 g/kWh. The Bush Equation (Eqn. 4.3) and Equation 4 were then used to calculate ε_s and P_{mass} from the average daily sunlight intensity on a month-by-month basis for each location. A TELCIM run for the month with the highest productivity at each site was used to size the facility (May was the peak sunlight month for Baton Rouge and Jacksonville, June for Bakersfield and Tucson, and July for Memphis). For each site, a simulation was run for each of the other eleven months, iterating on the CO_2 uptake rate until the design basis number of ponds was returned by the model. Annual performance statistics were computed using biodiesel volume-averaging. The results for several key performance indicators are shown in Table 4.4. For comparison, another set of simulations was run for the same five sites, using the same input data, but without correcting for the light saturation effect. The results of these simulations are also shown in Table 4.4.

Table 4.4: Alternative Site Analysis										
	With Light Saturation Effect					Without Light Saturation Effect				
	Bakersfield, California	Tucson, Arizona	Memphis, Tennessee	Baton Rouge, Louisiana	Jacksonville, Florida	Bakersfield, California	Tucson, Arizona	Memphis, Tennessee	Baton Rouge, Louisiana	Jacksonville, Florida
Number of Ponds	3863	3815	4260	4328	4197	2558	2445	3559	3742	3390
Biodiesel Production (MMgal/yr)	163	172	169	173	172	129	144	143	151	146
Areal Productivity (gal/acre-yr)	3285	3520	3123	3138	3214	3968	4643	3162	3162	3378
Net Energy Return (MJ/MJ)	0.57	0.57	0.56	0.57	0.57	0.57	0.58	0.57	0.57	0.58
Carbon Intensity (gCO_2/MJ)	84.3	84.9	86.0	85.0	84.3	85.9	82.6	85.6	84.7	83.6
Water Intensity (gal/gal)	778	516	42	18	63	688	401	40	17	58
Production Cost ($/gal)	5.65	5.49	5.79	5.77	5.67	5.34	4.95	5.78	5.75	5.56
Capital Cost Productivity ($/gal/yr)	24.77	23.45	25.85	25.74	24.98	23.02	20.01	26.49	26.11	24.84

The most striking outcome of this analysis is that when the light saturation effect is accounted for, there is almost no difference in unit manufacturing cost, NER, or CI among the five sites. The parameter which differs most significantly among the sites is water intensity, which is an order of magnitude higher for the two western sites (Bakersfield and Tucson) than for the sites located east of the Rocky Mountains. The capital productivity of the western sites is also slightly better, which appears to be the only benefit of the higher average sunlight intensity experienced by those sites. When the light saturation effect is ignored, the cost differences between sites are more pronounced, but the energy and carbon footprints are not significantly different.

4.6. Conclusions

Based upon the results of the simulations described in this article, coupling the conventional algae cultivation and bio-oil processing technologies modeled by TELCIM to produce biodiesel will not yield a renewable fuel with a sustainable net energy balance. Anaerobic digestion of the LEA significantly improves the biodiesel's NER while generating a favorable financial return, but this augmentation alone is insufficient to make the fuel environmentally sustainable. Even with anaerobic digestion, the large external energy demand imposed by a "conventional" biodiesel manufacturing process creates a very large carbon footprint; the full cradle-to-gate manufacturing process releases almost as much carbon dioxide as is incorporated into biomass in the growth step. As a result, biodiesel produced in this way has almost the same carbon footprint as diesel refined from petroleum. Faster microalgal cell growth and higher oil content increase the NER, but to achieve long-term sustainability it appears necessary to employ a different manufacturing process. Modeling suggests that reducing the extent to which the wet biomass must be dried before the lipid fraction is recovered holds significant potential for creating a positive net energy balance.

One of the objectives of this work was to determine how much impact seasonal variations in climate, and seasonal and diurnal variations in sunlight intensity, have on the KPI's of interest. It appears that for modeling purposes annual average climate data is adequate; using more fine-grained input does not significantly affect estimates of unit manufacturing cost, NER, or CI. However, this conclusion presumes that the biodiesel manufacturing facility is operated to maximize sunlight utilization. TELCIM predicts that operating the biodiesel facility to maximize CO_2 uptake will significantly increase capital and operating costs and adverse environmental impacts. A comparison of the results from the maximum and minimum productivity cases shows that the incremental cost of fully utilizing carbon is very high, which is unfortunate, since it would be preferable to take as much advantage as possible of the concentrated CO_2 in the industrial gas feeding the algae ponds. And although using monthly average climatological inputs instead of annual averages did not significantly change the NER, CI and unit manufacturing cost of the biodiesel, the production capacity (carbon dioxide conversion) and water intensity were sufficiently affected to warrant the use of finer-grain inputs, when available.

Incorporating the light saturation effect into the prediction of biomass productivity significantly reduces the seasonal variation in this parameter. When using the maximum productivity design basis, including the light saturation effect in the productivity calculation makes the facility size larger than it would be if the effect was ignored, but that also increases the annual biodiesel output for a given CO_2 source. Because of the "flattening" effect of the LSE on biomass productivity, the differences in climate conditions along the southern tier of the United States do not have a significant impact on the biodiesel's energy and carbon footprints. The potential advantage in biomass productivity offered by the higher sunlight intensities experienced in the southwestern United States is almost entirely lost when the light saturation effect is taken into account. But assuming the biological and/or technological barriers to long-term sustainability can be overcome, this suggests that the portion of the continental United States where microalgal biodiesel might be sustainably produced is much larger than first thought, and sites in the southeastern United States might be as suitable or even more suitable for microalgal biodiesel production than those in the southwest. As a result, local resource availability (e.g., carbon dioxide, water, land, labor, and electricity) and cost structures may be the deciding factors when siting manufacturing facilities.

Including precipitation as a source of make-up water creates a significant difference in water intensity for sites in the western United States versus those located east of the Rocky Mountains. But rainfall is an episodic phenomenon, and to take advantage of it some provision must be made in the production scheme for accumulating precipitation. Possible mechanisms include increased freeboard in the ponds, additional surface impoundments, storage in the subsurface, and dedicated tanks, all of which entail additional capital and operating costs that are not included in the base cost structures used in the simulations described in this article.

An unexpected outcome from the many TELCIM simulations performed to date is that NER and CI do not always move in the same direction, often because of assumptions about byproduct fates. This reinforces the importance of life cycle modeling, and in particular, appropriate selection of system boundaries and fully accounting for the fates of byproducts.

One of the limitations of this work is that the effect of ambient temperature on biomass growth rate is ignored. This was deemed an acceptable assumption because all of the locations which were modeled lay along the southern tier of the continental United States. Accounting for temperature effects may tend to increase the seasonal variation in biomass productivity, driving the predicted growth rates to more closely match those made when the light saturation effect is ignored. In fact, the cases with and without the light saturation correction may represent upper and lower bounds of actual performance, with the non-LSE cases representing more “ideal” or optimistic cases. A possible future enhancement of TELCIM is the inclusion of a more robust heat and mass transfer model of the raceway ponds, which would allow more accurate modeling of biodiesel production in locations at higher latitudes.

Finally, despite being a very large model, TELCIM is easy to work with and has a considerable amount of background information already loaded into it in the form of default input parameters. Selectively varying particular input values while holding all the other inputs constant allows the effect of specific parameter

selections and process assumptions to be systematically evaluated. And although perhaps not the obvious software choice for chemical process modeling, Excel has many features that make it a highly effective and accessible platform for integrated process-financial-LCI modeling.

4.7. References for Chapter 4

[1] Henson, M., R.A. Axelbaum and J.R. Turner. A techno-economic model of microalgal biodiesel manufacture (TELCIM). Manuscript in preparation. 2013.

[2] Wang., M. Updated Energy and Greenhouse Gas Emissions from Corn Ethanol. 15th International Symposium on Alcohol Fuels, 2005.

[3] Wang, M. GREET 1, v1.8d.1, Copyright 1999, University of Chicago Argonne, LLC.

[4] Olivares, J.A. Proceedings from Algal Biofuels Consortium, Algae R&D Activities Peer Review, Annapolis, MD, April 7-8, 2011.

[5] Spoehr, H.A., and H.W. Milner (1949). The chemical composition of Chlorella; the effect of environmental conditions. Plant Physiol. 24(1) (1949) 120-149.

[6] National Research Council of the National Academies. Sustainable development of algal biofuels in the United States. Prepublication copy. The National Academies Press, Washington, D.C., USA. 2013.

[7] Benemann, J.R., and W. J. Oswald. Systems and Economic Analysis of Microalgae Ponds for Conversion of CO_2 to Biomass – Final Report. 1996. Department of Energy, Pittsburgh, PA, 201 pp.

[8] Lundquist, T.J, I.C. Woertz, N.W.T. Quinn, and J.R. Benemann. A Realistic technology and engineering assessment of algae biofuel production. 2010. Energy Biosciences Institute, University of California, Berkeley, California, USA.

[10] Razon, L.F. and R.R. Tan. Net energy analysis of the production of biodiesel and biogas from the microalgae : *Haematococcus pluvialis* and *Nannochloropsis*. Applied Energy 88 (2011) 3507-3514.

[11] Frank, E.D., J. Han, I. Palou-Rivera, A. Elgowainy and M.Q. Wang (2011). Life Cycle Analysis of Algal Lipid Fuels with the GREET Model. Argonne National Laboratory, Energy Systems Division, ANL/ESD/11-5, August 2011.

[12] Weyer, K.M., D.R. Bush, A. Darzins, and B.D. Wilson. Theoretical maximum algal oil production. Bioenerg. Res. 3 (2010) 204-213.

[13] Wigmosta, M.S., A.M. Coleman, R.J. Skaggs, M.H. Huesemann, and L.J. Lane. National microalgae biofuel production potential and resources demand. 2011. Water Resources Research 47 W00H04, doi:10.1029/2010WR009966.

[14] Western Regional Climate Center, accessed at www.wrcc.dri.edu/cgi-bin/rawMAIN.pl?caZSSE, on various dates in 2013.

[15] California Climate Data Archive, accessed at www.calclim.dri.edu/ccda/comparative.html, on various dates in 2013.

[16] Chisti, Y. Biodiesel from microalgae. Biotech. Adv 25 (2007) 294-306.

[17] Melis, A. Solar energy conversion efficiencies in photosynthesis: Minimizing the chlorophyll antennae to maximize efficiency. Plant Scence 177 (2009) 272-280.

[18] Weissman, J.C. Bioconversion of solar energy. 1978. PhD Thesis, University of California, Berkeley, California.

[19] National Solar Radiation Database. Accessed at ftp://ftp.ncdc.noaa.gov/pub/data/nsrb-solar/summary-stats/dailystats/ on various dates in 2013.

[20] National Solar Radiation Database. Accessed at ftp://ftp.ncdc.noaa.gov/pub/data/nsrb-solar/summary-stats/hourlystats/ on various dates in 2013.

[21] National Climatic Data Center. Accessed at http://www.ncdc.noaa.gov/IPS/cd/cd.html%3bjsessionid=DE17457D54E2D27AB on various dates in 2013.

[22] Farnsworth, R.K. and E.S. Thompson (1982). Mean Monthly, Seasonal and Annual Pan Evaporation for the United States (NOAA Technical Report NWS 34). Office of Hydrology, National Weather Service, U.S. Department of Commerce.

5. OTHER ANALYSES AND RESULTS

5.1. Introduction

Several lines of inquiry pursued during the course of this research helped guide the direction of the work but did not relate directly to the results discussed thus far. Four of these secondary areas of research, which are representative of the types of supporting analyses that were performed during the course of this project, are discussed in this chapter. The first is an example of work done to test a basic assumption made when the production scheme modeled by TELCIM was selected: that conventional oilseed extraction technology will perform just as effectively with microalga

l biomass as with soybeans. The second topic is an example of work to identify mathematical relationships that model physical processes which occur in the manufacturing plant, allowing an optimization problem to be solved. The goal of this analysis was to optimize the residual water content based on its effects on the energy used during harvesting and the lipid recovery efficiency of the extraction process. The third study is an example of a detailed analysis of an individual process step, in which the effects of local climate conditions and standard operating conditions on the energy loads in the biomass drying operation were evaluated. The fourth topic is an example of a multi-parameter sensitivity analysis in which the sensitivity of the biodiesel's NER, CI, and unit cost to lipid content was evaluated under two different microalga growth rate assumptions.

5.2. Microalgal and Soy Lipids

As discussed in Section 1.1.4, some biodiesel production modelers have assumed that the same lipid extraction process commonly used in vegetable oil production will work similarly when the substrate is microalgal biomass. For example, Lundquist's techno-economic model of microalgal biodiesel production included a lipid extraction plant that was modeled after a comparably sized soybean oil extraction plant[1] (see Section 2.2.3 for a more detailed description of the lipid extraction process). To test this assumption,

the chemical profile of the neutral lipids present in a common microalga was compared to a profile typical of soybean oil.

Extraction with a pure hydrocarbon solvent is quite specific for neutral (i.e., non-polar) lipids, consisting primarily of triacylglycerides (TAG). TAG is a family of compounds in which three unbranched fatty acid molecules are esterified to glycerol. Figure 5.1 shows a breakdown of the compositions of TAG extracted from a *Chlorella* strain[2] and from soybean oil[3]. Table 5.1 lists some average properties of the fatty acids in the TAG produced by these two organisms.

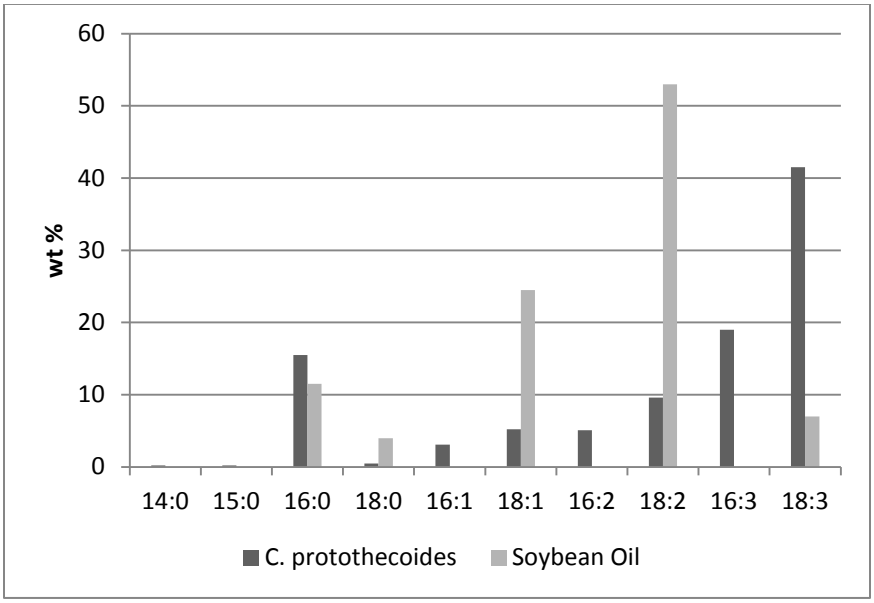

Figure 5.1: Lipid Profiles of Microalgal and Soybean Oil. Weight percentages of fatty acids in triacylglyceride extracted from *Chlorella protothecoides* and soybeans. The horizontal axis entries x:y indicate carbon chain length followed by the number of double bonds.

Table 5.1: Properties of Microalgal and Soybean Lipids		
	Microalgal Oil	**Soybean Oil**
Average Carbon Chain Length	17.1	17.8
Average Number of Double Bonds	2.2	1.5
Average Fatty Acid Molecular Weight (kg/kg-mol)	267	278
Average Triacylglyceride Molecular Weight (kg/kg-mol)	840	872

Figure 5.1 reveals some differences in the compositions of the fatty acids in the TAG recovered from *Chlorella* and soybeans. Roughly 75% (by weight) of the fatty acid in soybean TAG is comprised of oleic

acid (18:1) and linoleic acid (18:2), while these compounds represent less than 15% of microalgal TAG. Tri-unsaturated fatty acids constitute almost 60% of microalgal TAG, versus around 5% in soybean TAG. Despite these differences, the fatty acids in TAG from these two sources are very similar in average chain length and molecular weight. The most significant difference is in degree of unsaturation, which is roughly 50% higher in the microalgal TAG. While this difference may have implications with respect to biodiesel performance (e.g., viscosity, freeze point, pollutant formation), the chemical composition of these two materials is similar enough that microalgal oil can be expected to behave similarly to soybean oil during alkane extraction.

5.3. Effects of Residual Water on Oil Extraction

In the conventional production scheme modeled by TELCIM, the biomass drying step contributes significantly to the energy and carbon footprints of microalgal biodiesel. The extent to which the biomass must be dried is a constraint imposed by the lipid extraction process. Per Crown Iron Works, a leading supplier of vegetable oil recovery systems, hexane extraction has a very narrow water tolerance centered around 10% (wt.) residual water in the biomass[4]. It is clear from an overall system energy balance that allowing more water to enter the extraction step reduces the amount of energy consumed per unit of biodiesel produced. However, there is a concurrent loss in lipid recovery efficiency, which lowers the NER of every gallon of biodiesel produced. These offsetting factors create an optimization problem. If the relationships between residual water content and energy usage and lipid yield can be expressed mathematically and coded into TELCIM, the model can be used to identify the residual water content(s) that correspond to potential minima/maxima for NER, CI, and manufacturing cost.

If time effects such as different rates of drying are ignored, biomass drying can be modeled as a change of thermodynamic state, as discussed in Section 2.2.2. The curve describing the relationship between residual water content and energy usage is linear, and its slope is equal to the latent heat of vaporization of water. TELCIM's drying model is therefore already programmed to calculate the difference in energy loads represented by different residual water requirements.

The extraction of neutral lipids from biomass is a very complex process, and it may be better described as a leaching process than an extraction. Cooney and co-authors have reviewed the mechanisms by which neutral lipids are extracted from microalgal biomass using hydrocarbon solvents[5]. They conclude that there are multiple mechanisms involved in transferring lipids from microalgal cells to the extraction solvent, and that these mechanisms operate at different time scales:

- Solvation of accessible lipid droplets at the surface of the biomass (fast);
- Penetration of solvent into capillaries in the biomass matrix and diffusion of lipids from broken cells into those capillaries, followed by diffusion of the miscella out (slow); and
- Diffusion of solvent across intact cell membranes and diffusion of miscella back out (very slow).

Water interferes with mass transfer phenomena at the macro-scale by hindering solvent wetting of the biomass, and by inhibiting coalescence of miscella droplets. At the micro-scale, water occupies pores in the biomass matrix through which solvent and miscella must pass, converting a convective flow process into a much slower diffusion transport process. Dissolved water reduces the diffusivity of oil in the extraction solvent, and it increases the extraction of polar lipids, which reduces the solubility of TAG in the organic solvent. In addition to these detrimental effects when there is excess water, there are also adverse consequences when the biomass is "over-dried". At the bulk scale, the biomass becomes compacted, reducing the interfacial contact area. The solids also lose plasticity, resulting in an increase in the production of fine particulates, which tends to stabilize emulsions and inhibit coalescence. At the micro-scale, too little water leads to shrinkage and closure of pores in the biomass matrix, reducing access of the solvent to the oil[5]. In combination, these mechanisms create the potential for an optimum residual water concentration in the extraction process, and this is exactly what is seen in industrial soybean oil extraction plants using hexane extraction. In the Handbook of Soy Oil Processing and Utilization, G.C. Mustakas reports that "For optimum operation of the [hexane] solvent extraction process, 9.5 to 10% moisture is desirable…"[6]. And in "Introduction to Fats and Oils Technology," L.A. Johnson reports that "Moisture of the [soy] flakes is yet another factor affecting rate of solvent extraction. In most cases, 9-11% moisture is ideal."[7]

Other than these statements, no quantitative relationship correlating extraction efficiency with water content was found for hexane extraction of soybean oil. However, a reference in which the efficiency of soybean oil extraction by a different solvent – isopropanol – yielded the graph and equations shown in Figure 5.2[8]. These curves clearly show a maximum oil recovery at a relatively low residual water content, consistent with what has been reported for hexane extraction.

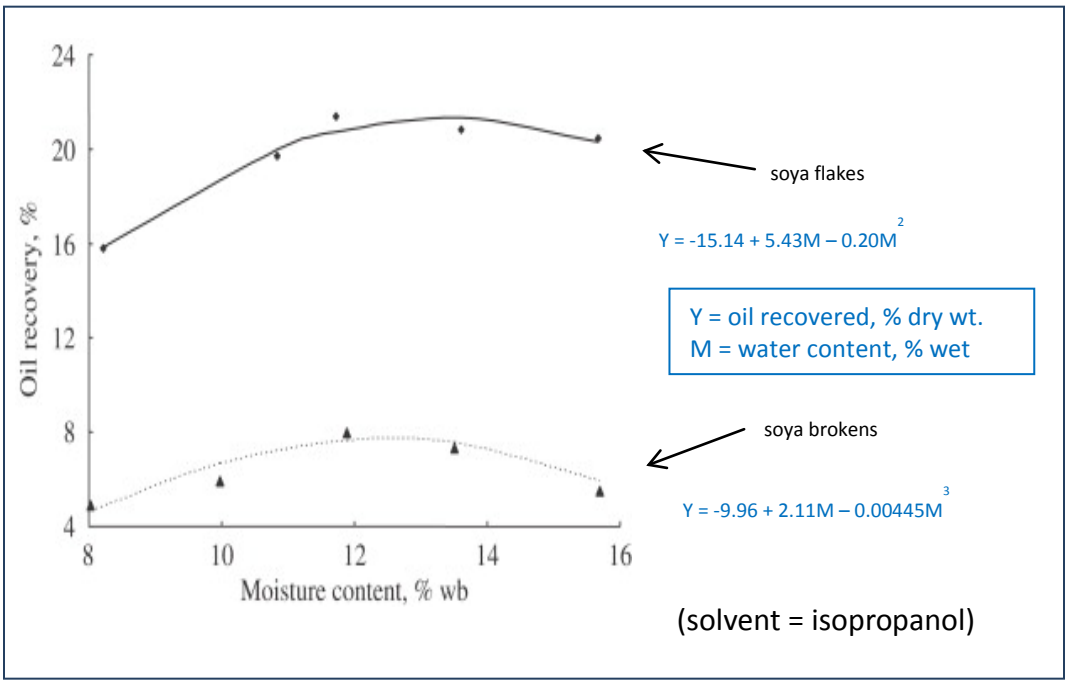

Figure 5.2: Effect of Water Content on Extractability of Soybean Oil. Efficiency of oil recovery from soy flakes and broken beans, on a moisture-free weight basis, using isopropanol as the extraction solvent. The curves not only show the sensitivity of oil extraction efficiency to residual water content, but the benefit of disrupting the solid matrix and expanding its surface to volume ratio, by flaking the biomass.

The optimum residual water content is a function of the relative magnitudes of the slope of the drying energy versus residual water content curve (the latent heat of vaporization of water), and the slope of the extraction yield versus water content curve. It is readily apparent from the curves in Figure 5.2 that the extraction efficiency is highly sensitive to water content, and therefore the optimum residual water content must lie very near the maximum of extraction yield (Y) versus water content (M).

5.4. Analysis of Biomass Drying

The potential microalgal biodiesel production locations evaluated during this research are subject to different climate conditions (see Section 4.5). An objective of this analysis was to evaluate the impact of these differences on the cost and energy and carbon footprints of the biomass drying process. The first part of the analysis was intended to determine whether the lower relative humidity experienced at the western sites, particularly Tucson, would translate into lower drying energy consumption. The second phase was intended to evaluate the effect on the biodiesel's NER, CI, and unit cost, of lowering the dryer inlet air temperature from the default value used in the Test Scenario. Phase 2 involved a set of simulations for the Tucson site, which had the lowest average relative humidity and highest average ambient temperature of the five sites evaluated in the Alternative Site Analysis.

The monthly average climate data assembled for the five sites evaluated in the Alternative Site Analysis were used to compute the annual average sunlight intensity, temperature, relative humidity, precipitation, and evaporation for each site[9,10,11,12]. The areal productivity of the microalga at the Memphis location was set equal to 20 g/m^2-day, and the lipid content to 50%, consistent with the NAABB R&D targets previously described (see Section 4.2)[13]. The remainder of the TELCIM inputs for these simulations were the same as the values used in the Test Scenario (see Section 3.2). The areal productivity at the other four sites was calculated based on the average sunlight intensity at those sites relative to that at Memphis, without correcting for the light saturation effect.

For the first (Phase 1) analysis, a single TELCIM simulation was run for each location using the default dryer conditions:

- Air temperature at inlet to Dryer #1 and Dryer #2 = 250^{o}F;
- Biomass water content at inlet to Dryer #1 = 73.5%;

- Biomass temperature at inlet to Dryer #1 = ambient (as specified by climate data for each site);
- Air and biomass temperature at outlet from Dryer #1 = 106°F;
- Biomass water content at outlet from Dryer #1 = 25%;
- Air and biomass temperature at outlet from Dryer #2 = 120°F; and
- Biomass water content at outlet from Dryer #2 = 10%.

The power loads for heating and compressing the inlet air at each site are reported in Table 5.2.

Table 5.2: Drying Energy Loads at Alternative U.S. Locations

PLANT LOCATION	AVERAGE TEMPERATURE (°F)	AVERAGE RELATIVE HUMIDITY (%)	DRYING AIR COMPRESSION (MW_e)	DRYING AIR HEAT LOAD (MW_{th})
Bakersfield, California	65.1	56	169	543
Tucson, Arizona	69.7	38	171	530
Memphis, Tennessee	62.8	67	168	550
Baton Rouge, Louisiana	67.2	75	168	537
Jacksonville, Florida	67.7	78	168	536

There is virtually no difference in the drying energy loads among the five sites. The drying air heat load is dominated by the latent heat required to evaporate sufficient water to achieve the target exit concentration of 10% (wt.). Because the rate of water evaporation is the same at all of the sites, the small differences in heat load arise from the slight variation in the inlet air and wet biomass temperature. And because the drying heat loads among the five sites are so similar, so too are the volumes of drying air required, leading to the similarity in compression electricity demand.

It appears that any benefit that might result from the low relative humidity at the Tucson site is lost because the drying air is being heated to such a high temperature (250°F) relative to its original, ambient

temperature (70°F). The second phase of this analysis was performed in order to determine whether lowering the inlet air temperature at Tucson would allow this advantage to become more apparent, and reduce the overall energy load of biomass drying. Two cases were considered in Phase 2 of the biomass drying analysis, representing two different dryer operating strategies. In the first, the dryer inlet air temperature was varied over the range of 175-250°F, while the exit temperatures from the dryers were held constant at their default values (106°F and 120°F for Dryers #1 and #2, respectively). The results of this case are shown in Table 5.3.

Table 5.3: Tucson Site Drying Cost Analysis – Constant Dryer Exit Temperature Operating Mode

	DRYER INLET AIR TEMPERATURE			
	250°F	**225°F**	**200°F**	**175°F**
Dryer #1 Outlet Temperature (°F)	106	106	106	106
Dryer #2 Outlet Temperature (°F)	120	120	120	120
Dryer #1 Outlet Relative Humidity (%)	82.6	70.4	58.3	46.1
Dryer #2 Outlet Relative Humidity (%)	47.7	40.0	32.3	24.7
Air Flowrate (million scfm)	5.83	7.08	9.00	12.3
Air Compression Power Load (MW_e)	171	207	263	362
Water Rejected (million kg/day)	9.79	9.79	9.79	9.79
Steam Thermal Load (MW_{th})	530	553	590	654
Drying Cost ($K/day)	712	816	976	1259
Biodiesel Production Cost ($/gal)	4.90	5.10	5.42	5.97

In this case, as the inlet air temperature is reduced, the air compression electricity load and the thermal load to preheat the air both increase significantly. Since the dryer outlet temperature conditions are being held constant, the dryer heat duty remains the same. As the inlet air temperature falls, enthalpy conservation requires the volume of air to increase correspondingly, which causes the compression energy duty to increase. The increase in the dryer thermal load with falling inlet temperature occurs because more sensible heat is required to heat a larger volume of air from the same inlet air temperature to the same exit temperature.

It is also noteworthy that the relative humidity of the air exiting both dryers falls as the inlet temperature is reduced. This is simply a dilution effect – the same amount of water is being evaporated

into a progressively larger volume of air. And while dryer exit temperature might be the normal control parameter for an operating dryer, in this case it would make more sense to operate the dryers based on exit humidity targets rather than exit temperature. To simulate this alternative operating strategy, another series of simulations was run, over the same inlet air temperature range 175-250 ^{o}F. The exit temperatures from the dryers were varied until the exit humidity from each dryer matched the default dryer humidities (82.6% from Dryer #1 and 47.7% from Dryer #2). Excel's "Goal Seek" function was used to perform these iterations. The results of this second case are shown in table 5.4. (This case optimistically assumes that the dryers can achieve the same exit humidity with a smaller temperature driving force.)

Table 5.4: Tucson Site Drying Cost Analysis – Constant Dryer Exit Relative Humidity Operating Mode

	DRYER INLET AIR TEMPERATURE			
	250^{o}F	**225^{o}F**	**200^{o}F**	**175^{o}F**
Dryer #1 Outlet Temperature (^{o}F)	106	102	98	93
Dryer #2 Outlet Temperature (^{o}F)	120	116	111	105
Dryer #1 Outlet Relative Humidity (%)	82.6	82.6	82.7	82.8
Dryer #2 Outlet Relative Humidity (%)	47.7	47.6	47.8	47.6
Air Flowrate (million scfm)	5.83	6.84	8.23	10.3
Air Compression Power Load (MW_e)	171	200	241	300
Water Rejected (million kg/day)	9.79	9.79	9.79	9.79
Steam Thermal Load (MW_{th})	530	535	539	543
Drying Cost ($K/day)	712	785	886	1031
Biodiesel Production Cost ($/gal)	4.90	5.05	5.24	5.53

The constant relative humidity case has a more favorable energy profile than the constant exit temperature case, but the energy loads still increase with decreasing inlet air temperature. The dryer thermal load is nearly constant, but the volume of air required still increases dramatically (due to the lower specific enthalpy of cooler air), which drives up the amount of electricity needed.

This analysis indicates that the dryer energy load is dominated by the evaporative load required to achieve the extraction step residual water concentration target, and that differences in ambient

conditions barely affect that load. The analysis of alternative dryer operating conditions suggests that the highest possible inlet air temperature should be used, since the impact on electricity usage for air compression is significant. The upper limit for the inlet temperature is dictated by the thermal stability of the biomass, and particularly the lipids, which are susceptible to oxidative degradation in the presence of hot air.

5.5. Lipid Accumulation

A limitation of many microalgae for the purpose of biodiesel production is that they contain relatively little usable oil. Consequently, considerable amounts of energy and cost are expended in the biodiesel manufacturing process producing carbohydrates, proteins and other biomolecules, which are undesired byproducts. Increasing the fraction of cell mass that is neutral lipid should have desirable effects on the KPI's. But due to thermodynamic and metabolic considerations, increasing the lipid fraction may slow the microalga's growth rate, which slows the rate of lipid production. Sensitivity analyses revealed that several of the KPI's of most interest - NER and unit cost - are strongly influenced by the microalga's oil content (see Section 3.2). But in those single parameter sensitivity analyses, the oil content was changed while all other parameters remained the same. One might instead expect that as TAG, a hydrophobic lipid, accumulates in a microalgal cell, the mass of water in that cell will decrease correspondingly. One possible model of lipid accumulation in microalgal cells is that the concentration of hydrophilic (non-lipid) compounds in water stays relatively constant as lipids accumulate. [This model is consistent with the hypothesis that cells that accumulate lipid do so at the expense of other energy storage polymers, such as glycogen.] If it is assumed that the mass ratio of non-lipid biomass to intracellular water remains constant, the change in residual water content corresponding to any given change in lipid content can be calculated.

If β is defined as the mass fraction of water in the wet biomass (i.e., residual water content), and α is defined as the mass fraction of lipid in the dry biomass, then one gram of wet biomass contains β grams of water, α(1-β) grams of lipid, and (1-α)(1-β) grams of non-lipid biomass. The assumption that the ratio of non-lipid biomass to residual water is constant is expressed by:

$$K = \frac{(1-\alpha)(1-\beta)}{\beta} = constant \tag{5.1}$$

For this analysis, the constant K was determined by substituting into Equation 5.1 the values of α and β used in the Test Scenario (0.25 and 0.735, respectively); this resulted in a value for K of 0.270. Equation 5.1 can be rearranged to solve for β:

$$\beta = \frac{(1-\alpha)}{(1-\alpha)+K} \tag{5.2}$$

A plot of the residual water content (β) as a function of oil content (α) is shown as Figure 5.3:

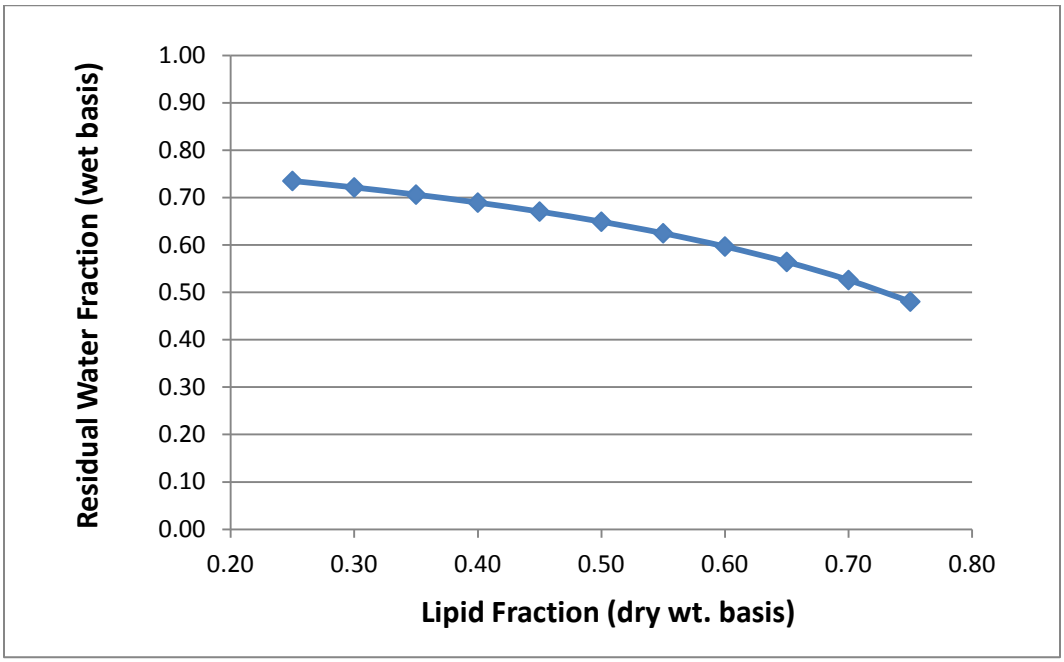

Figure 5.3: Plot of Residual water Content as a Function of Lipid Content, assuming the mass ratio of non-lipid biomass to residual water remains constant. Data points correspond to individual TELCIM simulations.

Two sets of TELCIM simulations were run; all input parameter values were as in the Test Scenario except as described below. In the first set of simulations, the oil content was varied over the range of 25-75% (centered on the NAABB target of 50%), and the residual water content was held constant at the default intracellular water fraction (0.735). In the second set, the oil content was varied over the same range, and for each value of the oil content, the residual water content was calculated from Equation 5.2. The values of NER, CI, and manufacturing cost generated by the two sets of simulations are shown in Figures 5.4 through 5.6, respectively.

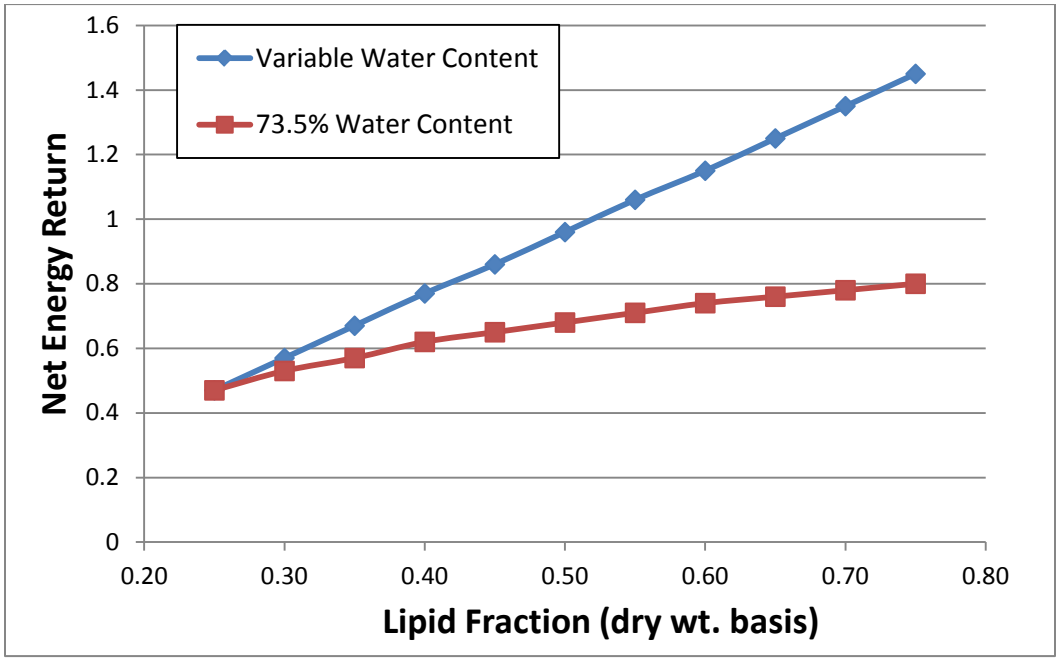

Figure 5.4: Effect of Lipid Accumulation on Net Energy Return.

In both cases, the NER improves with increasing oil content, since a larger fraction of the carbon being converted into biomass ends up in the form of biodiesel. The NER improves more quickly when the water content is variable since less water has to be evaporated in the dryers. When the residual moisture content is assumed to remain at 73.5%, the NER remains below 1.0 for the entire range of lipid

fractions. When the residual water content is assumed to vary with lipid content, the NER exceeds 1.0 when the lipid content is greater than around 50%.

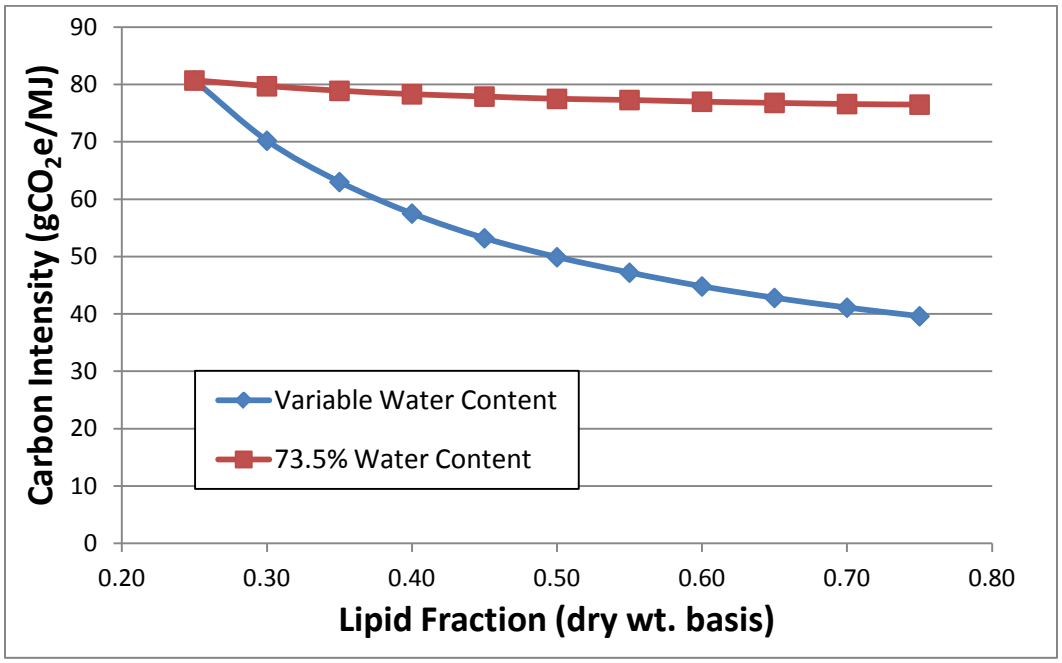

Figure 5.5: Effect of Lipid Accumulation on Carbon Intensity.

Figure 5.5 shows the effect of higher lipid content on the carbon intensity of the biodiesel product. When the water content is assumed to vary with lipid content, the carbon intensity falls off significantly as the lipid fraction increases. When the water content is held constant at 73.5%, the carbon intensity remains nearly constant. One might expect that even with constant water content, the carbon intensity of the biodiesel would fall as the lipid fraction increases, since more of the carbon dioxide that is converted to biomass ends up as fuel rather than a byproduct. To better understand why the carbon intensity responds so weakly to the lipid content, the contribution of each major process step to the biodiesel's overall carbon intensity was retrieved from TELCIM's Summary Results worksheet. To maximize the contrast, carbon intensity data from the simulations corresponding to the two extreme

data points on the upper curve in Figure 5.5 are compared in Figure 5.6. The data for the "75% Lipid" case in Figure 5.6 corresponds to the furthest data point on the right on that curve (oil content = 75%, carbon intensity = 77 gCO_2/MJ), while the "25% Lipid" data corresponds to the point furthest to the left (oil content = 25%, carbon intensity = 80 gCO_2/MJ).

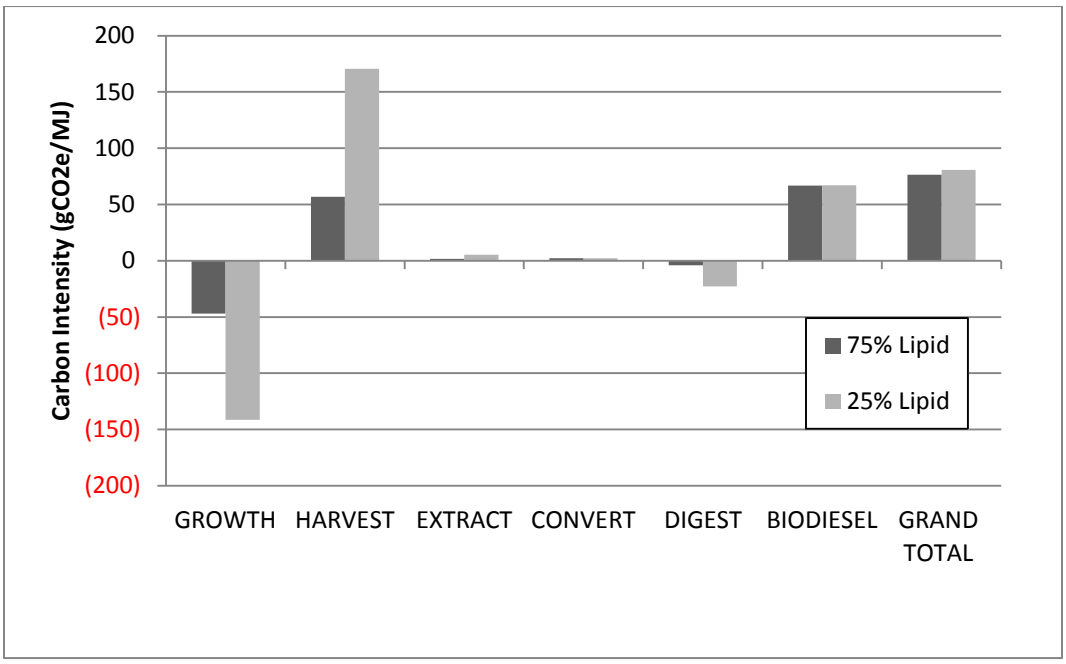

Figure 5.6: Breakdown of Carbon Intensity When Residual Water Content Is Held Constant. In both cases the residual water content is 73.5%. The remainder is biomass, of which lipid comprises either 25% or 75%.

In the simulation in which the lipid content of the biomass is 75%, three times as much carbon dioxide is being converted to lipid as in the case in which it is limited to 25%. As shown in Figure 5.6, the carbon intensity attributable to the growth step in the 75% case is roughly one-third that of the 25% case (in the carbon intensity calculation the same carbon dioxide flux is divided by a fuel energy content three times as large). The drying energy used in the harvesting step is the same in both cases (the model does not use different heat capacities for different cellular components), which results in the same carbon emissions, but again in the 75% case those emissions are divided by a number three times as large as in

the 25% case. Because the carbon dioxide fluxes in the growth and harvesting steps are (coincidentally) roughly equal in magnitude, these effects largely cancel one another, leading to little difference in the overall carbon intensity between the two cases.

It is also informative to compare the two simulations in which the oil content is constant%, but the water content is at its maximum difference (i.e., the furthest data point to the right on each of the upper and lower curves in Figure 5.5). Figure 5.7 shows a carbon intensity breakdown, by major process step, for those two cases. In both cases, the lipid content is 75% of the biomass on an ash-free, dry weight basis, but in the top curve the residual water content is 73.5%, and in the bottom curve it is around 48% (as determined from Equation 5.2 when α is equal to 0.75).

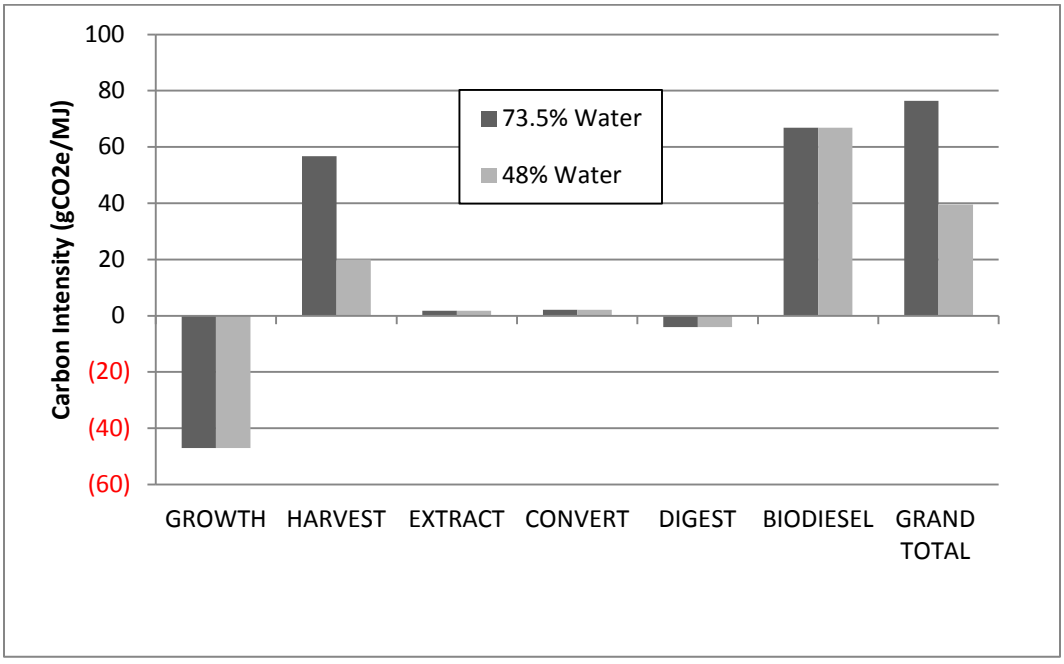

Figure 5.7: Breakdown of Carbon Intensity When Residual Water Content Is Allowed to Vary. In both cases the oil content is 75% of the biomass.

The only significant difference in carbon intensities is found in the harvesting step. Because the lipid content is the same in both cases, the carbon flux occurring in the growth step is divided by the same fuel energy content, so the carbon intensity of the growth step is unchanged. The amount of thermal energy required to achieve the target residual moisture content of 10% is obviously lower when the residual water content of the biomass entering the drying operations is 48% instead of 73.5%. And because the amount of heat that must be transferred to the biomass in the 48% water case is so much lower, so too is the electricity demand for air compression. In combination, the reduced natural gas and electricity demands create a sizeable reduction in the carbon emissions attributable to the harvesting step.

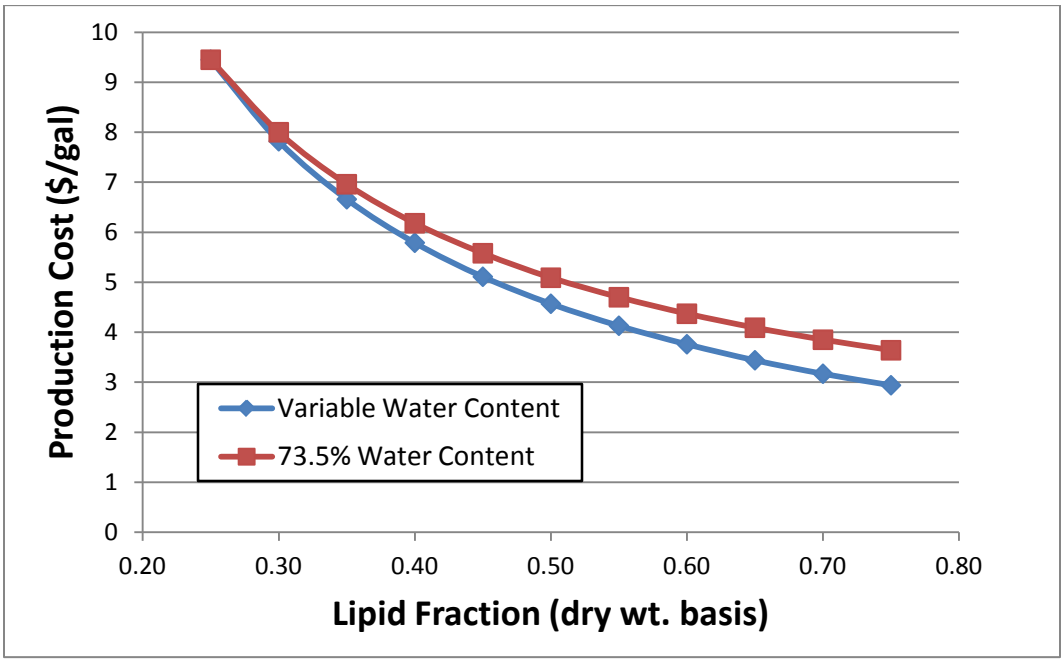

Figure 5.8: Effect of Lipid Accumulation on Unit Biodiesel Manufacturing Cost.

Figure 5.8 shows that the microalga's lipid content has a dramatic effect on unit biodiesel manufacturing cost, regardless of whether the residual water content is constant or variable. The cost reduction with

increasing lipid content merely reflects that purchased inputs, such as raw materials and energy, are more efficiently being converted into biodiesel, reducing each gallon's unit cost. There is still a net cost benefit from having less water in the biomass feeding the drying operations, but that effect is much smaller than the cost benefit derived from improving the yield of biodiesel from the carbon dioxide taken up in the ponds.

In this analysis the areal productivity of the microalga was assumed to be constant. This is a questionable assumption, since a cell that is accumulating large amounts of lipid may not be growing as quickly as one that is producing a more balanced slate of biomolecules. For example, researchers have substantially increased the lipid content of microalgal cells by starving them of nitrogen for extended periods of time[14]. But the cells do not grow and divide during the starvation period; essentially they are investing energy in converting other biomolecules into lipids. To investigate the potential impacts of this phenomenon, another set of simulations was run in which it was assumed that lipid productivity, rather than overall biomass productivity, remains constant. Thus cells with high lipid content tend to grow more slowly (on average) than those with a lower lipid content. Figures 5.9 through 5.11 reproduce Figures 5.4, 5.5 and 5.8, respectively, except the areal productivity was adjusted in each simulation so that the lipid productivity (i.e., grams of lipid per square meter per day) remain constant, at the same rate as in the Test Scenario (6.19 g lipid/m^2-day).

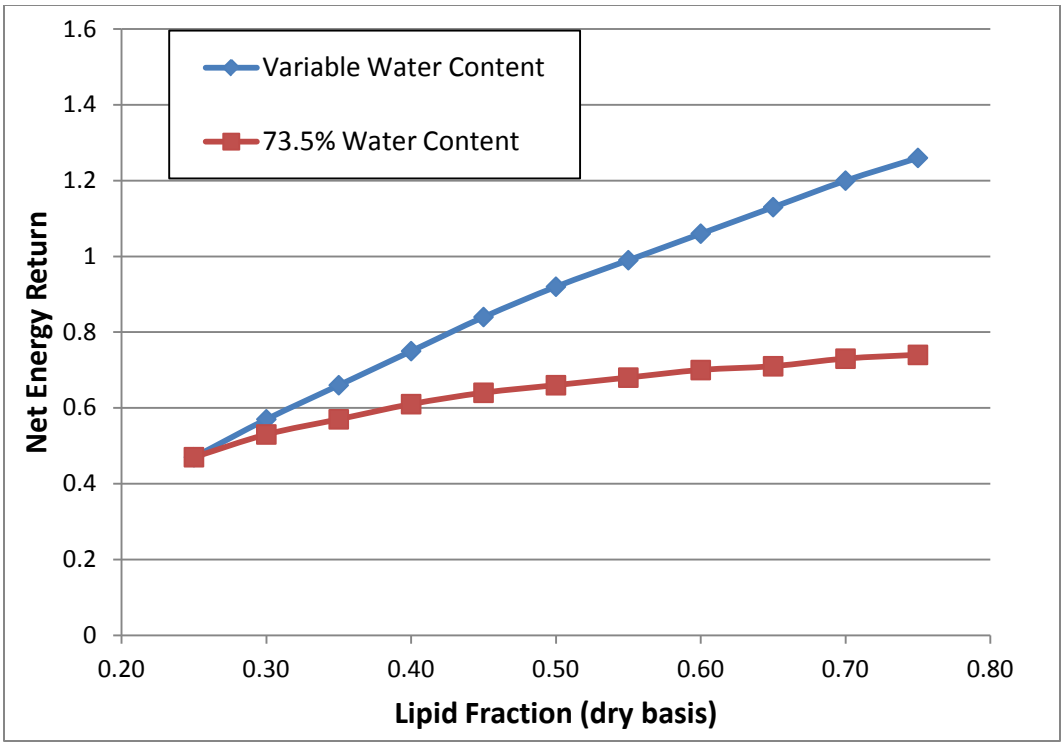

Figure 5.9: Effect of Lipid Accumulation on Net Energy Return Assuming Constant Lipid Productivity.

A comparison of Figures 5.9 and 5.4 shows that the assumption of constant lipid productivity reduces the benefit of lipid accumulation to the biodiesel's NER, especially in the case of variable water content. Assuming that lipid accumulation displaces water (the variable water content assumption), in both the constant biomass productivity and constant lipid productivity cases the NER climbs above the theoretical viability threshold of 1.0 at a lipid content of around 50%.

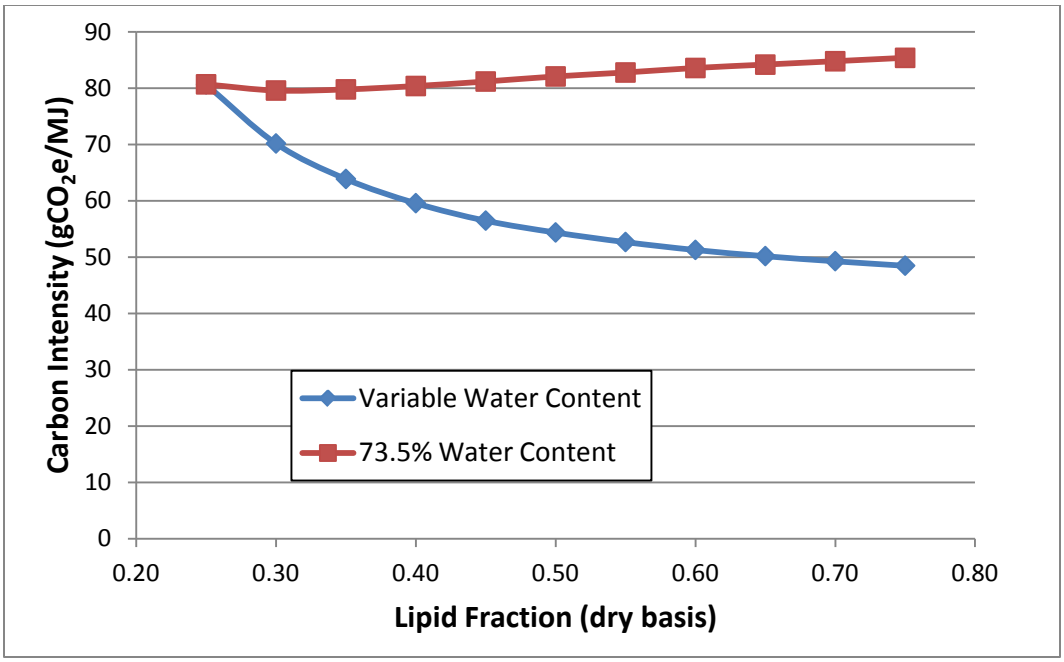

Figure 5.10: Effect of Lipid Accumulation on Carbon Intensity Assuming Constant Lipid Productivity.

The curves representing the response of the biodiesel's carbon intensity to lipid fraction, as shown in Figure 5.10, have much the same shape as those shown in Figure 5.5, but are slightly displaced upward, in the direction of higher carbon intensities. This degradation when modeling constant lipid productivity as compared to constant biomass productivity is caused by an increase in facility size, with corresponding increases in mixing and pumping energy expenditures and the embedded energy in the facility's capital assets.

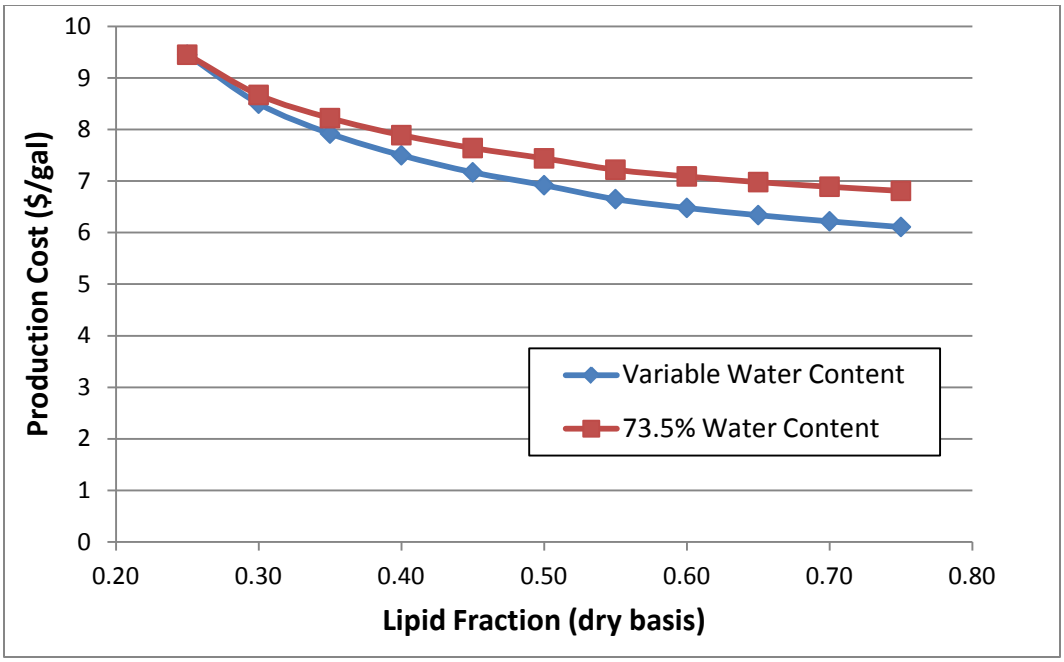

Figure 5.11: Effect of Lipid Accumulation on Unit Biodiesel Manufacturing Cost Assuming Constant Lipid Productivity.

The shape of the curves in Figures 5.8 and 5.11 are similar, but the slopes of the curves representing constant lipid productivity (Fig. 5.11) are much shallower than those simulating constant biomass productivity (Fig. 5.8). Because the size of the plant increases as the biomass productivity falls off (which happens as lipid content increases at constant lipid productivity), some of the cost benefits of higher lipid content seen in Figure 5.8 are offset by the higher energy and capital-dependent operating costs (e.g., maintenance, depreciation) resulting from a larger facility.

5.6. Conclusions

The results from the Test Scenario convincingly show that biomass drying imposes a large energy burden on the biodiesel manufacturing process, and this seriously degrades the NER, CI and unit cost of the fuel. The importance of this energy load, and the interplay between the requirements and capabilities of the drying and extraction steps, motivated all but the first of the four studies described in this chapter.

The attempt to optimize water content based on its effects on drying energy load and extraction efficiency led to a semi-quantitative conclusion (i.e., the optimum water content with respect to each of the NER, CI, and unit cost lies near the 10% target quoted in the literature) due to a lack of hard data on extraction efficiency when hexane is the solvent. Data on the extractability of lipids from microalgal biomass in commercial-scale equipment is needed to provide a more quantitative analysis.

The attempt to optimize dryer operating conditions did not identify any maxima or minima in the range of dryer inlet temperatures studied, but it showed the importance of the dryer operating strategy, which became another variable in the analysis. This study also revealed that local climate conditions have little effect on the NER, CI or cost of drying, whereas standard operating conditions can have a large effect. While this means that no potential biodiesel manufacturing site has an advantage due to its temperature and humidity, it also means no site will be disadvantaged because of its climate. (Note this applies only to biomass drying – ambient temperature may have an important impact on the microalgal growth rate when cultivated outdoors.)

The fourth analysis described in this chapter (lipid accumulation) shows how the detailed information available in TELCIM can be used to probe the underlying causes of results or trends. The use of the bar charts in Section 5.5 is an example of this. This study also shows how sensitivity analyses can be refined and extended by accounting for the potential dependencies between model parameters. This analysis explored three potentially interdependent input parameters: lipid fraction, residual water content, and lipid productivity. If high lipid content can be achieved without sacrificing biomass productivity, the NER, CI, and cost of manufacture are all significantly improved.

5.7. References for Chapter 5

[1] Lundquist, T.J., Woertz, I.C., Quinn, N.W.T., and Benemann, J.R. A Realistic Technology and Engineering Assessment of Algae Biofuel Production. Energy Biosciences Institute, University of California. October 2010. Berkeley, California.

[2] Dunstan, G.A., Volkman, J.K., Jeffrey, S.W., and Barrett, S.M. Biochemical composition of microalgae from the green algal classes Chlorophyceae and Prasinophyceae. 2. Lipid classes and fatty acids. J. Exp. Mar. Biol. Ecol. 161 (1992) 115-134.

[3] Kubatova, A., Luo, Y., Stavova, J., Sadramele, S.M., Aulich, T., Kozliak, E., and Seames, W. New path in the thermal cracking of triacylglycerols (canola and soybean oil). Fuel 90 (2011) 2598-2608.
[4] Ozer, R. Personal communication. May 16, 2011.
[5] Cooney, M., Young, G., and Nagle, N. – Extraction of bio-oils from microalgae. Separation & Purification Reviews 38 (2009) 291-325.
[6] Mustakas, G.C. Handbook of soy oil processing and utilization. Chap. 4 – Recovery of oil from soybeans. American Soybean Association and American Oil Chemists' Society. 1980. St. Louis, Missouri, USA.
[7] Johnson, L.A. Introduction to fats and oils technology, 2nd ed. (R.D. O'Brien, W. E. Farr and P.J. Wan, eds.). Chap. 7 – Recovery of fats and oils from plant and animal sources. American Oil Chemists' Society. 2000. Champaign, Illinois, USA.
[8] Seth, S., Y.C. Agrawal, P.K. Ghosh, D.S. Jayas and B.P.N. Singh. Oil extraction rates of soya bean using isopropyl alcohol as solvent. Biosystems Engineering 97 (2007) 209-217.
[9] National Solar Radiation Database. Accessed at ftp://ftp.ncdc.noaa.gov/pub/data/nsrb-solar/summary-stats/dailystats/ on various dates in 2013.
[10] National Climatic Data Center. Accessed at http://www.ncdc.noaa.gov/IPS/cd/cd.html%3bjsessionid=DE17457D54E2D27AB on various dates in 2013.
[11] California Climate Data Archive, accessed at www.calclim.dri.edu/ccda/comparative.html, on various dates in 2013.
[12] Farnsworth, R.K. and E.S. Thompson (1982). Mean Monthly, Seasonal and Annual Pan Evaporation for the United States (NOAA Technical Report NWS 34). Office of Hydrology, National Weather Service, U.S. Department of Commerce.
[13] Olivares, J.A. Proceedings from Algal Biofuels Consortium, Algae R&D Activities Peer Review, Annapolis, MD, April 7-8, 2011.
[14] Goodson, C., R. Roth, Z.T. Wang and U. Goodenough. Structural corrleates of cytomplasmic and chloroplast lipid body synthesis in Chlamydomonas reinhardtii and syimulation of lipid body production with acetate boost. Eukaryot Cell 10(12) (2011) PMC3232719.

6. CONCLUSIONS AND RECOMMENDATIONS

6.1 Introduction

There are many performance metrics that might be used to evaluate and compare alternative microalgal biodiesel manufacturing processes. The analyses conducted for this dissertation relied primarily on Net Energy Return, carbon intensity, and unit manufacturing cost for that purpose. NER is an especially relevant performance metric for a fuel, since it indicates the extent to which a particular manufacturing process is self-sufficient in terms of energy; the lower the NER, the higher the demand for externally supplied energy. An NER less than 1.0 is inherently unsustainable unless the energy deficit is supplied from renewable sources. TELCIM's LCI models differentiate between energy derived from renewable sources and fossil fuels, allowing an investigator to determine how much fossil energy is consumed to produce a quantity of microalgal biofuel. If more fossil energy is consumed to make a biofuel than the biofuel contains, then one must question whether it makes sense to produce that biofuel at all. However, some forms of energy are more valuable than others, and there may be situations in which it is appropriate to produce a fuel at a net energy deficit; examples might include a fuel used for military or other national security purposes. Carbon intensity is also a good performance metric for a fuel, since it indicates to what extent the life cycle of that fuel contributes to anthropogenic carbon emissions. One must question the merit of producing a biofuel that has higher net carbon emissions than the fossil fuel it is intended to replace. And manufacturing cost is the most commonly used measure of the resource intensity of a commodity, and provides a basis for gauging the ability of that commodity to compete in a fair and open marketplace.

TELCIM predicts many other performance measures that can be used to evaluate and compare biodiesel manufacturing schemes or scenarios. For example, the life cycle inventory models are designed to compile the indirect emissions of several air pollutants in addition to carbon dioxide. Some of these compounds are believed to contribute to global warming, others to adverse human health effects, ozone depletion, smog formation, etc. (Note that to construct a complete inventory of the emissions of these pollutants, any sources within the manufacturing plant must also be included. For example, hexane

emitted from the extraction step should be counted as VOC emissions, and fugitive methane emissions from the digestion step should be included in the inventory of greenhouse gases. TELCIM may have to be modified to estimate emissions of particular pollutants from the manufacturing plant.)

Other relevant performance measures that were used in this research include:

- Water intensity, which indicates the amount of stress a biodiesel plant will place on local water resources.
- Oil or biodiesel areal productivity, which is the volume of oil (biodiesel) produced per hectare per year. This metric is commonly used to evaluate the productivity of oilseed crops, and is an indicator of how much land is required to produce a quantity of fuel.
- Capital productivity, which is the total capital cost of the biodiesel plant divided by the annual biodiesel production volume. This is a measure of the investment required to produce a quantity of fuel.

An investigator will have to select the best performance indicators for the type of analysis being performed, and perhaps customize TELCIM to compute them..

6.2. Conclusions

6.2.1. The Viability of Microalgal Biodiesel

Assuming that the Test Scenario provides reliable indications of the approximate costs and energy and carbon footprints of producing microalgal biodiesel in the United States, it appears that conventional process technologies are inadequate to produce an environmentally sustainable and economically competitive fuel. The Net Energy Return is much less than 1.0, indicating that a significant amount of externally-supplied energy in excess of the energy content of the biodiesel must be expended to produce it. The biodiesel's carbon intensity is almost as high as that of conventional diesel produced from petroleum, so converting to microalgal biodiesel will not significantly slow the rate at which carbon dioxide is accumulating in the atmosphere. And the estimated production cost of microalgal biodiesel is several multiples of the current selling price of conventional diesel, meaning that switching would impose a substantial financial penalty. In addition, installing the production capacity to provide meaningful

quantities of microalgal biodiesel will require the investment of hundreds of billions of dollars. Under the circumstances, it hardly seems advisable to build microalgal biodiesel production plants that rely on current process technology.

Energy use within the biodiesel manufacturing process is the main driver for the NER, CI and manufacturing cost. Thermal energy for drying represents the largest energy user, followed (in descending order) by drying air compression, flue gas compression, pond mixing, and water pumping. Case studies showed that if the biomass drying load can be substantially reduced or eliminated, presumably by substituting an alternative "wet" extraction process for conventional oilseed extraction, the biodiesel's carbon intensity becomes negative, indicating net carbon sequestration. Among the many simulations performed during the course of this research, the "No Drying" case is the only scenario in which the biodiesel's carbon intensity is negative. Improving lipid productivity at constant biomass productivity can substantially reduce carbon intensity, but not enough to achieve net carbon removal from the atmosphere.

The case studies and sensitivity analyses indicate there may be several ways to improve the NER to above 1.0. In addition to implementing a wet extraction process, increasing the lipid faction of the biomass (on a dry basis) without appreciably slowing the microalga's growth rate can achieve that goal. This is very encouraging, since it suggests that advancements in both biology and process engineering can deliver substantial improvements in the biodiesel's energy footprint as well as dramatically reducing the fuel's manufacturing cost. In the analyses performed thus far, the biggest improvement in cost was achieved either by eliminating the need for drying, or by raising the lipid fraction of the dry biomass to greater than 60% without slowing the microalga's growth rate. Combining these two developments should deliver even greater benefits.

Among the more significant findings of the analyses conducted during this research is that there is little variation in the NER, CI, and unit manufacturing cost of biodiesel produced in different locations across the southern tier of the continental United States, from California to Florida. Energy usage, which drives

the KPI's, is only slightly affected by local climatological conditions. Differences in sunlight intensity barely affect biomass productivity, due to the light saturation effect. This finding suggests there is little benefit in locating biodiesel in peak sunlight areas, such as the desert Southwest, and that many other candidate sites will perform equally well or better, especially from the standpoint of make-up water requirements.

Finally, a massive amount of capital investment will be required to install manufacturing capacity for a meaningful amount of microalgal biodiesel. It is doubtful that private enterprise can or will make that investment unless dramatic process improvements and/or government incentives (e.g., land grants, favorable tax treatment, subsidies) make the economics more rewarding. Alternatively, if the driving forces become strong enough, biodiesel production may have to be viewed as a public utility at first, with production plants co-located and integrated with power and water treatment facilities. Government policy and funding may play a pivotal role in determining whether there is a future for microalgal biofuels in the United States.

6.2.2. Alternative Process Technologies

As previously discussed, energy use is the main driver of the three benchmark KPI's used in this research to characterize proposed biodiesel manufacturing schemes. The best way to improve these KPI's is to reduce the amount of energy consumed per gallon of fuel produced. Reductions in energy usage in biodiesel manufacture can be achieved by:

- Increasing the water tolerance of the oil extraction process. Allowing more water to enter the extraction step reduces the thermal and air compression energy loads in the harvesting step, the two largest energy users in the entire process.
- Lowering the microalga's intracellular water content. Reducing the amount of water entering the drying step also reduces the thermal and air compression loads in the drying operations. Increasing the lipid fraction of the dry biomass may also reduce the residual water content, giving a synergistic benefit.

- Using indirect drying. In an indirect dryer, the biomass comes into contact with a heated surface, so no hot air is needed. (Indirect dryers were not modeled in the Test Scenario because they are susceptible to fouling when drying biosolids like sewage sludge. Skin temperatures can also be high enough to accelerate undesired lipid degradation reactions. Replacing even just a portion of the total drying load with indirect drying should have favorable impacts.
- Increasing the drying air temperature. This will reduce the volume of air required, and with it the air compression energy load. (Higher temperatures may increase lipid decomposition reactions, however.)
- Reducing the mean channel velocity in the ponds. The ponds are circulated solely for the purpose of mixing, which ensures that adequate mass and heat transfer rates are maintained. Pond mixing should be kept at the absolute minimum necessary to ensure adequate performance.

Another way to improve the performance of the plant is to increase the amount of material and energy which is recovered and recycled within the process. Potential examples include:

- Anaerobic digestion of sewage sludge was the model for TELCIM's digestion process model. LEA may behave similarly, but any portion of it which is not decomposed and converted into a recoverable resource (i.e., biogas, nitrogen and phosphorus) is a lost opportunity. Some form of LEA pretreatment, such as acidic or enzymatic hydrolysis, may be justifiable on the basis of cost, energy return, and/or carbon balance.
- In the Test Scenario, heat is recovered from the exhaust from the biogas microturbine generators. This offsets some of the thermal energy load that would otherwise be met by burning natural gas. It may be possible to increase the efficiency of this and potentially other heat recovery operations in the plant.
- High volumes of humid air are rejected from the dryers, while at the same time there is a substantial need to replace evaporative losses from the ponds. Cooling towers to recover water from the dryer exhaust may be justified under some circumstances.

6.2.3. The Ideal Production Organism

Manufacture of microalgal biodiesel is at its heart a biological process, and compared to industrial organisms such as yeast or *E. coli*, microalgae are not yet well characterized or understood. Sensitivity analyses indicate that biological properties and characteristics are among the most influential on the biodiesel KPI's of interest. Biological factors affect the performance of virtually every step in the manufacturing process; for example:

- **Growth rate** affects the size of the ponds, which affects capital costs and the amount of energy used for pond mixing and water and flue gas pumping.
- **Lipid fraction** also affects the size of the ponds, and the size (capital cost) and performance (recovered energy) of the anaerobic digesters.
- **Lipid profile** affects the performance of the extraction and conversion steps, and influences the end use properties of the biodiesel.
- **Cell wall properties** affect the rate at which intracellular water is removed in drying, and the ease with which oil can be extracted..
- **Specific gravity** affects the pond mixing energy demand, and the size and operating costs of the clarifiers and thickeners in the harvesting step.
- **Cell number density** at the end of fermentation affects the size of the dewatering operations.
- **Intracellular water content** affects the size of the dryers and the amount of energy used in the drying step.
- **Thermotolerance** affects the growth rate, and influences the range of sites in which production facilities might be located.
- **Osmotolerance** also potentially affects the growth rate, the amount of water that can be recycled from the dewatering operations, and the quality of the water used as make-up.
- **Substrate specificity** determines which fertilizers can be used in the growth step, and can affect the growth rate of the organism.
- **Digestibility of LEA** affects the size and energy and nutrient recovery rates of the anaerobic digestion step.

TELCIM is an excellent tool with which to evaluate the relative importance of these properties, and to potentially identify the optimal mix of properties for a biodiesel production organism. Multi-dimensional sensitivity analyses might help guide bioprospecting, by directing researchers to microenvironments that should select for desirable properties. They might similarly influence efforts to create more effective production organisms using forced selection or genetic engineering techniques.

The goal of the growth step is to maximize lipid productivity (i.e., mass of lipid per unit illuminated surface area per unit time) rather than biomass productivity. But given that lipid productivity is the product of lipid fraction and cell growth rate, it should be recognized that, from a process standpoint, it is preferable to increase lipid fraction rather than growth rate. A higher lipid fraction reduces byproduct processing costs and waste. The value of higher lipid fraction is diminished only to the extent that energy is recovered from the residual biomass in the digesters.

The dependence of process performance on the biological, biochemical and physical properties of the microalga creates a need for close collaboration between biologists and engineers, so that the most advantageous characteristics of the organisms are identified, developed, and exploited.

6.2.4. TELCIM's Functionality

The benefits of an integrated Techno-Economic-LCI Model of biodiesel manufacture are evident in the results of the analyses described in this dissertation. Because TELCIM models the entire "cradle-to-gate" manufacturing process, including raw material and energy production and distribution, direct comparisons can be made to diesel produced by any other route. With TELCIM, an investigator can systematically evaluate the effects of alternative microorganisms, process technologies, and site conditions, on a wide range of technical, financial, and environmental performance measures. And this can be accomplished without the need to alter the underlying programming – every one of the variant cases and scenarios described in this dissertation was simulated only by changing input values from those used in the Test Scenario.

There were situations in which changes to the Test Scenario caused the NER and CI to move in opposite directions. For example, compared to the Test Scenario, adopting NAABB's productivity and lipid content targets caused the NER to improve while the CI got worse. The rich detail in TELCIM's supporting calculations allows an investigator to deconstruct aggregate measures like NER and CI to see precisely where changes are occurring in the manufacturing process, and how they contribute to changes in the performance metrics of interest.

In the Test Scenario, the extraction and conversion steps contribute little to the NER, CI and cost of the biodiesel. This raises the question of whether it is necessary to include these steps in the model, and whether the functional unit for the model should be expressed in terms of microalgal oil instead of biodiesel. It must be recognized that the purpose of the harvesting step is to render the biomass suitable for oil extraction, and that the harvesting step imposes the largest energy burden of all of the processing steps in the manufacturing process. In addition, large cost and energy savings are realized by digesting the LEA, which is a byproduct of the extraction step. Ignoring the extraction and conversion steps creates the risk of significantly distorting the ultimate costs and environmental impacts of biodiesel manufacture. It must also be recognized that due to the different cost scaling approaches used for the "modular" operations (growth, harvesting and digestion) versus the "unitary" process steps (extraction and conversion), the contributions of these two steps to the benchmark KPI's will be different at production scales other than the very large plant scale contemplated by the Test Scenario (as the plant size gets smaller, the relative contribution of the extraction and conversion steps to the NER, CI, and unit cost increases.)

6.2.5. TELCIM's Limitations

In a model such as TELCIM, there are trade-offs among size, accuracy, and flexibility. A model that is both highly accurate and flexible enough to model many different process schemes is likely to be very large and complex. TELCIM represents a reasonable balance among these competing priorities. Retaining the flexibility to model a range of physical processes while also constructing reliable financial and life cycle inventories required many simplifying assumptions, some of which are listed here:

- Quantitative nutrient uptake. It is assumed that 100% of the nitrogen, phosphorus and sulfur (if needed) added to the growth step is assimilated by the microalgae, and that no excess of these nutrients is needed. (This is a reasonable assumption as long as the blowdown ratio from the dewatering step is low, since most of the unused nutrients are recycled back to the ponds.)
- Autoflocculation. It is assumed that the biomass will flocculate and either settle or float without the aid of chemical additives, or resorting to an energy-consuming sedimentation process, such as dissolved air flotation or sonic focusing.
- No wastewater treatment. It is assumed that the blowdown and other wastewater streams generated during biodiesel manufacture can be disposed to the environment without additional treatment.
- Carbon dioxide uptake. Carbon dioxide is soluble in water, it undergoes rapid reactions with water to form carbonate and bicarbonate ions, and it participates in other biochemical and inorganic reactions. When fed flue gas at a high CO_2 concentration (relative to the concentration in the atmosphere), some carbon dioxide will escape from the ponds by offgassing. TELCIM models these complex phenomena with a simple linear correction to estimate the amount of carbon dioxide that is converted into biomass in the ponds.
- Cell growth. The microalga's areal productivity is probably the most influential input parameter in the entire model, and yet a number of complex biological, meteorological and operational phenomena are subsumed under this one variable. Results presented in this dissertation show that variations in this parameter over the time-scales being modeled can be significant, so the investigator must be careful to use appropriate input data for the type of analysis being undertaken.
- Capital costs. The capital cost structure for the harvesting step in the Test Scenario was prepared for a slightly different process than is represented by TELCIM's Harvesting Step Process Model. For example, the process model includes forced air dryers while the capital costs are based on solar drying beds. It was assumed that the changes in equipment size and/or type were small enough that the original capital cost estimates are still reasonably accurate.

TELCIM is a steady-state model simulating a process that is subject to variations of important process parameters that follow diurnal and seasonal cycles. Because it is an instantaneous model, small time steps can be used to simulate different meteorological and operating conditions, and those results can be integrated over time to build up a more accurate assessment of plant performance. The investigator must be careful to recognize the limitations on accuracy imposed by other uncertainties inherent in the model and the data used to populate it. Given these limitations, it may be advisable to place more importance on the trends and sensitivities predicted by TELCIM than the numerical values it produces.

6.3. Recommendations for Future Work

6.3.1. Uncertainty Analysis

TELCIM is a deterministic model – specific values are entered as input, calculations are made, and output is rendered in the form of numerical values for a large suite of process, financial, and environmental parameters. The model does not evaluate the validity of input parameter values, nor is it configured to estimate the uncertainty of its predictions. And although the processes modeled by TELCIM are plausible, they are still hypothetical, so there is undoubtedly some uncertainty in the model's predictions.

Some of the uncertainty in the predictions made by TELCIM arises because a single numerical value is supplied for each input parameter to the model. Many input parameters have a distribution of possible values, and although those selected as inputs to the Test Scenario and the other cases described in this dissertation represent reasonable or expected values, they were not the only values that might be defensibly used as input. Uncertainty also arises from the assumptions made about process type, sequence, and performance, or from other simplifying assumptions made to make the analysis more manageable. Because of TELCIM's structure, the uncertainty in parameters and assumptions related to the physical processes modeled by TELCIM is likely to be the most important, since predictions made by the process models are used as inputs to the financial and environmental models, and consequently process uncertainties propagate to the outputs from those models too. Price uncertainty only affects the model's financial predictions, except for the dependency of the resource usages and pollutant emissions

attributable to capital assets on monetary expenditures. Similarly, uncertainty in the resource and emission factors used in the life cycle inventories primarily affects the NER and CI calculations, and does not directly affect the engineering or financial predictions made by the model.

Now that the integrity and functionality of TELCIM have been demonstrated, an uncertainty analysis should be considered as a future project. For deterministic models like TELCIM, uncertainty is often addressed by performing Monte Carlo simulations. But Monte Carlo analysis is subject to one of the same limitations that single parameter sensitivity analysis is prone to – all variables are treated as independent, when there may be hidden or complex interdependencies that are not reflected by the mathematical models. Allowing these interdependencies to go unrecognized may actually suppress the uncertainty in the model's predictions, so it is recommended that a thorough review of the input parameter set is made, looking for interdependencies that are not reflected by the program. Wherever possible, these dependencies (e.g., residual water content as a function of lipid content, the interrelationship between growth rate and lipid fraction) should be expressed mathematically and coded into TELCIM. In addition, some of the process assumptions might be replaced with mathematical expressions. For example, quantitative uptake of nutrients could be replaced with an uptake efficiency factor that can be treated as a variable in an uncertainty analysis.

The following is a general outline of a plan for an uncertainty analysis that can be performed with TELCIM:

1. Review the complete set of input parameters and identify those between which there are dependencies. Develop mathematical relationships describing those interdependencies, thereby reducing the number of input parameters that must be specified.
2. Review process assumptions, and wherever possible, replace assumptions that limit model flexibility (e.g., allow for incomplete nutrient uptake in the ponds, allow for the use of a flocculant in the sedimentation step). This may add more input parameters that must be specified, but also allows for additional sensitivity analyses.

3. Perform comprehensive sensitivity analyses testing all input variables for their influence on a defined set of performance metrics. While selecting the range over which each variable is to be evaluated, initial consideration should be given to the type and characteristics of the probability distribution for that parameter.
4. Select the most influential variables. Prepare probability distributions from operational or experimental data, interviews with subject matter experts, and/or best technical judgment. (A reference work on preparing probability distributions and interviewing subject matter experts is "Uncertainty", by Morgan and Henrion, published by Cambridge University Press in 1990.)
5. Run Monte Carlo simulations using Oracle's Crystal Ball software, which is an Excel add-in. Predict frequency distributions for KPI's of interest, and determine confidence limits and other measures of uncertainty from those distributions (Training on Crystal Ball is available through Technology Partnerz; www.crystalballservices.com.)

6.3.2. Enhanced Physical Models

One of the design objectives for TELCIM was to make it easy for an investigator to evaluate different processing schemes for the manufacture of microalgal biodiesel. Several such alternatives are discussed in this dissertation, including a scenario in which biomass drying in the harvesting step is bypassed, and another in which the anaerobic digestion step is deleted from the process. All of the alternative scenarios described in this dissertation were performed by altering certain of the input data to neutralize the effects of certain operations (e.g., no separation across a dryer, no nutrient recovery or biogas production in a digester). To model other alternative operating schemes, it may be necessary to revise one or more of the physical models that comprise TELCIM's process models.

Prior results indicate that the three benchmark KPI's predicted by the Test Scenario can be greatly improved by adopting an oil extraction process that has a much higher water tolerance than the hexane extraction process commonly used for vegetable oil extraction. The "No Drying" variant case described in Chapter 4 was modeled by bypassing the drying operations from an operational standpoint, while retaining the capital and non-energy operating costs of the drying and extraction operations as

representative of the corresponding costs of a novel, but as yet undefined, wet extraction process. As more information becomes available on alternative lipid recovery processes, the following steps can be followed to model them in TELCIM:

- Retain the dewatering operations in the harvesting step process model.
- Revise the drying target if the water tolerance of the extraction process cannot be met by mechanical dewatering operations alone. A single drying step may be sufficient to reach that target, or the load may be split between sequential dryers, as in the Test Scenario.
- Develop a physical model for the extraction step that relates the amount of oil recovered to some process variable(s). This may be as simple as an oil recovery efficiency factor, or as sophisticated as an integrated model of solvation, pore diffusion, and coalescence. Express this model mathematically and incorporate it into TELCIM's programming.
- Develop correlations between extraction process performance and mass and energy flows, so that material and energy balances can be closed around the new process. Ensure that all of the outputs required from the Extraction Step Process Model are generated and correctly identified as inputs by any other models that use them. In addition, new entries in the financial and LCI models may have to be made to reflect new raw materials, energy carriers, capital spending categories, emission categories, etc.

If the extraction solvent contains the alcohol to which the the fatty acids will be esterified in the conversion step, some or all of the transesterification reaction may occur in the extraction step. In that case, some changes may also need to be made to the conversion step process model, or it may need to be bypassed altogether.

One of the environmental factors that can affect microalgal growth rate is the temperature of the ponds. TELCIM does not account directly for the effect of pond temperature on growth rate; it assumes that the areal productivity value selected by the user accounts for any such effects. By analyzing only sites along the southern rim of the United States, it was assumed that temperature effects on areal productivity would be insignificant, or would be the same at all of those sites. A more explicit heat balance around the ponds could be performed and incorporated into the Growth Step Process Model. This would allow differences

in productivity arising from lower ambient temperatures at more northerly sites to be predicted. To do this correctly, the investigator must be able to correlate changes in growth rate to water temperature. If such a model is implemented, TELCIM might be used to determine over what temperature range it is justifiable to continue running the plant, or to estimate how much external heat must be supplied to overcome low ambient temperatures and maintain the biomass growth rate at the desired level.

In the Test Scenario, carbon uptake in the ponds is modeled as a linear process – a fixed percentage of the carbon dioxide fed to the ponds is converted to biomass. Carbon dioxide conversion is a complicated process, since equilibration is occurring between atmospheric carbon dioxide, soluble carbon dioxide, dissolved carbonate and bicarbonate species, the biological reactions involving these chemical species, and perhaps other inorganic reactions (e.g., solids precipitation and dissolution). A more sophisticated model of these simultaneous mass transfer and reaction phenomena could be used to predict the rate at which carbon is converted into biomass. Another valuable alternative is to develop a model that predicts the efficiency of carbon dioxide transfer from the flue gas to the liquid phase in the ponds, based on gas composition and properties, fluid composition and properties, and the design and operating conditions of the gas spargers. Such a model could even investigate the effect of gas injection on the local and mean velocities of the circulating fluid in the ponds. Along similar lines, a carbonate balance around the system could be attempted.

In TELCIM, nutrient uptake in the ponds is assumed to be quantitative. This simplistic model can be replaced with a more complicated one, in which an uptake efficiency factor is either entered, or is calculated from relevant physical properties and operating conditions. Or elemental balances can be performed around the growth, harvesting and digestion steps to determine steady state concentrations of usable nitrogen and phosphorus species. These balances will predict required feed rates from steady state concentrations in the various process, product, and byproduct streams.

Although TELCIM assumes that microalgal cells will autoflocculate, in practice a chemical flocculant may be needed to achieve acceptable levels of clarifier and thickener performance. A simple mass or volume ratio can be used to estimate the consumption of flocculant, or a more sophisticated settling model can be constructed to calculate the settling characteristics of the biomass, and predict chemical addition rates.

6.3.3. Alternative models

In addition to enhancing some of its physical models, TELCIM could also be modified to simulate different processes. For example, the growth step could be based on photobioreactors (PBR's) instead of raceway ponds. This would require the redesign of most of the growth steps physical models, but the overall configuration of the Growth Step Process Model can be retained. The Stoichiometry Model will remain unchanged, precipitation and evaporation can be deleted from the water balance model, the pressure drop in the bioreactors will have to be revised, etc.

TELCIM currently treats all growth ponds the same, and the model is based on continuous, well-mixed flow reactors. A more sophisticated growth model that more accurately reflects the growth characteristics of the production organism could be developed. For example, some of the ponds might be used for production of inoculum. One set of reactors could be configured to promote biomass production, while another could be designed to maximize lipid production.

An assumption that was built into the model is that it is preferable to use microturbines distributed around the facility for power generation, rather than collecting and pumping biogas to a central power generation unit. Another design assumption built into TELCIM which could easily be replaced is the use of trucks to haul biomass to and from the extraction plant. Alternative systems could be considered, such as conveyor belts, or a pneumatic system.

One of the potential advantages of using microalgae to produce biodiesel is that many strains are capable of thriving in brackish, saline, or otherwise degraded water. TELCIM uses the salt tolerance of the organism to assist with closing the system water balance. An analysis of the impact of allowable water

quality on the KPI's can be performed to identify the expected benefits of using an osmotolerant organism. The ability to grow in degraded water may also be an absolute requirement for sites at which fresh water supplies are limited. There may be financial and operational synergies if the algae ponds can be used to treat some form(s) of wastewater, and the biodiesel is credited with avoided costs at an industrial or municipal wastewater treatment plant. Tests may have to be conducted to determine how effectively microalgae can remove conventional and other organic pollutants from wastewater, and what effect the presence of pollutants might have on its growth rate and lipid fraction.

Finally, the pressure drop calculations performed by TELCIM are based on highly simplified piping arrangements. In the Test Scenario, gas and water pumping are the second and third largest consumers of energy (following the heat energy used in biomass drying), so more accurate estimates may improve the quality of the KPI estimates generated by TELCIM. Sensitivity analyses on piping friction factors and equivalent pipe lengths will indicate whether this analysis is warranted.

6.3.4. Other Analyses

Because local climatological conditions appear to have little impact on the cost of manufacture at the five alternative US sites considered, the availability of required resources and local price structures will determine which is the most economical. Utility rates (electricity, natural gas, and water) will be among the most influential, along with labor rates. TELCIM's financial models can be populated with data specific to different sites. Another local criterion is the availability of sufficient quantities of water of suitable quality. Water procurement may involve additional capital and operating costs, such as for extraction wells and electricity for pumping groundwater. Local data can also be used to extend TELCIM's analysis into a Life Cycle Assessment. This would involve characterizing the complete life cycle of the byproducts from the biodiesel manufacturing plant, and assigning impacts to the data compiled in the LCI models.

TELCIM is programmed to model a microalgal biodiesel manufacturing facility. It assumes there is a source of carbon dioxide at the center of the facility, but no other interactions between that source and the

biodiesel plant are modeled. Similarly, TELCIM allows that part of the water brought in to the facility is wastewater treatment plant effluent, but no other connection between that plant and the biodiesel plant is modeled. Instead of viewing these as distinct facilities functioning in a traditional supplier-consumer relationship, the facility being modeled could be a utility enterprise that integrates municipal wastewater treatment, electricity generation, and biodiesel production. In that case, the biogas from the digesters could be co-fired with natural gas in the central power unit. Optimizing the production of biodiesel, electricity, and delivery of wastewater treatment services could lead to more cost effective and environmentally sustainable operating platforms when combined rather than operating individually.

In its current configuration, TELCIM does not model the extraction and conversion steps at the level of individual unit operations, as it does with the growth and harvesting steps. Instead, it models each of the extraction and conversion steps as a single activity in which all of that step's inputs and outputs are linearly related to its oil throughput. The original models for the basis extraction and conversion plants modeled by TELCIM were developed using chemical process simulators such as Aspen Plus. To better characterize the relationships between material and energy flows and oil throughput in these two major process steps, several simulations could be run over the range of relevant oil throughputs, and mathematical models entered into TELCIM.

As pointed out in Section 5.5, there are likely to be interdependencies between a microalga's lipid fraction, intracellular water content, and growth rate. TELCIM currently treats these biological properties as independent variables. When performing sensitivity analyses on these parameters, two possible relationships among these variables were proposed: the ratio of intracellular water to non-lipid biomass in the microalgal cells remains constant, and that the lipid productivity of the cells remains constant. These relationships, or other likely relationships among these three cell properties, can be expressed mathematically and coded into TELCIM.

The flue gas used as a source of carbon dioxide in the Test Scenario was assumed to originate at a coal-fired electric power plant. The offgas from other types of industrial sources, including power plants using

different fuels, will have different compositions. A series of TELCIM simulations could be used to estimate the impact on the KPI's of using flue gas from electric power plants fueled by natural gas, or that use advanced technologies such as oxycoal combustion. More concentrated carbon dioxide sources will reduce pumping energy and pipe sizes, reducing capital and operating costs and energy and carbon footprints, perhaps significantly.

For the Test Scenario, the COD removal efficiency in the anaerobic digesters was set at 65%, a value commonly achieved when sewage sludge is digested. However, LEA may be a more consistent, biodegradable material than sewage sludge, in which case the actual COD removal efficiency may be higher than 65%. On the other hand, because fatty acids are relatively reduced molecules, the LEA will be more oxidized than whole microalgae, and the methane yield might be lower than for sewage sludge. As production quantities of LEA become available it will be instructive to study how it behaves in an anaerobic digestion process.

Appendix - Derivation of Process Models

A.1. Introduction

The primary purpose of this Appendix is to provide the derivations of the governing relationships of several of TELCIM's process models. Another purpose is to capture the major assumptions underlying these models. Knowing the bases for TELCIM's physical models makes it easier to assess the reliability and accuracy of their predictions.

A.2. Models for Predicting Microalga Productivity

One of the most influential input parameters used by TELCIM to predict the technical, financial and environmental performance of proposed microalgal biodiesel manufacturing schemes is the areal productivity of the microalga strain to be grown. This parameter determines the amount of illuminated surface area required to produce a given amount of biomass, and affects energy loads, pollutant emissions, and capital and operating costs. Ideally, a value for this critically important parameter is available from actual operating data, or can be estimated from experimental data. But in the absence of such data, TELCIM includes two alternative methods for predicting it.

A.2.1. Photosynthesis Model

The first method for estimating the areal productivity of a microalga strain is adapted from techniques used by Weyer[1] and Wigmosta[2]. Their approach is to estimate the efficiency with which the energy of incident sunlight is converted into biochemical energy, using either the energy density of whole algal cells (Weyer), or the typical energy density of lipid, protein, and carbohydrate, and a representative microalgal cell composition (Wigmosta). TELCIM uses a similar formulation, but employs a carbon mass balance rather than an energy balance to estimates a microalga's productivity:

$$P_{mass} = \frac{E_s C_{PAR} \tau_p \varepsilon_f \varepsilon_s \varepsilon_a M_A}{Q_r C_c \hat{E}_p} \qquad \text{(A.2.1)}$$

where:

P_{mass} = areal productivity of microalga [kg/m^2-day];

E_s = sunlight intensity [kJ/m^2-day];

C_{PAR} = fraction of sunlight that is photosynthetically active [none];

τ_p = sunlight transmission efficiency [none];

ε_f = efficiency loss due to fluorescence [none];

ε_s = efficiency loss due to light saturation [none];

ε_a = efficiency of sunlight conversion to biomass [none];

M_A = nominal molecular weight of microalga [kg/kg-mol];

Q_r = quantum yield [kg-mol photons/kg-mol CO_2];

C_c = molar carbon concentration [kg-mol carbon/kg-mol microalga]; and

$\hat{E}_p$ = average energy content of photosynthetically active radiation [kJ/kg-mol photons].

This approach is based on the assumption that all of the carbon atoms in new microalgal cells are ultimately obtained from carbon dioxide via photosynthesis reactions. It uses the detailed microalga composition data already available in TELCIM, and obviates the need to have a measured or estimated value for the microalga's energy density.

All of the parameters on the right side of Equation A.2.1 are entered as constants, except for the efficiency factor for light saturation. TELCIM computes the light saturation efficiency using a form of Bush's Equation[3]:

$$\varepsilon_s = \begin{cases} \frac{E_0}{E_s}\ln\left(\frac{E_s}{E_0}+1\right), if\ E_s > E_0 \\ 1 \qquad\qquad\qquad\quad , if\ \ E_s \le E_0 \end{cases} \tag{A.2.2}$$

where:

E_0 = light saturation constant [kg/m^2-day]; and

E_s =actual sunlight intensity [kJ/m^2-day].

A.2.2. CSTR Model

The second method is a simplified chemical reactor model that uses the microalga's doubling time and several properties of the growth vessel to estimate the microalga's areal productivity. It assumes that the growth vessel is a perfectly mixed, flow-through reactor (also known as a continuously-stirred tank reactor, or CSTR), operating at steady state, and that growth kinetics can be modeled as first order in biomass concentration (i.e., exponential growth). An expression for these kinetics is:

$$C = C_0 e^{kt} \tag{A.2.3}$$

where:

C = microalga concentration at time 't' [kg/m^3];

C_0 = microalga concentration at time zero [kg/m^3];

k = pseudo-first order rate constant [1/day]; and

t = reaction time [days].

The microalga's doubling time can be used in Equation A.2.3 to find the pseudo-first order rate constant 'k':

$$k = \frac{1}{t_D}\ln\left(\frac{C}{C_0}\right) = \frac{\ln 2}{t_D} = \frac{0.693}{t_D} \tag{A.2.4}$$

where:

t_D = microalga's doubling time [1/day].

The reaction rate, which is the rate of microalga production, is found by differentiating Equation A.2.3 with respect to time, and using Equation A.2.4:

$$r_A = \frac{dC}{dt} = kC_0 e^{kt} = kC = 0.693\frac{C}{t_D} \tag{A.2.5}$$

where:

r_A = microalga production rate [kg/m^3-day].

Finally, the volumetric productivity (r_A) is converted into an areal productivity by dividing it by the ratio of the reactor's illuminated surface area to its volume, and including an efficiency factor (f_t) to account for less than peak illumination:

$$P_{mass} = 0.693 \frac{f_t CV}{A_i t_D} \quad \text{(A.2.6)}$$

where:

f_t = efficiency factor [none];

V = reactor volume [m^3]; and

A_i = reactor illuminated surface area [m^2].

(As a first approximation, f_t can be estimated as the fraction of the day during which the sun is shining.) This alternative is a crude approach to estimating areal productivity, since microalgae growth is exceedingly complex, and does not remain exponential even when all required growth factors are present. And because mixing in reactors as large as raceways ponds will almost certainly be less than perfect, local nutrient and/or light limitations will also reduce the microalga's growth rate. The efficiency factor can be used to account for these non-idealities.

A.3. Predicting Fertilizer Addition Rates (The "Stoichiometry Model")

The primary purpose of the Stoichiometry Model is to estimate the minimum amounts of chemical supplements ("fertilizers") that must be added to satisfy the composition of the microalgal strain being grown. The following inputs are required to perform mass balance calculations around the growth step: the amount of carbon dioxide that will be converted to biomass, the elemental composition of the microalga, and the elemental composition of each of the chemical fertilizers that will be used to supply nitrogen, phosphorus, and sulfur to the growing microalgae. (It is assumed that the requirements for other trace elements and micronutrients are satisfied by the make-up water streams being fed to the bioreactors.) In addition, TELCIM allows for two other sources of nitrogen and phosphorus: treated

sewage, and recycle from the anaerobic digestion step. These additional sources of nitrogen and phosphorus can offset some or all of the demand for purchased fertilizers.

The elemental composition of the microalga is entered in the form of the mass fraction of each element (e.g., grams of carbon per gram of microalga). TELCIM requires input data for carbon, nitrogen, oxygen, hydrogen, phosphorus, and sulfur. The mass fractions of several other elements (e.g., iron, calcium, and magnesium) are recorded, but do not factor into subsequent mass balance calculations, which are done an ash-free, dry weight basis. TELCIM converts the mass fractions to mole fractions on the basis that one "molecule" of alga contains exactly one atom of phosphorus. This artificial construct is very useful when performing subsequent mass balance calculations, which are much more conveniently done as molar balances.

The elemental composition of the nitrogen, phosphorus, and sulfur sources are specified by entering each compound's molecular weight and the number of atoms of nitrogen, phosphorus, sulfur, carbon, hydrogen and oxygen each contains. The amount of carbon dioxide that is to be converted into biomass is entered directly, or is calculated by TELCIM from a power plant rating and an appropriate CO_2 emission factor (e.g., gCO_2/kWh). A CO_2 uptake efficiency factor is entered to account for any losses due to offgassing from the ponds.

Mole balances around the growth ponds are performed for six elements: carbon, nitrogen, phosphorus, sulfur, hydrogen and oxygen. The most general statement of these balances takes the following form:

$$\sum_{i,j,k} \nu_{i,j} M_{j,k} Q_k = 0 \qquad \text{(A.3.1)}$$

where:

$\nu_{i,j}$ = stoichiometric coefficient for element 'i' in compound 'j' [kg-mol/kg-mol];

$M_{j,k}$ = molar concentration of compound 'j' in stream 'k' [kg-mol/m^3]; and

Q_k = volumetric flowrate of stream 'k' [m^3/day].

Values of Q_k are considered to be positive if entering the ponds, and negative if exiting the ponds.

Several key assumptions are made to simplify the elemental balances, and to ensure that the minimum required amounts of fertilizers are calculated:

- No more than one unique chemical compound is used as the primary source of nitrogen, of phosphorus, and of sulfur (the primary supplement for one element may include one or both of the other elements, however);
- All macronutrient elements (C, N, P and S) feeding the ponds are converted quantitatively into microalgal cells (consequently, the filtrate from the harvesting operations contains no usable C, N, P or S);
- There is no usable carbon in the make-up water (q_{fresh} in Figure 4.1, below), sewage water (Q_{SEWAGE}), and recycle from the digesters ($q_{recycle}$); and
- There is no usable nitrogen, phosphorus or sulfur in the make-up water stream.

Given these assumptions, an elemental balance on carbon simplifies to:

$$C_{TOT} = C_{CO_2} + C_N + C_P + C_S \quad \text{(A.3.2)}$$

where:

C_{TOT} = total amount of carbon to be converted to microalgae [kg-mol/day];

C_{CO_2} = amount of carbon in the CO_2 that is converted to microalgae [kg-mol/day];

C_N = amount of carbon in the nitrogen source added to the growth step [kg-mol/day];

C_P = amount of carbon in the phosphorus source added to the growth step [kg-mol/day]; and

C_S = amount of carbon in the sulfur source added to the growth step [kg-mol/day].

Balances on nitrogen, phosphorus and sulfur can also be written, accounting for the amounts of these elements that are present in any sewage water used as make-up, and in the recycle from the anaerobic digestion step:

$$N_{FED} = N_N + N_P + N_s + N_{SEW} + N_{REC} \quad \text{(A.3.3)}$$

$$P_{FED} = P_N + P_P + P_s + P_{SEW} + P_{REC} \quad \text{(A.3.4)}$$

$$S_{FED} = S_N + S_P + S_s + S_{SEW} + S_{REC} \quad \text{(A.3.5)}$$

where:

N_{FED} = total amount of nitrogen added to the microalgae growth step [kg-mol/day];

N_N = amount of nitrogen in the nitrogen source added to the growth step [kg-mol/day];

N_P = amount of nitrogen in the phosphorus source added to the growth step [kg-mol/day];

N_s = amount of nitrogen in the sulfur source added to the growth step [kg-mol/day];

N_{SEW} = amount of nitrogen added in the sewage wastewater [kg-mol/day];

N_{REC} = amount of nitrogen recycled from the digesters [kg-mol/day]; and

etc.

Carbon is used as a “key” element, allowing the amount of nitrogen, phosphorus and sulfur incorporated into biomass to be related to the amount of carbon that is converted to new cells:

$$N_{TOT} = k_{NA} C_{TOT} \quad \text{(A.3.6)}$$

$$P_{TOT} = k_{PA} C_{TOT} \quad \text{(A.3.7)}$$

$$S_{TOT} = k_{SA} C_{TOT} \quad \text{(A.3.8)}$$

where:

N_{TOT} = total amount of nitrogen to be incorporated into microalgae [kg-mol/day];

k_{NA} = molar ratio of nitrogen to carbon in the microalgae [kg-mol/kg-mol]; and

etc.

An additional set of nine relationships can be written based on the relative numbers of atoms in the fertilizers used to supply nitrogen, phosphorus, and sulfur. For example:

$$N_N = k_{NC} C_N \quad \text{(A.3.9)}$$

where:

k_{NC} = molar ratio of nitrogen to carbon in the nitrogen source [kg-mol/kg-mol].

To support microalgal growth, enough nitrogen, phosphorus and sulfur must be added to satisfy the microalga's composition:

$$N_{FED} \geq N_{TOT} \quad \text{(A.3.10)}$$

$$P_{FED} \geq P_{TOT} \quad \text{(A.3.11)}$$

$$S_{FED} \geq S_{TOT} \quad \text{(A.3.12)}$$

This system of relationships (A.3.2 – A.3.12) constitutes an optimization problem, which, due to the unbounded nature of the composition and stoichiometry of the fertilizers, is very complex. The first step in setting mathematical constraints to allow a solution to emerge is to consider whether any physical constraints might limit the possible solution set. The initial problem statement allowed for all fertilizers to contain any number of carbon, nitrogen, phosphorus and/or sulfur atoms. While this is the most general case, it is also physically unrealistic, so the following additional simplifying assumptions are made:

1. Fertilizers to provide phosphorus and sulfur are most likely to be inorganic phosphate or sulfate salts, containing no organic carbon. By further assuming these macronutrients contain no inorganic carbon, then the only potential source of carbon for cell growth other than carbon dioxide is the compound added as a nitrogen source. As a result, C_P = C_S = 0.
2. If a supplemental phosphorus source is required, it is assumed that the phosphorus source contains a negligible amount of nitrogen and/or sulfur. As a result, $P_N = P_S$= 0.
3. If a supplemental sulfur source is required, it is assumed that this material contains a negligible amount of nitrogen and/or phosphorus. As a result, $S_N = S_P$ = 0.

These heuristics acknowledge that in typical algal biomass, the number of nitrogen atoms (per cell, or per unit mass) greatly exceeds the number of atoms of phosphorus and sulfur. Thus a nitrogen source that

contains phosphorus or sulfur (e.g., $(NH_4)_3PO_4$, $(NH_4)_2SO_4$) will most likely deliver more than enough phosphorus or sulfur to meet that element's requirement.

Applying these heuristics to the elemental balances yields the following simplifications:

$$C_{TOT} = C_{CO_2} + C_N = C_{CO_2} + k_{CN}N_N \quad \text{(A.3.13)}$$

$$N_{FED} = N_N + N_{SEW} + N_{REC} \quad \text{(A.3.14)}$$

$$P_{FED} = P_P + k_{PN}N_N + P_{SEW} + P_{REC} \quad \text{(A.3.15)}$$

$$S_{FED} = S_S + k_{SN}N_N + S_{SEW} + S_{REC} \quad \text{(A.3.16)}$$

where:

k_{CN} = molar ratio of carbon to nitrogen in the nitrogen source; and

etc.

The amount of usable nitrogen contained in the sewage wastewater fed to the microalgae growth step is the product of the sewage water flowrate and its nitrogen concentration:

$$N_{SEW} = n_{SEW}Q_{SEW} \quad \text{(A.3.17)}$$

where:

n_{SEW} = concentration of usable nitrogen in the sewage wastewater [kg-mol/m^3]; and

Q_{SEW} = volumetric flowrate of sewage wastewater [m^3/day].

The amount of usable nitrogen that is recycled from the anaerobic digesters to the growth step is a function of the performance of the harvesting, extraction and digestion steps, which can be modeled as a linear function:

$$N_{REC} = f_N N_{TOT} \quad \text{(A.3.18)}$$

where:

f_N = fraction of the usable nitrogen contained in the microalgae exiting the ponds that is recycled to the growth step.

Combining Equations A.3.3, A.3.10, A.3.14, A.3.17, and A.3.18, and given that the amounts of usable nitrogen in the sewage water and digester recycle are specified by user inputs, the following relationship can be written:

$$N_N \geq k_{NA}(1 - f_N)C_{TOT} - n_{SEW}Q_{SEW} \quad \text{(A.3.19)}$$

Recognizing that the first term on the right-hand side of Equation A.3.19 represents the demand for nitrogen that is NOT satisfied by the digester recycle stream, this relationship merely states that the minimum amount of nitrogen that must be added to the ponds is equal to that unsatisfied demand less the amount present in the incoming sewage waste. Because the amount of nitrogen fertilizer added cannot be less than zero, it can be concluded that:

$$if \;\; n_{SEW}Q_{SEW} \geq k_{NA}(1 - f_N)C_{TOT}, \qquad then \; N_N = 0 \quad \text{(A.3.20)}$$

$$if \;\; n_{SEW}Q_{SEW} < k_{NA}(1 - f_N)C_{TOT}, \qquad then \; N_N = k_{NA}(1 - f_N)C_{TOT} - n_{SEW}Q_{SEW} \quad \text{(A.3.21)}$$

It is also apparent that if no nitrogen source is needed, the only source of carbon for microalgal growth is carbon dioxide, so:

$$if \;\; n_{SEW}Q_{SEW} \geq k_{NA}(1 - f_N)C_{TOT}, \qquad then \; C_{TOT} = C_{CO_2} \quad \text{(A.3.22)}$$

and Equation A.3.22 can be rewritten as:

$$if \;\; n_{SEW}Q_{SEW} \geq k_{NA}(1 - f_N)C_{CO_2}, \qquad then \; C_{TOT} = C_{CO_2}, and \;\; N_N = 0 \quad \text{(A.3.23)}$$

Note that Equation A.3.21 specifies N_N if $n_{SEW}Q_{SEW} < k_{NA}(1-f_N)C_{TOT}$, while Equation A.3.23 specifies N_N if $n_{SEW}Q_{SEW} \geq k_{NA}(1-f_N)C_{CO_2}$. But because $C_{TOT} \geq C_{CO_2}$, there is overlap between these intervals, in the region in which:

$$k_{NA}(1-f_N)C_{CO_2} \leq n_{SEW}Q_{SEW} < k_{NA}(1-f_N)C_{TOT}$$

Because Equation A.3.23 is unbounded, it must hold that in this interval $C_{TOT} = C_{CO_2}$. And because N_N is a continuous function over all values of C_{TOT}, the transition point at which N_N becomes nonzero must be at $k_{NA}(1-f_N)C_{CO_2}$. In that case, Equation A.3.21 can be rewritten as:

$$if \quad n_{SEW}Q_{SEW} < k_{NA}(1-f_N)C_{CO_2}, \qquad then\ N_N = k_{NA}(1-f_N)C_{TOT} - n_{SEW}Q_{SEW} \tag{A.3.24}$$

Substituting Equation A.3.24 into A.3.13 gives:

$$if \quad n_{SEW}Q_{SEW} < k_{NA}(1-f_N)C_{CO_2}, then\ C_{TOT} = C_{CO_2} + k_{CN}[k_{NA}(1-f_N)C_{TOT} - n_{SEW}Q_{SEW}] \tag{A.3.25}$$

which can be rearranged to:

$$if \quad n_{SEW}Q_{SEW} < k_{NA}(1-f_N)C_{CO_2}, \qquad then\ C_{TOT} = \frac{C_{CO_2} - k_{CN}n_{SEW}Q_{SEW}}{[1 - k_{CN}k_{NA}(1-f_N)]} \tag{A.3.26}$$

The only unknown in Equations A.3.23 and A.3.26 is C_{TOT}, allowing direct numerical calculation of this parameter from input data. (Note that if the nitrogen source contains no carbon, k_{CN} is identically zero, and Equation A.3.26 simplifies to $C_{TOT} = C_{CO_2}$, which is the expected result (i.e., carbon dioxide is the only source of carbon in the ponds). Similarly, as f_N approaches one, indicating that all of the nitrogen contained in the microalgae is being recycled, the condition described by Equations A.3.20 and A.3.22 is met, and TELCIM predicts that no additional nitrogen source is required, and $C_{TOT} = C_{CO_2}$.)

Once C_{TOT} is calculated, N_N is found from Equations A.3.20 and A.3.21. The only remaining unknowns in the simplified system of relationships are P_P and S_S, the amounts of phosphorus and sulfur supplements that must be added. The phosphorus and sulfur balances for the growth step expressed by Equations A.3.15 and A.3.16 are solved in a manner similar to that used to resolve the nitrogen balance, except that the nitrogen source may be another supplemental source of phosphorus and/or sulfur.

The complete solution for determining the total amount of carbon converted to microalgae, and the minimum addition rates of nitrogen, phosphorus and sulfur supplements, is given by:

$$C_{TOT} = \begin{cases} \dfrac{(C_{CO_2} - k_{CN} n_{SEW} Q_{SEW})}{[1 - k_{CN} k_{NA}(1 - f_N)]}, & if\ n_{SEW} Q_{SEW} < k_{NA}(1 - f_N) C_{CO_2} \\ C_{CO_2}, & if\ \ n_{SEW} Q_{SEW} \geq k_{NA}(1 - f_N) C_{CO_2} \end{cases} \quad \text{(A.3.27)}$$

$$N_N = \begin{cases} k_{NA}(1 - f_N) C_{TOT} - n_{SEW} Q_{SEW}, & if\ n_{SEW} Q_{SEW} < k_{NA}(1 - f_N) C_{TOT} \\ 0, & if\ \ n_{SEW} Q_{SEW} \geq k_{NA}(1 - f_N) C_{CO_2} \end{cases} \quad \text{(A.3.28)}$$

$$P_P = \begin{cases} k_{PA}(1 - f_P) C_{TOT} - p_{SEW} Q_{SEW} - k_{PN} N_N, & if\ (p_{SEW} Q_{SEW} + k_{PN} N_N) < k_{PA}(1 - f_P) C_{TOT} \\ 0, & if\ k_{PA}(1 - f_P) C_{TOT} \geq (p_{SEW} Q_{SEW} + k_{PN} N_N) \end{cases} \quad \text{(A.3.29)}$$

$$S_S = \begin{cases} k_{SA}(1 - f_S) C_{TOT} - s_{SEW} Q_{SEW} - k_{SN} N_N, & if\ (s_{SEW} Q_{SEW} + k_{SN} N_N) < k_{SA}(1 - f_S) C_{TOT} \\ 0, & if\ k_{SA}(1 - f_S) C_{TOT} \geq (s_{SEW} Q_{SEW} + k_{SN} N_N) \end{cases} \quad \text{(A.3.30)}$$

The Stoichiometry Model also predicts the amount of water consumed in photosynthesis reactions. This is accomplished by performing an elemental balance on hydrogen around the ponds, with the following assumptions:

- The hydrogen content of the nitrogen, phosphorus, and sulfur-containing compounds in sewage water is negligible (consistent with the effluent from a secondary treatment system);
- The nitrogen recycled to the ponds from the digester is in the form of ammonia, and the concentration of reduced sulfur in this stream is negligible; and
- Sufficient water is oxidized in photosynthesis reactions to exactly satisfy the hydrogen balance around the ponds.

With these assumptions, the following balance on hydrogen atoms can be written:

$$H_{TOT} = H_{RXN} + k_{HN}N_N + k_{HP}P_P + k_{HS}S_S + 3f_N N_{TOT} \quad \text{(A.3.31)}$$

where:

H_{TOT} = total amount of hydrogen to be incorporated into microalgae [kg-mol/day];

H_{RXN} = amount of hydrogen obtained from water of reaction [kg-mol/day];

k_{HN} = molar ratio of hydrogen to nitrogen in the nitrogen source [kg-mol/kg-mol]; and

etc.

Making the appropriate substitutions and rearranging gives:

$$H_{RXN} = (k_{HA} - 3k_{NA}f_N)C_{TOT} - k_{HN}N_N - k_{HP}P_P - k_{HS}S_S \quad \text{(A.3.32)}$$

Because all of the parameters on the right-hand side of Equation A.3.32 are TELCIM inputs, or outputs from prior computations, H_{RXN} can be calculated. This approximates the amount of water consumed in photosynthesis reactions, which is an input to TELCIM's Water Balance Model, as described in Section A.4 of this Appendix.

The Stoichiometry Model also predicts the amount of oxygen gas liberated by photosynthesis reactions. This calculation relies on the following assumptions:

- The oxygen content of the nitrogen, phosphorus, and sulfur-containing compounds in sewage water and digester recycle is negligible; and
- The oxygen released as gas from the ponds exactly satisfies the oxygen balance around the ponds.

An elemental balance on oxygen around the ponds, analogous to Equation A.3.29, can be written, and upon rearrangement, takes the following form:

$$O_{GAS} = k_{ON}N_N + k_{OP}P_P + k_{OS}S_S + 0.5H_{RXN} - k_{OA}C_{TOT} \quad \text{(A.3.33)}$$

where:

O_{GAS} = amount of oxygen released as gaseous oxygen (on atomic basis) [kg-mol/day]; and

etc.

All of the parameters on the right side of Equation A.3.33 are known, allowing O_{GAS} to be calculated.

A.4. Predicting Make-up Water Requirements (The "Water Balance Model")

To complete the mass balances around the microalgae growth step, it is necessary to perform a water balance around the ponds. It was already noted that water is a reactant in photosynthesis reactions, and the amount of water consumed by those reactions was calculated in the stoichiometric analysis described in the prior section. Figure A.4.1 shows the other water streams entering and leaving the bioreactors (the water consumed in photosynthesis reactions is shown as $Q_{REACTION}$). Because there is likely to be water available to be recycled to the growth step from the dewatering operations, this is included in the water balance for the growth step. (Note that the process model assumes that a portion of this recycle water stream passes through the anaerobic digestion step, where it solubilizes recovered nitrogen and phosphorus, before being returned to the ponds. Since this diversion through the digestion step does not affect the water balance, it is not indicated in Figure A.4.1.)

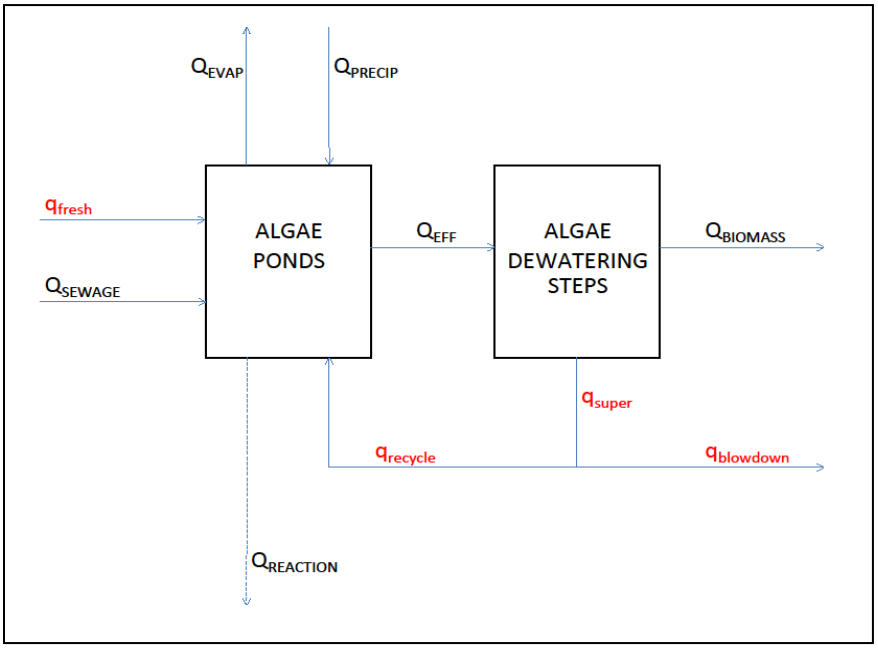

Figure A.4.1. Water Balance Schematic.

In Figure A.4.1, the water flowrates that are known are shown in uppercase (Q_{SEWAGE}, Q_{PRECIP}, $Q_{REACTION}$, Q_{EVAP}, Q_{EFF}, and $Q_{BIOMASS}$), and those which are unknown are shown in lowercase (q_{fresh}, $q_{recycle}$, q_{super} $q_{blowdown}$). The effluent from the bioreactors is known because the biomass concentration in that stream is specified by the user, and the biomass production rate is fixed by C_{TOT} and the nominal molecular weight of the algae. The amount of water in the dewatered biomass is known because the biomass recovery rates across the dewatering operations, as well as the concentration of biomass in the subnatant (concentrate) from those operations, are supplied as inputs. The flow rates of evaporated water, precipitation, and sewage make-up are also specified.

From Figure A.4.1, it is apparent that four water balance relationships can be written:

- Around the growth step and dewatering operations (see Equation A.4.1, below);
- Around the ponds (A.4.2);
- Around the dewatering operations (A.4.3); and
- Around the flow splitter on the supernatant (filtrate) from the dewatering operations (A.4.4).

These water balances take the following form:

$$q_{fresh} + Q_{SEWAGE} + Q_{PRECIP} = Q_{REACTION} + Q_{EVAP} + Q_{BIOMASS} + q_{blowdown} \quad \text{(A.4.1)}$$

$$q_{fresh} + Q_{SEWAGE} + Q_{PRECIP} + q_{recycle} = Q_{REACTION} + Q_{EVAP} + Q_{EFF} \quad \text{(A.4.2)}$$

$$Q_{EFF} = Q_{BIOMASS} + q_{super} \quad \text{(A.4.3)}$$

$$q_{super} = q_{recycle} + q_{blowdown} \quad \text{(A.4.4)}$$

where:

q_{fresh} = volumetric flow rate of non-sewage make-up water feeding the ponds [m^3/day];

Q_{SEWAGE} = volumetric flow rate of treated sewage water feeding the ponds [m^3/day];

Q_{PRECIP} = volumetric flow rate of precipitation entering the ponds [m^3/day];

$Q_{REACTION}$ = equivalent volumetric flow rate of water consumed in biomass synthesis reactions [m^3/day];

Q_{EVAP} = volumetric flow rate of water evaporated from the ponds [m^3/day];

$Q_{BIOMASS}$ = volumetric flow rate of water in the dewatered biomass [m^3/day];

$q_{blowdown}$ = volumetric flow rate of supernatant (filtrate) from the dewatering operations that will not be recycled to the ponds [m^3/day];

$q_{recycle}$ = volumetric flow rate of supernatant from the dewatering operations that will be recycled to the ponds [m^3/day];

Q_{EFF} = volumetric flow rate of aqueous medium leaving the ponds [m^3/day]; and

q_{super} = volumetric flow rate of supernatant produced by the dewatering operations [m^3/day].

Although these four water balance equations contain four unknowns, the system is underspecified because only three of the equations are linearly independent (Equation A.4.1 is the sum of A.4.2 through A.4.4.) This is consistent with our intuition that the fraction of the supernatant which is recycled versus that which is rejected as blowdown is a degree of freedom.

If possible, the lowest cost and least environmentally burdensome operating mode is the one in which all of the supernatant is recycled. However, net evaporation removes essentially pure water, so a blowdown stream may have to be removed in order to control the accumulation of dissolved chemical species in the growth medium. A mass balance for a dissolved, non-volatile chemical species present in the system can be written as:

$$q_{fresh}C_{fresh} + Q_{SEWAGE}C_{SEWAGE} = Q_{BIOMASS}C_{BIOMASS} + q_{blowdown}C_{blowdown} \quad \text{(A.4.5)}$$

where:

C_i = Mass concentration of dissolved, non-volatile chemical species in stream “i” [kg/m^3]

Recognizing that the concentration of this species in the blowdown and the aqueous fraction of the biomass stream are identical to that in the supernatant, Equation A.4.5 can be rewritten as:

$$q_{fresh}C_{fresh} + Q_{SEWAGE}C_{SEWAGE} = (Q_{BIOMASS} + q_{blowdown})C_{super} \quad \text{(A.4.6)}$$

Presumably, the maximum concentration that a non-volatile dissolved species can be allowed to reach in the growth medium without adversely affecting microalgal growth or lipid content can be specified. If it is assumed that this concentration is reached in the ponds, the supernatant stream will have the same concentration of that dissolved species. Assuming that the concentration of this constituent in each of the make-up water streams (C_{fresh} and C_{SEWAGE}) is also specified, the system now consists of four independent equations in four unknowns. Serial substitution allows the unknown water flowrates ($q_{blowdown}$, q_{fresh}, $q_{recycle}$, and q_{super}) to be found from Equations A.4.2 through A.4.4 and A.4.6.

But these water balance equations can, under certain circumstances, generate negative values for flowrates, which is physically impossible. For example, when precipitation greatly exceeds evaporation, the water balance may indicate a negative make-up water flowrate (q_{fresh}). To avoid these outcomes, the following constraints must be imposed:

- The maximum amount of water that can be recycled to the ponds cannot exceed the amount of supernatant that is available; and
- If inflow to the ponds exceeds outflow, even when the make-up water flowrate (q_{fresh}) is zero, then the recycle water flowrate is calculated solely on the basis of the water balance.

With these constraints in place, the system water balance is solved in the following steps. First, q_{super} is found from Equation A.4.3. The maximum amount of supernatant that can be recycled to the ponds is then found from A.4.6, after substituting into it Equations A.4.2 through A.4.4 and rearranging:

$$q_{recycle,max} = Q_{EFF} + Q_{SEWAGE}\frac{(C_{SEWAGE} - C_{FRESH})}{(C_{FRESH} - C_{super})} + (Q_{EVAP} + Q_{REACTION} - Q_{PRECIP})\frac{C_{FRESH}}{(C_{FRESH} - C_{super})} \quad \text{(A.4.7)}$$

If the quantity on the right-hand side of Equation A.4.7 is greater than q_{super}, then $q_{recycle,max}$ is limited to q_{super}. TELCIM then checks whether the total influx to the pond exceeds the total efflux, assuming that

q_{fresh} is zero. If so, q_{fresh} is set equal to zero, and $q_{recycle}$ is determined strictly by water balance. For any case between these two extremes, $q_{recycle}$ is determined using the salt balance. In summary:

$$q_{recycle} = \begin{cases} q_{super} & if\ q_{recycle,max} > q_{super} \\ Q_{RXN} + Q_{EVAP} + Q_{EFF} - Q_{PRECIP} - Q_{SEWAGE}, & if\ \left(Q_{RXN} + Q_{EVAP} + Q_{EFF} - Q_{PRECIP} - Q_{SEWAGE} - q_{recycle,max}\right) < 0 \\ q_{recycle,max} & otherwise \end{cases} \quad \text{(A.4.8)}$$

(It can easily be confirmed from Equation A.4.2 that the first two conditions expressed in Equation A.4.8 cannot both be met at the same time.)

TELCIM now calculates the amount of make-up water that is needed to satisfy the system water balance using Equation A.4.2 and the second constraint listed above, as follows:

$$q_{fresh} = \begin{cases} 0, & if\ \left(Q_{RXN} + Q_{EVAP} + Q_{EFF} - Q_{PRECIP} - Q_{SEWAGE} - q_{recycle,max}\right) < 0 \\ Q_{RXN} + Q_{EVAP} + Q_{EFF} - Q_{PRECIP} - Q_{SEWAGE} - q_{recycle}, & otherwise \end{cases} \quad \text{(A.4.9)}$$

Finally, the volumetric flowrate of the blowdown stream is found from Equation A.4.4.

With the completion of this water balance, all of the mass balances around the algae growth system are closed. The mass flowrates of macronutrients (nitrogen, phosphorus and sulfur sources), and the volumetric flowrate of make-up water that must be added to the system to sustain growth and maintain the water balance are calculated by TELCIM. Also determined are:

- The mass flowrate of algal biomass;
- The supernatant recycle ratio; and
- The water consumed and oxygen produced by photosynthesis.

A.5. Predicting Raceway Pond Mixing Energy Requirements

The water in the ponds must be well mixed in order to:

- Ensure nutrients are well distributed;

- Inhibit cells from settling or adhering to surfaces;
- Allow all of the microalgal cells to gain exposure to sunlight; and
- Prevent thermal stratification.

Mixing is typically accomplished in ponds by inducing rapid flow in a single (horizontal) direction along the long axis of the pond. Friction along the interfaces between the flowing water and the solid pond floor and walls impedes flow, and energy must be supplied to the fluid to overcome friction and maintain the desired velocity.

Flow in raceway ponds can be modeled as a form of open channel flow, in which the driving force for flow is a hydraulic gradient (i.e., a change in elevation along the flow path). Open channel flow is characterized by the Manning Equation[4]:

$$v = \frac{R^{2/3} s^{1/2}}{n} \quad \text{(A.5.1)}$$

where:

v = mean channel velocity [m/sec];

R = hydraulic radius =A/P [m];

s = hydraulic gradient = ΔD/L [none];

A = cross sectional area perpendicular to flow = DW [m^2];

P = wetted perimeter = W+2D [m];

D = water depth [m];

L = channel length [m];

ΔD = change in elevation (or depth) [m]; and

n = Manning friction factor [$sec/m^{1/3}$].

Equation A.5.1 can be reconfigured to solve for the change in elevation, or “head”, required to induce a desired mean channel velocity in a pond of specified dimensions:

$$\Delta D = \frac{L v^2 n^2}{R^{4/3}} \quad \text{(A.5.2)}$$

Another source of energy dissipation in fluid flow is changes in flow direction. TELCIM accounts for two types of flow direction changes. The first, which is typical of all raceway ponds, is the 180^o bends at the ends of the pond. TELCIM also allows for changes in water flow direction in carbonation sumps. A diagram of a potential carbonation sump is shown as Figure A.5.1. The head loss associated with these changes in flow direction is estimated using the following correlation[5]:

$$h_L = \frac{K v^2}{2g} \quad \text{(A.5.3)}$$

where:

h_L = head loss [m];

K = friction loss coefficient [none]; and

g = acceleration due to gravity [m/sec^2].

The head losses due to friction and bends are combined and converted to an electric power load using the following relationship[6]:

$$P = k \frac{Q\rho(\Delta D + h_L)}{e} \quad \text{(A.5.4)}$$

where:

k = unit conversion factor =0.0098066 kW-sec/kg-m;

P = power usage [kW];

Q = volumetric flowrate [m^3/sec];

ρ = fluid density [kg/ m^3]; and

e = electric motor efficiency [none].

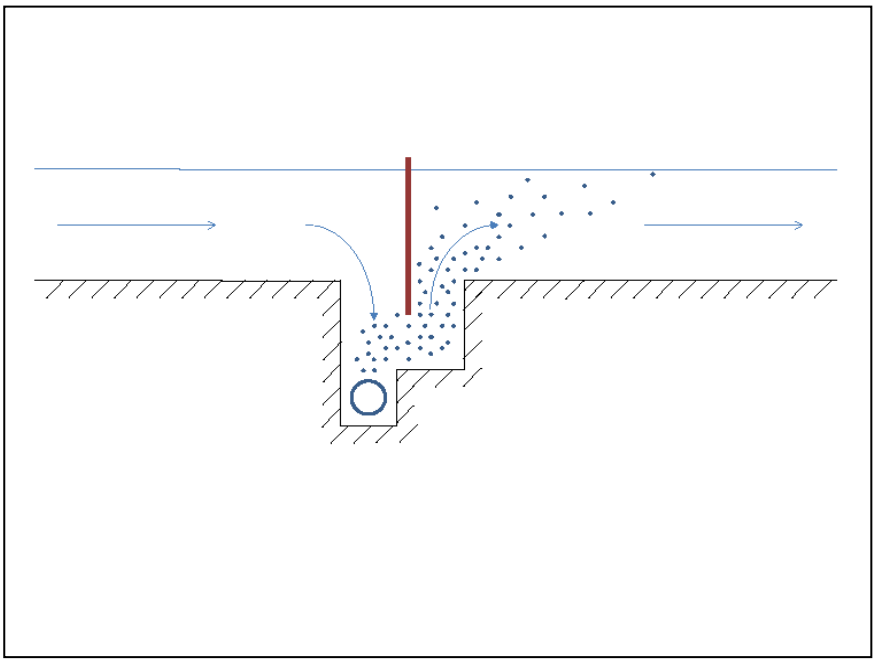

Figure A.5.1: Cross-section of a possible carbonation sump. A vertical baffle directs water flow downward, countercurrent to the gas flow. As the water passes around the baffle, and back upward, the gas bubbles are carried upward and then horizontally as the water changes flow direction. The water makes the equivalent of two 180^{o} changes in flow direction as it passes through the sump.

A.6. Predicting Flue Gas Pumping Energy Requirements

The energy required to pump flue gas from a centralized source to a biomass production module (a cluster of ponds and associated equipment) is a function of the amount, composition and physical properties of the gas, and the length and characteristics of the pipeline through which the gas flows.

The composition of the flue gas is entered as the volume percent of oxygen, carbon dioxide and nitrogen (it is assumed that water vapor has been condensed and the concentrations of other gases are negligible). The total mass flowrate of flue gas is calculated from the volume fraction and mass flowrate of carbon dioxide, which are inputs to the Stoichiometry Model.

The Stoichiometry Model predicts the amount of carbon that is converted into microalgae. The amount of illuminated pond surface area required is calculated from the carbon mass fraction of the microalgae and

its areal mass productivity (kg/m^2-day). Ponds are assumed to be clustered into biomass production modules, and TELCIM computes the number of modules needed to provide the required illuminated surface area. The total mass flowrate of flue gas is apportioned evenly among that number of modules, and it is assumed that each module has a dedicated flue gas pipeline, or "header".

In order to calculate the pressure drop in the flue gas headers, it is necessary to estimate the viscosity of the flue gas. The viscosity of gas mixtures can be very non-ideal (i.e., non-linear with composition), so TELCIM employs a semi-empirical method first developed by Wilke in the 1950's to estimate the viscosity of the flue gas at the specified inlet temperature[7].

Another gas property that is used in the calculation of the power required for compression is the ratio of the gas's heat capacity at constant pressure to its heat capacity at constant volume. The heat capacity of the gas mixture at constant pressure is assumed to be the molar average of the heat capacities of the constituent gases. The heat capacity of the gas mixture at constant volume is calculated from the following property of ideal gases[8]:

$$C_V = C_P - R \tag{A.6.1}$$

where:

C_V = Heat capacity at constant volume [kJ/kg-mole-K];

C_P = Heat capacity at constant pressure [kJ/kg-mole-K]; and

R = Universal gas law constant = 8.3145 kJ/kg-mole-K.

The estimated pressure at the outlet of the gas header is an input to the model. This outlet pressure should account for the static head from water in the ponds above the gas sparger, the pressure drop across the sparger, and the pressure drop due to valves and fittings in the flue gas distribution system within the biomass production module. A pipe diameter is specified, and TELCIM computes the Reynolds number for flow in the header using the following relationship:

$$Re = \frac{\rho v D}{\mu} = \frac{\rho(\frac{Q}{A})D}{\mu} = \frac{(\rho Q)(\frac{4}{\pi D^2})D}{\mu} = \frac{4\dot{m}}{\pi \mu D} \quad \text{(A.6.2)}$$

where:

Re = Reynolds number [none];

ρ = gas density [kg/m^3];

v = linear gas velocity [m/sec];

D = pipe inside diameter [m];

μ = gas viscosity [kg/m-sec];

Q = gas volumetric flowrate [m^3/sec];

A = pipe cross-sectional area [m^2]; and

$\dot{m}$ = gas mass flowrate [kg/sec].

The Fanning friction factor, which is a function of the Reynolds number, pipe diameter and surface roughness, is then entered. TELCIM computes the header inlet pressure necessary to overcome frictional losses using the following form of the Bernoulli Equation for isothermal flow of a compressible fluid in circular pipes[9]:

$$\dot{m} = \left(\frac{\pi}{8}\right)\sqrt{\frac{(P_1^2 - P_2^2)g_c D^5 M}{fLRT}} \quad \text{(A.6.3)}$$

where:

$\dot{m}$ = Gas mass flowrate [lb$_m$/sec];

P_1 = Header inlet pressure [lb$_f$/ft^2];

P_2 = Header outlet pressure [lb$_f$/ft^2];

g_c = Gravitational constant = 32.174 lb$_m$-ft/lb$_f$-sec^2;

D = Pipe inside diameter [ft];

M = Gas molecular weight [lb$_m$/lb-mole];

f = Fanning friction factor [none];

L = Pipe length [ft];

R = Universal gas law constant =1546 ft-lb_f/lb-mole-^oR; and

T = Absolute temperature [^oR].

The pressure at the inlet to the gas header is assumed to be the outlet pressure from a compressor. The energy required to compress the flue gas to that outlet pressure is calculated from the following equation for adiabatic compression[9]:

$$H_{ad} = \left(\frac{k}{k-1}\right) RT \left[\left(\frac{P_{out}}{P_{in}}\right)^{(k-1)/k} - 1\right] \quad \text{(A.6.4)}$$

where:

H_{ad} = adiabatic head [kJ/kg-mole]

k = ratio of heat capacities = C_P/C_V [none];

P_{out} = compressor outlet pressure [atm]; and

P_{in} = compressor inlet pressure [atm].

The adiabatic head is converted to a power load using the following equation:

$$P = \frac{H_{ad}\dot{m}}{eM} \quad \text{(A.6.5)}$$

Depending on the number of biomass production modules in the modeled facility, modules may be located at different distances from the gas source. In that case, the discharge pressures calculated by Equation A.6.3 will be different, as will the power loads calculated by Equations A.6.4 and A.6.5. TELCIM uses the Flue Gas Pumping Distance Model to determine how many modules there are at each pumping distance, and then aggregates the total power load for flue gas pumping.

A.7. Predicting Water Pumping Energy Requirements

Water pumping energy calculations are performed in a similar fashion to the flue gas pumping energy calculations described in Section A.6, except that water is an incompressible fluid. In general, the volumetric flowrate of a particular water stream is either specified or is calculated by the Water Balance Model. TELCIM apportions that volumetric flow based either on the number of modules (for streams entering the facility, such as sewage water), or the total number of ponds (for streams that transfer water to or from the ponds, such as pond effluent feeding the first dewatering operation). The pumping distance and pipe diameter are specified, and TELCIM calculates the Reynolds number using Equation A.6.2. Based on the Reynolds number, pipe diameter and surface roughness, the appropriate Fanning friction factor is entered, and TELCIM calculates the head loss due to friction using a form of the Darcy Equation[5]:

$$h_L = \frac{2fLv^2}{Dg} \tag{A.7.1}$$

where:

h_L = head loss [m]

g = acceleration due to gravity = 9.81 m/sec^2

To this head loss is added any change in elevation between the inlet and outlet of the water header, and the total change in head is then converted to a power load using Equation A.5.4. In the special case of water transfers between harvesting operations, it is assumed that the pumping distances are negligible, and that the elevation change is the dominant source of head loss. To the elevation change can be added the equivalent head losses due to valves and fittings, if these are known or can be estimated.

A.8. Mass Balance Model of Microalgal Biomass Harvesting

The microalgae harvesting step in TELCIM allows for as many as five sequential dewatering operations followed by as many as five sequential drying operations. TELCIM requires two input data for each of these ten steps: the biomass recovery rate and the ash-free, dry weight concentration (wt. %) of the

biomass in the concentrate stream from that operation. The separation steps are modeled as described by the following schematic:

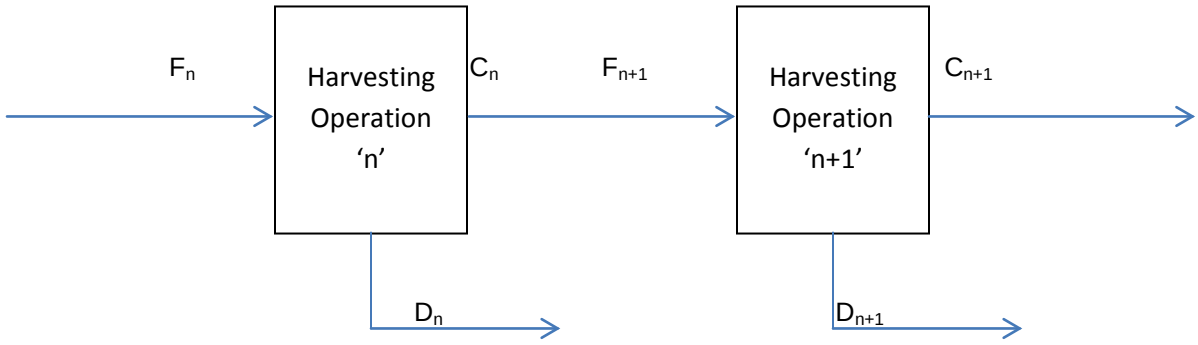

Figure A.8.1

where F_n is the feed stream to harvesting operation 'n', C_n is the stream exiting harvesting operation 'n' which is more concentrated in biomass (the "concentrate"), and D_n is the stream exiting harvesting operation 'n' which has become more dilute in biomass (the "filtrate" or "supernatant"). As shown, the concentrate from harvesting operation 'n' is the feed to harvesting operation 'n+1'. A mass balance on microalgal biomass around harvesting operation 'n' can be written as:

$$M_{F_n} = M_{C_n} + M_{D_n} \tag{A.8.1}$$

where:

M_{F_n} = mass flowrate of algal biomass in the feed to harvesting operation 'n' [kg/day];

etc.,

and all mass flowrates are on an ash-free, dry weight basis.

Because the solids recovery rate for each harvesting operation is provided as input, the following relationship can be written:

$$M_{C_n} = r_n M_{F_n} \tag{A.8.2}$$

where:

r_n = microalgal biomass recovery rate for harvesting operation 'n' [kg/kg];

Because the concentrate from one harvesting operation is the feed to the next:

$$M_{C_n} = M_{F_{n+1}} \tag{A.8.3}$$

The mass flowrate of biomass entering the first harvesting operation (M_{F_1}) is calculated by the Growth Step Process Model. Using Equations A.8.2 and A.8.3, the mass flowrate of biomass in all concentrate and feed streams can be calculated. The mass flowrate of microalgal biomass in all of the reject (dilute) streams can be found from Equation A.8.1.

Because the weight fraction of microalgal biomass in each concentrate is also provided as an input, the following relationship can be written:

$$k_n = \frac{M_{C_n}}{M_{C_n} + W_{C_n}} \tag{A.8.4}$$

where:

k_n = mass fraction of microalgal biomass in concentrate stream C_n [none]; and

W_{C_n} = mass flowrate of water in concentrate stream C_n [kg/day].

Equation A.8.4 can be rearranged to the following:

$$W_{C_n} = M_{C_n} \frac{(1 - k_n)}{k_n} \tag{A.8.5}$$

Because the mass flowrate of microalgal biomass in all concentrate streams is known, TELCIM can calculate the mass flowrate of water in each concentrate stream. A water balance around harvesting operation 'n' provides that:

$$W_{F_n} = W_{C_n} + W_{D_n} \quad \text{(A.8.6)}$$

Because the mass concentration of biomass in the effluent from the ponds is specified, W_{F_1} is known. That allows TELCIM to calculate W_{D_1} from Equations A.8.5 and A.8.6. And since the concentrate from each harvesting operation is the feed to the next:

$$W_{F_{n+1}} = W_{C_n} \quad \text{(A.8.7)}$$

TELCIM can calculate the mass flowrate of water in every concentrate and filtrate stream. These water mass flowrates are also converted to volumetric flowrates using the following relationship:

$$Q_{D_n} = \frac{W_{D_n}}{\rho} \quad \text{(A.8.8)}$$

where:

Q_{D_n} = volumetric flowrate of filtrate (dilute) stream D_n [m^3/day]; and

ρ = density of water [kg/m^3].

TELCIM aggregates the volumetric flowrates of the filtrate (dilute) streams from the five dewatering operations, and reports this to the Water Balance Model as the maximum amount of water available for recycle to the microalgae growth step from the harvesting step.

At this point, the mass flowrates of microalgal biomass and water in every concentrate and dilute stream in the harvesting step are known. A harvesting operation involving fewer than five dewatering and/or fewer than five drying operations can be simulated by "bypassing" any unwanted operations. This is accomplished by setting the biomass recovery rate for each unwanted harvesting operation to 100%, and the biomass concentration in the concentrate stream equal to the biomass concentration of the concentrate exiting the prior harvesting operation. Because the concentrate from one harvesting

operation is the feed to the next, these input parameter selections cause the concentrate from the unwanted operation to be the same as its feed; in other words, no separation occurs in that operation.

A.9. Thermodynamic Model of Forced Air Drying of Microalgal Biomass

This section describes the model used to calculate the energy demand of forced air drying to remove intracellular water from the microalgal biomass. Each drying operation in the harvesting process is modeled as a two-step process. In the first step, ambient air is heated to a specified temperature using an external heat source. In the second step, this preheated air is contacted with wet biomass, evaporating sufficient water to achieve a specified residual moisture content at a specified dryer exit temperature. TELCIM performs simultaneous mass and enthalpy balances to compute the volume of air required and the amount of heat energy that must be supplied to achieve the specified dryer exit conditions. TELCIM models as many as five sequential drying operations, in which the biomass exiting one stage becomes the feed to the next stage. The calculation strategy is the same for all drying stages, so it is only described once.

The first step of the two-step drying process comprising each drying stage is illustrated as follows:

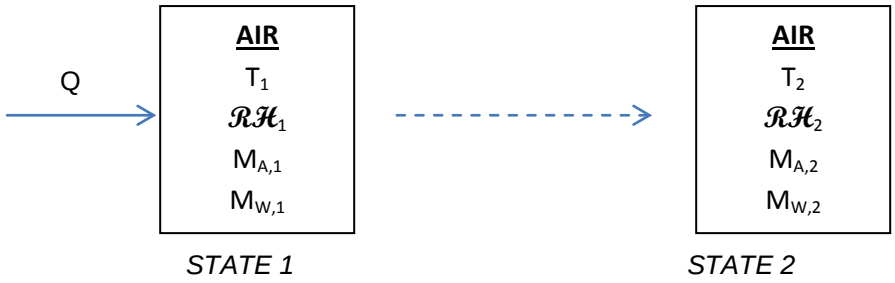

Figure A.9.1

where:

Q = heat energy [kJ];

T_i = temperature of state i [K];

$\mathcal{RH}_i$ = relative humidity of state i [%];

$M_{A,i}$ = mass of bone dry air in state i [kg]; and

$M_{W,i}$ = mass of water vapor in state i [kg].

In this change of state, the thermodynamic system is considered to be closed with respect to mass and open with respect to heat energy. Since all of the water in State 1 is water vapor, no change of phase occurs, and the following mass balances can be written:

$$M_{A,1} = M_{A,2} \tag{A.9.1}$$

$$M_{W,1} = M_{W,2} \tag{A.9.2}$$

An energy balance over the system requires that:

$$Q = \Delta H = \Delta H_A + \Delta H_W = M_{A,1}\left(\Delta\overline{H}_{A,2} - \Delta\overline{H}_{A,1}\right) + M_{W,1}\left(\Delta\overline{H}_{W,2} - \Delta\overline{H}_{W,1}\right) \tag{A.9.3}$$

where:

ΔH = change in enthalpy between states 1 and 2 [kJ];

ΔH_A = change in enthalpy in the air phase between states 1 and 2 [kJ];

ΔH_W = change in enthalpy in the water phase between states 1 and 2 [kJ];

$\Delta\overline{H}_{A,i}$ = specific enthalpy of the air phase in state i [kJ/kg]; and

$\Delta\overline{H}_{W,i}$ = specific enthalpy of the water phase in state i [kJ/kg].

To specify the enthalpies of the air and water phases in any state, a reference state must first be selected for each phase. For this analysis, the standard state for air is specified as 0^oF and 1 atmosphere (abs.), and the standard state for liquid water is specified as 32^oF and 1 atmosphere (abs.). The enthalpies of air and water vapor in any other state can then be calculated using the following:

$$\Delta\overline{H}_{A,1} = \overline{C}_{p,A}(T_1 - T_A^o) \tag{A.9.4}$$

$$\Delta\bar{H}_{A,2} = \overline{C}_{p,A}(T_2 - T_A^o) \quad \text{(A.9.5)}$$

$$\Delta\bar{H}_{W,1} = \overline{C}_{p,W}(T_{VAP} - T_W^o) + \Delta\bar{H}_{VAP} + \overline{C}_{p,WV}(T_1 - T_{VAP}) \quad \text{(A.9.6)}$$

$$\Delta\bar{H}_{W,2} = \overline{C}_{p,W}(T_{VAP} - T_W^o) + \Delta\bar{H}_{VAP} + \overline{C}_{p,WV}(T_2 - T_{VAP}) \quad \text{(A.9.7)}$$

where:

$\overline{C}_{p,A}$ = specific heat capacity of air [kJ/kg-K];

$\overline{C}_{p,W}$ = specific heat capacity of liquid water [kJ/kg-K];

$\overline{C}_{p,WV}$ = specific heat capacity of water vapor [kJ/kg-K];

T_A^o = reference temperature for air [K];

T_W^o = reference temperature for water [K];

T_{VAP} = temperature at which the heat of vaporization of water is reported [K]; and

$\Delta\bar{H}_{VAP}$ = specific heat of vaporization of water at T_{VAP} [kJ/kg].

TELCIM uses mathematical correlations to estimate the specific heat capacities of air and water vapor at specified temperatures[10]. The specific heat capacity of liquid water is assumed to be a constant over the relevant temperature range, and the value used for the latent heat of vaporization of water was measured at 25°C[11]. Because the temperature of the inlet air (T_1) and the target air temperature (T_2) are specified, the specific enthalpies of the inlet and outlet materials can be calculated. Finally, a correlation is used to estimate the vapor pressure of water at the target air temperature, allowing the relative humidity at that condition ($\mathcal{RH}_2$) to be calculated[12].

The second step in the drying process is illustrated as:

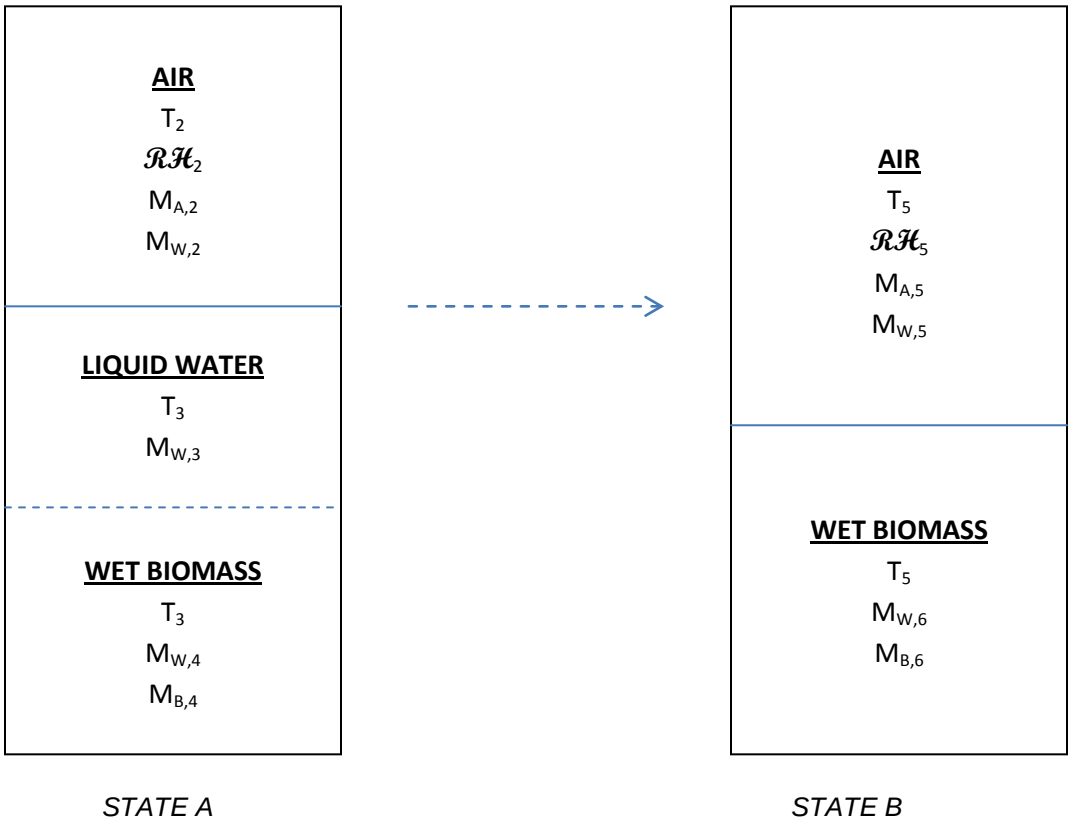

Figure A.9.2

This process, which is closed to both mass and energy transfer, involves contacting wet biomass with the warm air produced in the first step. The sensible heat lost when the air temperature drops from T_2 to T_5 provides the latent heat necessary to evaporate some water and heat the wet biomass to the dryer exit temperature. The biomass entering the dryer is treated as an ideal mixture of water and bone dry biomass. A portion of the liquid water in the incoming biomass is to be evaporated ($M_{W,3}$); that water is identified separately as "liquid water", while the incoming liquid water that is not evaporated is designated as $M_{W,4}$.

Because the system is closed, the following mass and enthalpy balances can be written:

$$M_{A,5} = M_{A,2} \tag{A.9.8}$$

$$M_{W,5} = M_{W,2} + M_{W,3} \tag{A.9.9}$$

$$M_{W,4} = M_{W,6} \tag{A.9.10}$$

$$M_{B,4} = M_{B,6} \tag{A.9.11}$$

$$\begin{aligned} M_{A,2}\Delta\overline{H}_{A,2} + M_{W,2}\Delta\overline{H}_{W,2} + M_{W,3}\Delta\overline{H}_{W,3} + M_{W,4}\Delta\overline{H}_{W,4} + M_{B,4}\Delta\overline{H}_{B,4} = \ldots \\ \ldots = M_{A,5}\Delta\overline{H}_{A,5} + M_{W,5}\Delta\overline{H}_{W,5} + M_{W,6}\Delta\overline{H}_{W,6} + M_{B,6}\Delta\overline{H}_{B,6} \end{aligned} \tag{A.9.12}$$

Substituting Equations A.9.8 – A.9.11 into Equation 9.12 and rearranging gives:

$$\begin{aligned} M_{A,2}\left(\Delta\overline{H}_{A,2} - \Delta\overline{H}_{A,5}\right) = M_{W,2}\left(\Delta\overline{H}_{W,5} - \Delta\overline{H}_{W,2}\right) + M_{W,3}\left(\Delta\overline{H}_{W,5} - \Delta\overline{H}_{W,3}\right) + \ldots \\ \ldots + M_{W,4}\left(\Delta\overline{H}_{W,6} - \Delta\overline{H}_{W,4}\right) + M_{B,4}\left(\Delta\overline{H}_{B,6} - \Delta\overline{H}_{B,4}\right) \end{aligned} \tag{A.9.13}$$

The ratio of $M_{W,4}$ to $M_{B,4}$ is fixed by the residual water content feeding the extraction step, which is an input to the model. And because the moisture content of the biomass feeding the drying step is also an input to the model, the ratio of $M_{W,3}$ to $M_{B,4}$ is also fixed. The mass of incoming water vapor can be related to the mass of incoming air by its relative humidity, per the following expression:

$$M_{W,2} = \mathcal{RH}_2(\mathcal{H}_{\text{SAT},2})M_{A,2} \tag{A.9.14}$$

where:

$\mathcal{H}_{\text{SAT},2}$= saturated humidity of air at Temperature 2 [kg/kg].

The specific enthalpies of air and water at all conditions are determined in the same manner as shown in Equations A.9.4 – A.9.7 above. And rather than define a standard state for biomass, it is sufficient to note that since no phase change occurs, and the heat capacity of biomass is likely to be a weak function of temperature over the relevant temperature range, the following relationship will hold:

$$\left(\Delta\overline{H}_{B,6} - \Delta\overline{H}_{B,4}\right) = \overline{C}_{p,B}(T_5 - T_3) \tag{A.9.15}$$

Substituting Equations A.9.14 and A.9.15 into A.9.13 and rearranging gives:

$$M_{A,2}[(\Delta\bar{H}_{A,2} - \Delta\bar{H}_{A,5}) - \mathcal{RH}_2(\mathcal{H}_{\text{SAT},2})\,(\Delta\bar{H}_{W,5} - \Delta\bar{H}_{W,2})]=\ldots$$
$$\ldots = M_{W,3}(\Delta\bar{H}_{W,5} - \Delta\bar{H}_{W,3}) + M_{W,4}(\Delta\bar{H}_{W,6} - \Delta\bar{H}_{W,4}) + M_{B,4}(\Delta\bar{H}_{B,6} - \Delta\bar{H}_{B,4}) \quad \text{(A.9.16)}$$

Given that all of the specific enthalpies in Equation A.9.16 are known, and the ratios of $M_{W,4}$ and $M_{W,3}$ to $M_{B,4}$ are also known, once $M_{B,4}$ is specified, $M_{A,2}$ can be calculated. And once $M_{A,2}$ is determined, the heat load on the dryer (Q) can be calculated from Equation A.9.3.

Because the dryer outlet temperature is specified as an input, TELCIM performs one additional check to ensure that the relative humidity of the air in State B does not exceed 100% (this might occur if the specified dryer outlet temperature, T_5, is too low, since as this temperature goes down, more sensible heat is converted to latent heat, but at the same time the "water carrying capacity" of the air is reduced). Based on the mass flowrates and dryer exit temperature, TELCIM calculates the relative humidity of the air exiting the dryer. The selected dryer outlet temperature should be tuned so that a reasonable value of this relative humidity is reported by TELCIM.

A.10. Estimating the Biogas Yield from Residual (Lipid-Extracted) Biomass

The Chemical Oxygen Demand (COD) of activated sludges generated in secondary wastewater treatment is often used as the basis for estimating the amount of methane that will be produced when those sludges are decomposed in anaerobic digesters. Because the residue generated when lipids are extracted from microalgal biomass is likely to be similar in composition and physical properties to activated sludge, it seems reasonable to assume that its COD can be used to estimate its methane yield during anaerobic digestion. TELCIM is programmed to accept an experimentally measured value for the COD of the residual microalgal biomass, or to estimate its COD based on its elemental composition.

The elemental composition of the whole microalgal biomass is determined by TELCIM from input data, as discussed in Section A.3 (the Stoichiometry Model). The elemental composition of the lipids recovered in the extraction step is determined based on two input parameters: the average number of carbon atoms and the average number of double bonds per fatty acid moiety in the recovered lipids. Assuming all of the recovered lipid is in the form of triacylglyceride, TELCIM makes the following calculation:

$$M_{TAG} = 12.011[3(x+1)] + 15.9994[6] + 1.0079[6(x-y)+2] \quad \text{(A.10.1)}$$

where:

M_{TAG} = Average molelcular weight of triacylglyceride molecule [kg/kg-mole];

x = average number of carbon atoms per fatty acid moiety [none]; and

y = average number of double bonds per fatty acid moiety [none].

Dividing the mass flowrate of lipid recovered in the extraction step by M_{TAG} determines the molar flowrate of triacylglyceride, and the molar flowrates of carbon, oxygen and hydrogen in the recovered lipid are easily calculated. TELCIM subtracts these from the molar flowrates of the elements feeding the extraction step to estimate the molar flowrates of carbon, oxygen, hydrogen, and nitrogen, phosphorus and sulfur in the residual biomass.

TELCIM then computes the COD of the residual biomass assuming the following chemical reactions occur in the COD test:

$$C + 2O \rightarrow CO_2$$

$$2H + O \rightarrow H_2O$$

$$P + 3H + 4O \rightarrow H_3PO_4$$

$$S + 2H + 4O \rightarrow H_2SO_4$$

$$N + 3H \rightarrow NH_3$$

TELCIM computes the amount of oxygen required to satisfy all of these reactions, assuming that only the hydrogen in excess of that consumed in the reactions producing ammonia and phosphoric and sulfuric

acids is oxidized to water, and after accounting for the oxygen already present in the residual biomass. (Note that organic nitrogen tends to be reduced rather than oxidized in the standard potassium dichromate COD test[13].)

With the additional inputs of:

- COD removal efficiency in the anaerobic digesters [%];
- biogas yield per unit mass of COD removal [m3 per kg COD removed]; and
- methane content of the biogas [vol. %];

TELCIM calculates the volume of methane produced in the anaerobic digesters. Using the heat of combustion of methane, and assuming ideal gas behavior, this volume is converted into an energy production rate. TELCIM also calculates the carbon dioxide produced in the digesters (on the basis that the biogas contains only methane and CO_2), and when the methane produced there is burned for energy recovery.

A.11. References for Appendix A

1 Weyer, K.M., Bush, D.R., Darzins, A., and Wilson, B. D. Theoretical Maximum Algal Oil Production. Bioenerg. Res. (2010) 3:204-213.

2 Wigmosta, M.S., A.M. Coleman, R.J. Skaggs, M.H. Huesemann, and L.J. Lane. National microalgae biofuel production potential and resources demand. Water Resources Research 47 (2011) W00H04 doi:10.1029/2010WR009966.

3 Huesemann, M.H., T.S. Hausmann, R. Bartha, M. Aksoy, J.C. Weissman, and J.R. Benemann (2009). Biomass productivities in wild type and pigment mutant of Cyclotella sp. (Diatom). Appl Biochem Biotechnol 157:507-526.

4 Oswald, W.J. (1988). Micro-algal biotechnology; Chap. 14 (Borowitka & Borowitzka, eds.). Cambridge University Press, Great Britain.

5 Welty, J.R., C.E. Wicks, R.E. Wilson, and G. Rorrer (2001). Fundamentals of Momentum, Heat and Mass Transfer (4th ed.). John Wiley & Sons, Inc. Hoboken, NJ, USA.

6 Lundquist, T.J, I.C. Woertz, N.W.T. Quinn, and J.R. Benemann (2010). A Realistic technology and engineering assessment of algae biofuel production. Energy Biosciences Institute, University of California, Berkeley, California, USA.

7 Bird, R.B., W. E. Stewart, and E.N. Lightfoot (2007). Transport phenomena (2nd ed.).John Wiley & Sons. New York, NY, USA.

8 Smith, J.M., and H.C. Van Ness. Introduction to chemical engineering thermodynamics (3rd ed.). 1975. McGraw-Hill Book Company. New York, NY, USA.

9 Perry, R.H. and C.H. Chilton (1973). Chemical Engineers' Handbook, 5th ed. McGraw-Hill Inc. USA.

[10] Himmelblau, David M. (1974). Basic principles and calculations in Chemical Engineering; 3rd ed. Prentice Hall. Englewood Cliffs, NJ, USA.
[11] Thompson, Edward V. (2005). Thermodynamic information and tables of data for Chemical Engineers. Stillwater Press. Orono, ME, USA.
[12] Bosen, Julius F. (1960). A formula for approximation of the saturation vapor pressure of water. Monthly Weather Review. August, 1960.
[13] Sawyer, C. N., P.L. McCarty and G. F. Parkin (2003). Chemistry for environmental engineering and science (5th ed.). McGraw-Hill. New York, NY, USA.